DETECTION AND EVALUATION OF INDOOR AIR PARAMETERS

A PROJECT REPORT
Submitted by

Neha.M Rai (1BM15BT019)
Nikhil.BV (1BM15BT020)
Sanjana.S (1BM15BT031)

in partial fulfilment of the academic requirements for the award of

BACHELOR OF ENGINEERING
IN
BIOTECHNOLOGY

Under the Guidance of:
N. Prathibha
Asst. Professor, BMSCE

B.M.S. College of Engineering
DEPARTMENT OF BIOTECHNOLOGY
Bull Temple Road, Bengaluru - 560019, Karnataka, India.
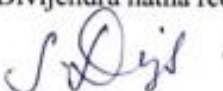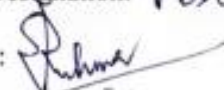**(June 2019)**

1

B.M.S. College of Engineering
DEPARTMENT OF BIOTECHNOLOGY
Bull Temple Road, Bengaluru - 560019, Karnataka, India

BONAFIDE CERTIFICATE FOR STUDENT BATCH

This is to certify that the project report titled, **"Detection and Evaluation of Indoor Air Parameters"** is a bonafide record of the project work done by Neha M Rai (1BM15BT019), Nikhil BV (1BM15BT020), Sanjana. S (1BM15BT031)

Head of the Department	Guide
Name: Dr. Divijendra natha reddy	Name: N. Prathibha
Signature:	Designation: Assistant Professor
Seal: HOD-Biotechnology BMS College of Engineering	Signature: N. Pran. Le
Date: Bangalore-560 019	Date: 7/6/19

Submitted for the University Examination held on ....

Internal Examiner	External Examiner
Name: Chandraprasad	Name: Dr Reshma SV
Designation:	College/Designation: PESU
Signature:	Signature:
Date: 7/6/19	Date: 7-6 2019

ACKNOWLEDGEMENT

We would like to express our gratitude to all those who have contributed in all possible ways to help us complete this project.

We thank our guide Ms. N. Prathibha, Asst. Professor, Department of Biotechnology, for giving us an opportunity to carry out this project and for her continuous support and guidance. We are grateful to all the other professors of the department for providing a helping hand at various stages of our project. Our Internal evaluators for monitoring our progress and helping us meet the demand for better development of the project.

Our sincere thanks to Dr.Divijendranatha Reddy. S, Professor and Head of the Biotechnology Department, BMSCE, for granting us the permission to work in the department and use the facilities such as laboratories. We would also like thank Dr Ravishankar B V, Principal, BMSCE for giving us this platform to showcase our skills and knowledge.

Last but not the least, we take this opportunity to thank all the laboratory assistants and our friends and family for extending their support and timely co-operation to enable us to complete our work in an resourceful manner.

ABSTRACT

With upcoming development and urbanisation the quality of air is not only deteriorating but also becoming a leading cause for death in humans. Ailments including asthma, emphysema or chronic obstructive pulmonary disease. The micro-organisms like bacteria, fungi and spores also contribute for various allergic and respiratory tract infections.

Air pollution is one of the world's largest killers, responsible for 6.4 million deaths per year. Recent evidence suggests that air pollution is also linked to higher risk of diabetes, autism, and lower IQ.

Air pollution, is actually a mixture of small particles such as: black carbon gases like nitrogen oxides, ozone, and sulfur dioxide. Particulate matter include small airborne particles like dust, soot, and drops of liquids. The majority of PM in urban areas is formed directly from burning of fossil fuels by power plants, automobiles, non-road equipment, and industrialfacilities.

Nitrogen oxide (NO) and Nitrogen dioxide (NO_2) are produced primarily by the vehicles. Ozone is formed in the atmosphere through reactions of volatile organic compounds and nitrogen oxides, both of which are formed as a result of combustion of fossil fuels. Short-term exposure to ozone can cause chest pain, coughing, throat irritation, while long term exposure can lead to decreased lung function and cause chronic obstructive pulmonarydisease (COPD). In addition, ozone exposure can aggravate existing lung diseases. SO_2 is emitted into the air by the burning of fossil fuels that contain sulfur. Coal, metal extraction and smelting, ship engines, and heavy equipment diesel equipment burn fuels that contain sulfur. Sulfur dioxide causes eye irritation, worsens asthma, increases susceptibility to respiratory infections, and impacts the cardiovascular system.

There are set standards for outdoor air quality, according to National Ambient Air Quality Standards (NAAQS),[1] which ensures that one must maintain the parameters within the limit for a healthy lifestyle.

Indoor Environmental Quality (IEQ) has another sent of parameters for indoor environment as follows,[2] :

IEQ parameter	Ambient levels	Health risk levels
Humidity	40–70%	$70 > H > 40\%$
Temperature	16–24°C	$24 > T > 16°C$
PM2.5	$<35\ \mu g/m^3$	$>35\ \mu g/m^3$
PM10	$<150\ \mu g/m^3$	$>150\ \mu g/m^3$
Total VOC	50–325 ppb	>500 ppb
CO_2	350–1000 ppm	>5000 ppm
CO	0–10 ppm	>10 ppm
Illuminance	200–500 lux	<100 lux
Sound levels	0–70 dB	>80 dB

IEQ parameter	"Good"	"Average"	"Poor"	"Bad"
Humidity	40–50%	50–60%	60–70%	$70 > H > 40\%$
Temperature	20–24°C	16–20°C	24–26°C	$26 > T > 16°C$
PM2.5	$0–10\ \mu g/m^3$	$10–15\ \mu g/m^3$	$15–35\ \mu g/m^3$	$>35\ \mu g/m^3$
PM10	$0–50\ \mu g/m^3$	$50–80\ \mu g/m^3$	$80–150\ \mu g/m^3$	$>150\ \mu g/m^3$
Total VOC	0–200 ppb	200–350 ppb	350–500 ppb	>500 ppb
CO_2	350–500 ppm	500–1000 ppm	1000–5000 ppm	>5000 ppm
CO	0–3 ppm	3–8 ppm	8–10 ppm	>10 ppm
Indoor air quality	0–10 ppm	10–25 ppm	25–50 ppm	>50 ppm

This project involves the detection of Air quality parameters including temperature, humidity, gas and biological particles present in the at most surrounding. The integration of the microbe detector to the sensors is the major part of electrically connecting it via indirect mode of detection. The fluorescence is detected with the intensity detector GY 20. The biological particles were charged using the electrodes that were then moved via the micro fluidic channel for providing the higher surface area and for east detection.

Since all the components selected were made sure to be kept small for easy integration into a compact device, they were provided a common voltage of 5V and the devices were activated using Arduion nano and its functioning was done by installing the necessary libraries and writing codes for instrumentation.

The final device was fabricated, soldered and complete dark room was ensured for selective detection of the intensity purely generated by the presence of microbe. This setup is ready to detect temperature, humidity, gasses and the microbes when powered with electricity.

CHAPTER 1

INTRODUCTION

Indoor air quality is becoming more and more significant matter for public health. Air in the indoor environment can be polluted by number of pollutants and contains many airborne micro organisms such as bacteria and fungi. These pathogens are linked with several infections such as gastrointestinal tract, respiratory tract infections, skin disorders etc. These findings would be an alert to students, staff and workers to these pathogens.

Microbes grow in very diverse conditions, which explains why they are found nearly everywhere on Earth. The airflora depends on the area and type of people moving in that vicinity.[1] When trying to control humidity in a building, it's important to realize that humidity typically rises and falls in response to current outdoor conditions. As a general rule, though, the more moisture, the more microorganisms there will be found. Thus moistureplays a very important role in growth of microorganism.[5]

CHAPTER 2
LITERATURE REVIEW

Babichenko et. al. Air Samplers for Microbiological Monitoring of Air Quality, the company KANOMAX in this article demonstrated the use of Heated Auto-fluorescence to identify the content of pathogen in the indoor environment. BioSentinel is able to detect them in real- time, providing early warning of a breach in the controlled environment and making it easier to pinpoint the source. The only drawback was seen to be its high cost and low shelf life.[1]

Detection of bacterial cells and antibodies using surface micromachined thin silicon cantilever resonators. According to the paper Amit Gupta et.al, figured that all the process has the ability to detect small amounts of materials, especially bacterial organisms, important for medical diagnostics and national security issues. Fabricated micromechanical system provided one approach for constructing multifunctional, highly sensitive, real-time, immunospecific biological detectors. Detection was achieved due to the change in the surface stress on the cantilever surface in situ upon binding of a small number of bacteria. This system provided numerous advantages such as high sensitivity and selectivity, low analyte volume, possibility to create portable and implantable devices. In addition, the fabrication process was easily adapted to batch fabrication, multiplexing and integration with other semiconductor processes to produce "on chip" complete sensing devices.[2]
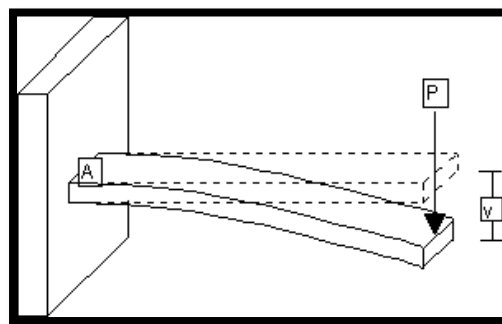
Fig 1 : The deflection is based on the mass absorbed and
the variation of intrinsic resonance of the substrate material.

Device using a laser to rapidly detect bacteria, a beam of laser i.e. single photon was passed through the sample that interacts with a bacterium. It was seen to diverts from its perfectly linear course, and it started to fly off in any random direction. It will further hit another bacterium, or hit the inside of the sphere. But eventually, all the photons will be seen by the photodetector on the inside of the sphere. And all this happens at the speed of light, so it's more or less instantaneous.[3]

Fig 2 : The detection based on scattering of laser beam.

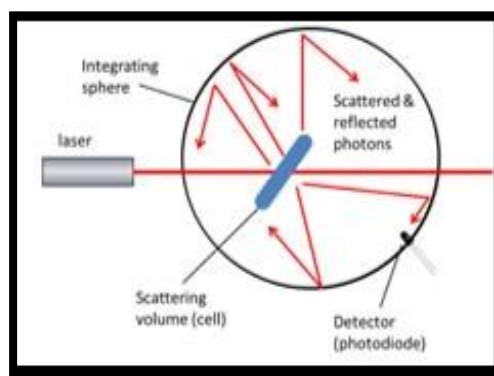Detection of microbial volatile organic compounds (MVOCs) by ion-mobility spectrometry Preliminary analysis done in this paper of indoor air was completed by the use of the IMS system in less than five minutes. These results showed that IMS is a very sensitive system for in-situ detection of microbial volatile organic compounds in indoor environments. Mixtures of MVOCs gave complex spectra, because of interference of signals and interaction of ionic species; this limits identification to five substances present, the ion-mobility values being inversely proportional to the mass-to-charge ratio of the substances investigated.[4]

Hans Miessner et.al. used Scattering to Identify Bacterial Pathogens the paper, Elastic Laser Scattering was sufficiently advanced technology to thwart sophisticated act of bioterrorism. It has the ability to monitor the signature pattern of the pathogen. The technology involves unique potential to rapidly identify and distinguish between the electronic signatures or fingerprints of high-priority agents like anthrax, botulism and plague versus those that cause more common threats such as water and food contamination, ricin toxin and viral encephalitis. It allowed quick assess to the potential risk and initiate the appropriate responseeven before the precise identity of that organism is known.[5]

According to Dr.Vijaylakshmi et.al, her research related to gram positive bacteria *Streptococcus pneumonia* uses the auto inducer peptides unlike the gram negative bacteria that has enzymes or genes acting as AI(auto inducers). The peptide used as autoinducer in Gram-positive quorum sensing is secreted through an ATP Binding Cassette transporter

(ABC). These bacteria use two component adapter response proteins for the detection of the peptide autoinducer and a phosphorylation/ dephosphorylation cascade regulates the two component signalling.[6]
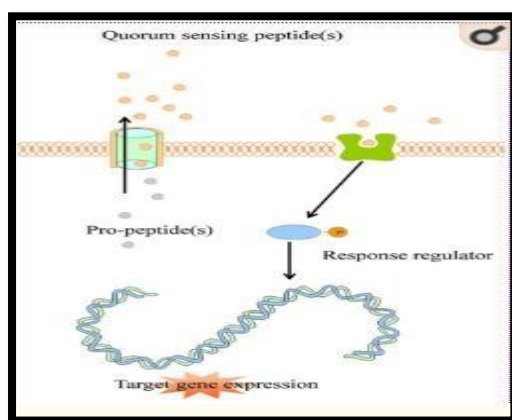

Fig 3: Regulation of Protein Response to density gradient.

XiaoLin Tian et. al came out with a successful structure-activity detection concluding, to detect Activation of quorum sensing for genetic competence and other co-ordinated activities in these species requires at least six gene products encoded by comCDE, comAB, and comX. The comC gene encodes a competence-stimulating peptide (CSP) precursor, which is cleavedand exported through a peptide-specific ABC transporter encoded by comAB, releasing CSP into a extracellular environment. The comDE encodes a two-component system consisting of a histidine kinase sensor protein (ComD) and its cognate response regulator (ComE) that specifically senses and responds to CSP. At a critical concentration, the CSP activates autophosphorylation of the ComD of neighboring cells. The phosphate group is then transferred to the ComE, which in turn activates its target genes, including comX that encodes a competence-specific sigma factor recognizing a consensus sequence (com-box) at the promoter regions of late competence genes, triggering the signaling cascade for genetic competence.[7]

Various peptide that activate the quorum sensing in bacteria was identified. A variety of analytical techniques have been reported in the literature for the qualitative and quantitative analysis of quorum sensing molecules, by Frederick Verbeke et. al.[8]
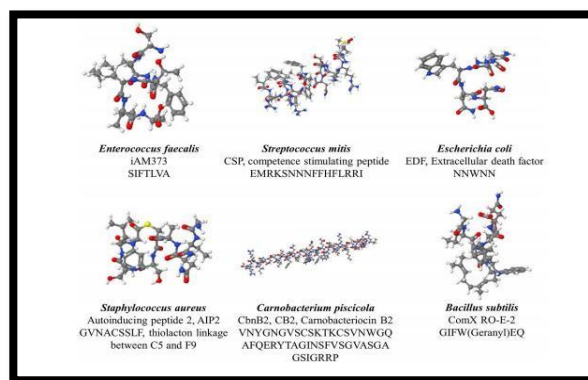
Fig 4: Different types of protein involved in quorum sensing.

Craney, A et. al have constructed a luxCDABE gene cluster optimized for expression in high-GC bacteria and established that the cluster is active in S. coelicolor. Fusions of this cluster to promoters for the genes hrdB, ramC and whiE faithfully report their activities via spontaneous bioluminescence. The quorum sensing was found to be much efficient in AT rich sequence and not much activity was seen to be that efficient in case of GC rich bacteria negative bacteria.[9]
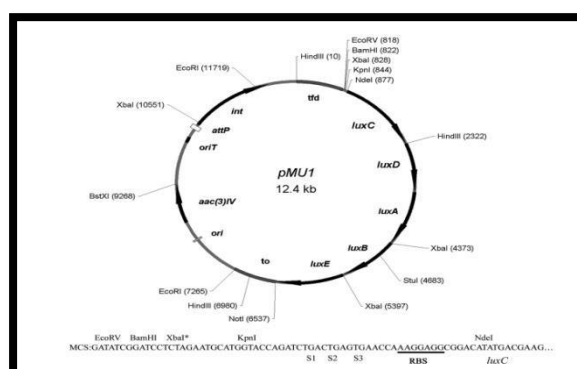
Fig 5: The final plasmid structure for the up regulation of quorum sensing effect in GC rich bacteria.

Gary m. Dunny et. Al The electroporation system and shuttle vector described have facilitated a number of experiments involving cloning and transfer of streptococcal genes in laboratories. The EcoRI fragments of pCF10, which have been cloned into the low-copy- number shuttle vector pWM402, could not be cloned in pUC vectors or other vectors useful for sequencing. These same fragments were stably maintained in E. coli and in E. faecalis when inserted into pDL276, which utilizes the same replicon as the pUC family of plasmids. On the basis of the relative intensity of plasmid DNA bands on ethidium bromide-stained

agarose gels, estimate that the copy number of pDL276 and pDL276-derived chimeric plasmids is four to five times that of pWM402 in both E. coli E. faecalis hosts. says. Gary m. Dunny et. Al.[10]

Natalia Romo et. al came up with this tool, possible to develop genetic circuits and new bioelectronic devices for the detection of pathogens. As biosensors are a suitable tool for the detection of molecules related to environmental quality problems or health risks. In this sense, the development of new bioelectronic devices that consider a sampler unit, a biosensor unit and a receptor unit, remotely connected through online systems represents an advance that allows to efficiently act against pathogens in indoor environments.[11]

Jungho Hwang et.al ,goal was fast monitoring of indoor bioaerosol concentrations with ATP bioluminescence assay using a bioaerosol sampler. For this purpose, a novel hand-held electrostatic rod-type sampler (110 mm wide, 115 mm long, and 200 mm tall) was developed and used with a commercial luminometer, which employs the Adenosine triphosphate (ATP) bioluminescence method. The sampler consisted of a wire-rod type charger and a cylindrical collector, and was operated with an applied voltage of 4.5 kV and a sampling flow rate of 150.7 lpm.Thus ATP bioluminescence method may be effective for fast monitoring of indoor bioaerosol concentrations.[12]

The scientist from IIT Delhi designed a biosensor relies on hydrogen sulphide gas produced by microorganisms. It is a gaseous signalling molecule that transmits biological signals in living system. In the heart of the biosensor are silver nanorod sensors that react with hydrogen sulphide to form black coloured silver sulphide. The colour and water wetting properties of silver nanorods change when exposed to microbes, while dead ones do not do any such thing.[13]

CHAPTER 3
OBJECTIVE

- Integration of Dht22 and MQ135 Sensor.

- Sampling .

- Statistical analysis of indoor air quality parameters.

- Microbial detector

- Optimization of components in the device for detection of indoor air quality parameters .

- Finalize the design of air quality parameter detector.

- Fabrication of indoor air quality detector.

CHAPTER 4

MATERIALS AND METHODOLOGY

4.1 MATERIALS USED:

- Arduion nano board
- Dht 22 temperature and humidity sensor
- MQ135 gas sensor
- Electrodes
- Air pump
- Water pump – solenoid
- Microfluidic channel
- Flouroscent dye
- Light intensity sensor (GY 20)
- LED display

4.2 METHODOLOGY :

4.2.1 Integration of Dht22 and MQ135 Sensors :

From the study , temperature and humidity plays a major role in microbe growth, hence its control becomes a prime importance. "Dht22" Temperature and Humidity sensor was used which measures the highest accuracy and wide ambient temperature and relative moisture content in the air as humidity in the tested location. Particulate being the soot emitted from the vehicles exhaust, it turns to smoke as it reached a certain height in the air. Regulation of this is very much important.

So, "MQ135" the gas sensor was used which senses the Air Quality, volatile gases, and smoke in ppm. A cumulative of all the gases present in air.

All this was integrated on to the "Arduion nano" onto the breadboard using connecting wires. Common of 5V was provided at one pin, grounded the other and the final pin was connected to data output pin. (Fig 1)
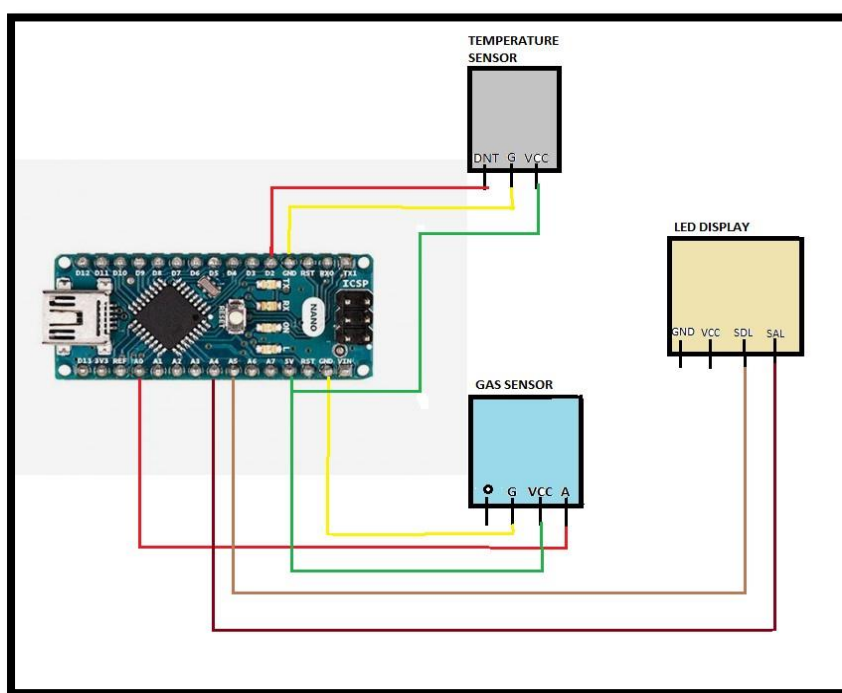
Fig1

4.2.2 Sampling

Microbial sample collection was done at 20 different places at morning and afternoon hours by placing 2% agar plates for 1hr at 1m height and 1m away from the side walls, then incubated for 24hrs at the bacterial incubator at 37ºC. simultaneously, the designed circuit was used to record the air parameters like temperature, humidity and gas.

The colonies obtained was counted using the microbial counter and then was converted to cfu/m 2 , using the formula

5a*10 ^{4} (bt) $^{-1}$

Where a = number of microbial colonies (cfu)

b = dish surface (cm 2)

t = exposure time (min)

The results were tabulated (table 1,2,3,4,5 & 6) for further analysis.

4.2.3 Statistical analysis of indoor air quality parameters

20

Statistical analysis is then undertaken considering the hypothesis with p = 5% , to be:

H_0 = " There Is No Significant Difference In Microbial Count With Change In Time, External Parameters And Its State Of Occupancy."

H_A = " There Is Significant Difference In Microbial Count With Change In Time, External Parameters And Its State Of Occupancy."

IBM SPSS software was used as the platform to arrive to all the statistical results. Anova, Regression, Independent Sample Test, Spearman correlation and Pearson Co-relation were performed. Microbial sensor was designed according to the protocol and it was integrated with the other sensor .

4.2.4 Microbial Detector

Our sampler is a type of single-stage electrostatic sampler, where in charging and collection of the airborne particles take place almost simultaneously.

When a high voltage is applied between the discharge electrode and the ground electrode of the sampler, unipolar air ions are generated from the tip of the discharge electrode by corona discharge.

The generated air ions then drift toward the ground electrode by the electric field and described by Han et al.

The air flow and the liquid flow rate was controlled using the electronic control panel. The bioluminescence detector was replaced with the fluorescent detector in our model.

The microfluidic channel is given a serpentine-shaped. The channel width, height, length, and gap were 500 mm, 500 mm, 50 cm, and 200 mm, respectively. The channel was given for 3D printing which was photo lithographically moulded by **think 3D**. [17]

4.2.5 Optimization of components in the device for detection of indoor air quality parameters .

The Dht22 was effective sensor compared to other sensors like SE121, DS18B20, TGS etc. the reason being its cost effectiveness and easy compatibility with other sensors used in the

circuit with high accuracy to detect both temperature and humidity.

MQ135 was the gas sensor, predominantly known to detect most of the air components like oxides of Carbon sulphur and nitrogen, along with volatile organic compounds and smoke. Where as other sensors don't show this all in one detection capability hence being very particular.

Out of various other methods to detect the microbe like Temperature, antibody coating based method provided a chance of the microbes to get resistant with time, hence finally losing the efficiency of the device to detect them. Other methods like quorum sensing and mass based cantilever based detection, though being highly sensitive and specific to microbes needed a lot of research time. Amongst all these constraints, the best was to choose the indirect mode of detection i.e. via light intensity.

Fluorescence was used over ATPase kit for its cost efficiency, large chemical needs and having low range of detection capability. EtBr being carcinogenic and having various health related issues confined its useage. Hence Rhodamine-B was preferred for detection.

Mini solenoid, electromechanical actuated valve to control the flow of liquid was used at 5V to control the rhodamine flow via the air sample and the channel. The nest part of it being electrically controlled to help integrate to the circuit over other huge water flow pumps. Thingbits, help get this compact version of solenoid to enable assembling.

4.2.6 Finalize the design of air quality parameter detector.

The final step was to connect one sensor to another at a common voltage base to provide uniform power source with 5V.
The integration of the microbe detector using the air and the liquid pump with electrically controlled flow at 5V.
The electrical components were soldered to make it even more compact and permanent and efficient connections.

4.2.7 Fabrication of indoor air quality detector.

B-Automate and the integration of the biotechnical project with electronic and electrical department helped us with connections and to fabricate it to make an end product out of all the separate components.
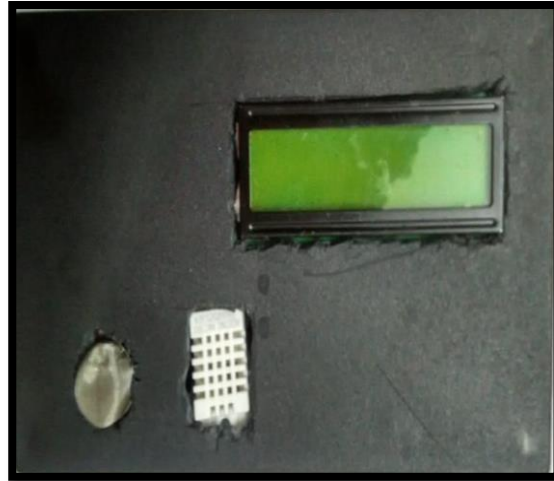

Fig 2 : The top and the bottom view of the device

CHAPTER 5

RESULTS AND DISCUSSION

Day 1 Morning

Location	Temp 1a (°C)	Humidity 1a (%)	Gas 1a (ppm)	Count 1a (cfu)	Count 1a (Cfu/m²)
MBG	27.8	21.8	178	78	8125
CMB	27.5	22.2	169	50	5952.38
BT-3	27.4	22.6	133	77	7825
BT-1	26	21	90	116	10175.43
BT-Office	27.4	22.6	118	44	5238.09
Staffroom	27.6	24	121	54	6428.57
Datacentre	27.5	20.7	79	32	3809.52
Coffee Kuteera	27	22	76	220	19298.24
R & D	28.1	24	371	50	5952.38
Canteen	27.6	22.7	56	102	8947.36
Power electronics	28.5	24.1	120	35	4166.66
Environmental Lab	27	23.8	104	96	9756
Indoor	27.7	23.7	63	79	8028.45
Store room	27.3	23.7	231	35	4166.66
BEE	27.4	22.6	81	111	9736.84
EEE	27.3	22.6	82	60	7142.85
Relay lab	27.5	23.1	77	76	7723.57
Concrete Lab	27.8	23.3	81	80	8130.08
Chemical Room	27	21	75	35	4166.66
Parking	27.5	24.8	127	304	26666.66

Table 1

Descriptive Statistics

	Mean	Std. Deviation	N
Count 1a (Cfu/m²)	8571.8200	5440.04034	20
Temp 1a (°C)	27.445	.4947	20
Humidity 1a (%)	22.815	1.1375	20
Gas 1a (ppm)	121.600	73.1749	20

Correlations

		Count 1a (Cfu/m²)	Temp 1a (°C)	Humidity 1a (%)
Pearson Correlation	Count 1a (Cfu/m²)	1.000	-.220	.258
	Temp 1a (°C)	-.220	1.000	.523
	Humidity 1a (%)	.258	.523	1.000
	Gas 1a (ppm)	-.166	.329	.319
Sig. (1-tailed)	Count 1a (Cfu/m²)	.	.176	.136
	Temp 1a (°C)	.176	.	.009
	Humidity 1a (%)	.136	.009	.
	Gas 1a (ppm)	.242	.079	.085
N	Count 1a (Cfu/m²)	20	20	20
	Temp 1a (°C)	20	20	20
	Humidity 1a (%)	20	20	20
	Gas 1a (ppm)	20	20	20

Fig1

ANOVA^a

Model		Sum of Squares	df	Mean Square	F	Sig.
1	Regression	153436632.505	3	51145544.168	2.002	.154^b
	Residual	408850107.336	16	25553131.708		
	Total	562286739.841	19			

a. Dependent Variable: Count 1a (Cfu/m²)

b. Predictors: (Constant), Gas 1a (ppm), Humidity 1a (%), Temp 1a (°C)

fig 2

Coefficients^a

Model		Unstandardized Coefficients B	Unstandardized Coefficients Std. Error	Standardized Coefficients Beta	t	Sig.
1	(Constant)	84189.713	68044.339		1.237	.234
	Temp 1a (°C)	-4890.006	2808.232	-.445	-1.741	.101
	Humidity 1a (%)	2645.767	1216.986	.553	2.174	.045
	Gas 1a (ppm)	-14.596	17.068	-.196	-.855	.405

One-Sample Statistics

	N	Mean	Std. Deviation	Std. Error Mean
Temp 1a (°C)	20	27.445	.4947	.1106
Humidity 1a (%)	20	22.815	1.1375	.2544
Gas 1a (ppm)	20	121.600	73.1749	16.3624
Count 1a (Cfu/m²)	20	8571.8200	5440.04034	1216.43000

			Test Value = 0		95% Confidence Interval of the Difference
	t	df	Sig. (2-tailed)	Mean Difference	Lower
Temp 1a (°C)	248.114	19	.000	27.4450	27.213
Humidity 1a (%)	89.696	19	.000	22.8150	22.283
Gas 1a (ppm)	7.432	19	.000	121.6000	87.353
Count 1a (Cfu/m²)	7.047	19	.000	8571.82000	6025.8027

Fig 3

Non parametric tests

Correlations

		Temp 1a (°C)	Humidity 1a (%)	Gas 1a (ppm)
Temp 1a (°C)	Pearson Correlation	1	.523*	.329
	Sig. (2-tailed)		.018	.157
	N	20	20	20
Humidity 1a (%)	Pearson Correlation	.523*	1	.319
	Sig. (2-tailed)	.018		.170
	N	20	20	20
Gas 1a (ppm)	Pearson Correlation	.329	.319	1
	Sig. (2-tailed)	.157	.170	
	N	20	20	20
Count 1a (Cfu/m²)	Pearson Correlation	-.220	.258	-.166
	Sig. (2-tailed)	.352	.272	.484
	N	20	20	20

Correlations

			Temp 1a (°C)	Humidity 1a (%)
Spearman's rho	Temp 1a (°C)	Correlation Coefficient	1.000	.460*
		Sig. (2-tailed)	.	.041
		N	20	20
	Humidity 1a (%)	Correlation Coefficient	.460*	1.000
		Sig. (2-tailed)	.041	.
		N	20	20
	Gas 1a (ppm)	Correlation Coefficient	.193	.297
		Sig. (2-tailed)	.415	.203
		N	20	20
	Count 1a (Cfu/m²)	Correlation Coefficient	-.205	.076
		Sig. (2-tailed)	.385	.750
		N	20	20

Fig4

28
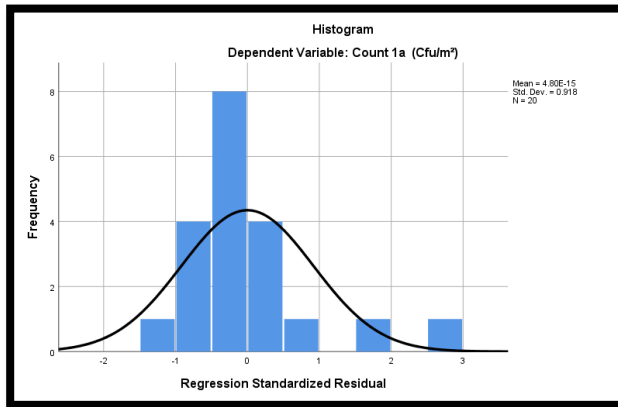
Fig5
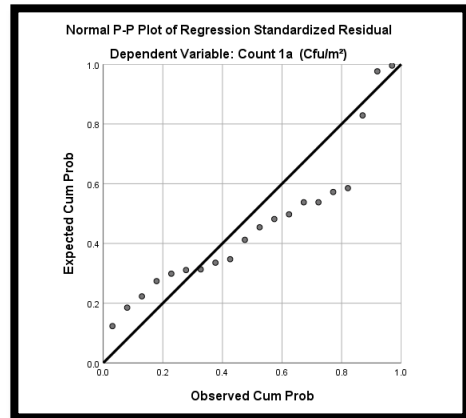
Fig6
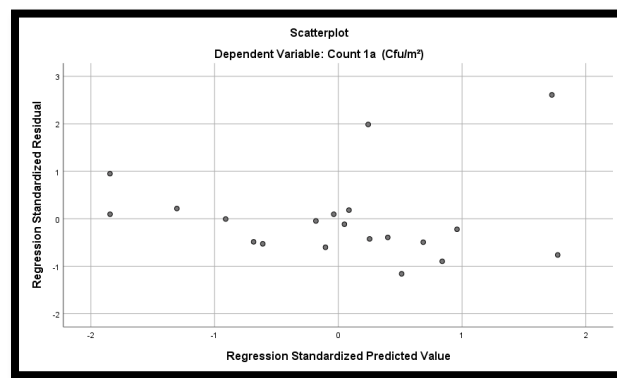
Fig 7

DAY 1 Evening

Location	Temp 1b (°C)	Humidity 1b (%)	Gas 1b (ppm)	Count 1b (cfu)	Count 1b (Cfu/m²)
MBG	29.2	8.7	178	143	13240.74
CMB	29.4	8.2	138	96	10000
BT-3	29.5	7.1	103	31	3690.47
BT-1	29.5	7.3	105	15	5952.38
BT-Office	29.5	7.4	99	50	5952.38
Staffroom	29.7	8.7	84	24	2857.14
Datacentre	29	7.5	86	72	7500
Coffee Kuteera	30	5	63	142	13148.14
R & D	29	13	419	107	9907.4
Canteen	31.2	4.5	78	283	26203.7
Power electronics	30	9	120	60	7142.85
Environmental Lab	29.7	8.4	95	33	3928.57
Indoor	31.7	7.9	67	70	7291.66
Store room	29	7.4	231	25	2976.19
BEE	29	11.1	82	87	9062.5
EEE	29.3	9.7	91	112	10370.37

Relay lab	29.1	8.6	92	385	35648.14
Concrete Lab	29	9.9	79	212	19629.62
Chemical Room	30.1	7.1	89	45	5357.145
Parking	30.9	7.4	99	233	21574.07

Table 2

Descriptive Statistics

	Mean	Std. Deviation	N
Count 1b (Cfu/m²)	11071.67325	8579.785234	20
Temp 1b (°C)	29.690	.7766	20
Humidity 1b (%)	8.195	1.8861	20
Gas 1b (ppm)	119.900	80.5951	20

Correlations

		Count 1b (Cfu/m²)	Temp 1b (°C)	Humidity 1b (%)
Pearson Correlation	Count 1b (Cfu/m²)	1.000	.139	-.109
	Temp 1b (°C)	.139	1.000	-.515
	Humidity 1b (%)	-.109	-.515	1.000
	Gas 1b (ppm)	-.135	-.359	.552
Sig. (1-tailed)	Count 1b (Cfu/m²)	.	.279	.324
	Temp 1b (°C)	.279	.	.010
	Humidity 1b (%)	.324	.010	.
	Gas 1b (ppm)	.285	.060	.006
N	Count 1b (Cfu/m²)	20	20	20
	Temp 1b (°C)	20	20	20
	Humidity 1b (%)	20	20	20
	Gas 1b (ppm)	20	20	20

Fig8

ANOVA[a]

Model		Sum of Squares	df	Mean Square	F	Sig.
1	Regression	38651440.774	3	12883813.591	.152	.927[b]
	Residual	1359990137.663	16	84999383.604		
	Total	1398641578.437	19			

a. Dependent Variable: Count 1b (Cfu/m²)

b. Predictors: (Constant), Gas 1b (ppm), Temp 1b (°C), Humidity 1b (%)

Fig 9

Coefficients[a]

Model		Unstandardized Coefficients B	Unstandardized Coefficients Std. Error	Standardized Coefficients Beta	t	Sig.
1	(Constant)	-21369.953	100631.900		-.212	.835
	Temp 1b (°C)	1137.439	3194.855	.103	.356	.726
	Humidity 1b (%)	-11.642	1472.692	-.003	-.008	.994
	Gas 1b (ppm)	-10.288	31.654	-.097	-.325	.749

One-Sample Statistics

	N	Mean	Std. Deviation	Std. Error Mean
Temp 1b (°C)	20	29.690	.7766	.1736
Humidity 1b (%)	20	8.195	1.8861	.4217
Gas 1b (ppm)	20	119.900	80.5951	18.0216
Count 1b (Cfu/m²)	20	11071.67325	8579.785234	1918.498301

One-Sample Test

Test Value = 0

	t	Df	Sig. (2-tailed)	Mean Difference	95% Confidence Interval of the Difference Lower
Temp 1b (°C)	170.981	19	.000	29.6900	29.327
Humidity 1b (%)	19.431	19	.000	8.1950	7.312
Gas 1b (ppm)	6.653	19	.000	119.9000	82.180
Count 1b (Cfu/m²)	5.771	19	.000	11071.673250	7056.210160

Fig10

Non Parametric test

Correlations

		Temp 1b (°C)	Humidity 1b (%)	Gas 1b (ppm)
Temp 1b (°C)	Pearson Correlation	1	-.515*	-.359
	Sig. (2-tailed)		.020	.120
	N	20	20	20
Humidity 1b (%)	Pearson Correlation	-.515*	1	.552*
	Sig. (2-tailed)	.020		.012
	N	20	20	20
Gas 1b (ppm)	Pearson Correlation	-.359	.552*	1
	Sig. (2-tailed)	.120	.012	
	N	20	20	20
Count 1b (Cfu/m²)	Pearson Correlation	.139	-.109	-.135
	Sig. (2-tailed)	.559	.647	.570
	N	20	20	20

Correlations

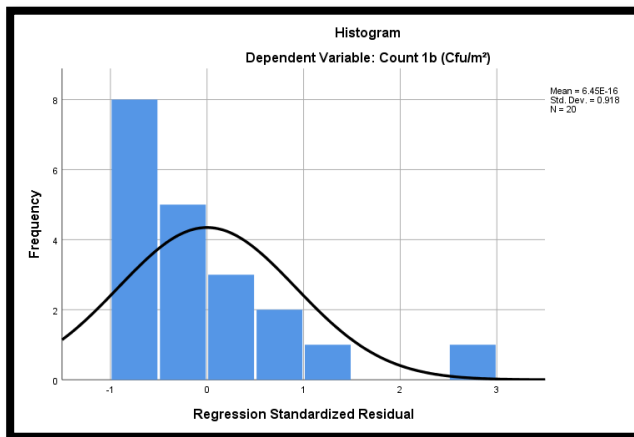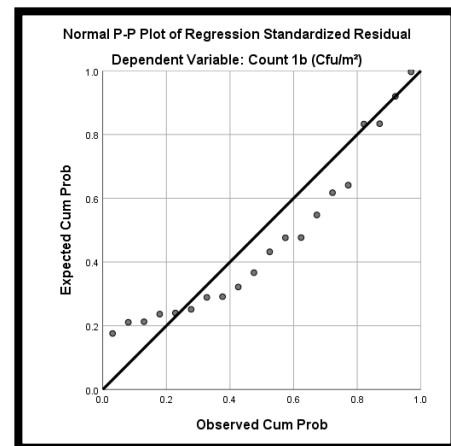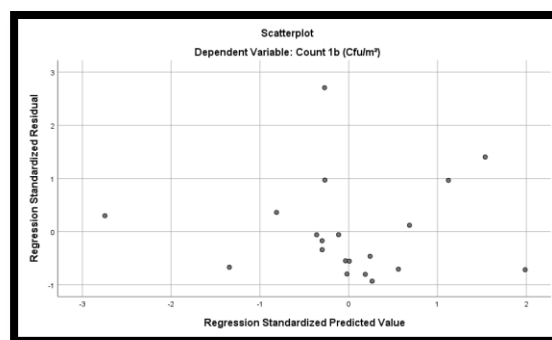|			Temp 1b (°C)	Humidity 1b (%)
Spearman's rho	Temp 1b (°C)	Correlation Coefficient	1.000	-.548*
		Sig. (2-tailed)	.	.012
		N	20	20
	Humidity 1b (%)	Correlation Coefficient	-.548*	1.000
		Sig. (2-tailed)	.012	.
		N	20	20
	Gas 1b (ppm)	Correlation Coefficient	-.337	.175
		Sig. (2-tailed)	.147	.461
		N	20	20
	Count 1b (Cfu/m²)	Correlation Coefficient	-.058	.133
		Sig. (2-tailed)	.809	.575
		N	20	20

Fig 11

Fig 12

Fig 13

Fig 14

Table description :

A Pearson correlation is a number between -1 and 1 that indicates the extent to which two variables are linearly related.(fig 1,8)

The one-way analysis of variance (ANOVA) is used to determine whether there are any statistically significant differences between the means of three or more independent(unrelated) groups (fig 2,9)

When you perform a t-test, you're usually trying to find evidence of a significant difference between population means (2-sample t) or between the population mean and a hypothesized value (1-sample The t-value measures the size of the difference relative to the variation in your sample data.(fig3, 10)

Spearman's Rho is a non-parametric test used to measure the strength of association between two variables (fig4, 11)

Day 2 Morning

Location	Temp 1c (°C)	Humidity 1c (%)	Gas 1c (ppm)	Count 1c (cfu)	Count 1c (Cfu/m²)
MBG	28.2	21.8	96	159	14722.22
CMB	28.2	22.6	91	100	9259.25
BT-3	28.3	22.1	81	110	10185.18
BT-1	28.3	21.4	70	17	2023.8
BT-Office	28.3	21.6	74	40	4761.9
Staffroom	28.4	21.4	68	65	6605.69
Datacentre	28.6	18.4	71	94	9552.84
Coffee Kuteera	29.5	18.8	54	140	4444.4
R & D	28.4	23.2	160	59	5995.93
Canteen	30.5	16.6	60	156	14444.44
Power electronics	29.2	19.4	88	14	1666.66
Environmental Lab	29	20.2	57	90	9146.34
Indoor	30.8	17.4	63	35	4166.66
Store room	28.5	20.9	225	26	3095.23
BEE	28.5	22.5	65	138	12777.77
EEE	29	25	69	139	12870
Relay lab	28.1	21.6	68	100	10161.2
Concrete Lab	29	22.8	56	75	7621.95
Chemical Room	28.3	21.8	110	51	6071.42
Parking	28	22	75	310	28703.7

Table 3

Descriptive Statistics

	Mean	Std. Deviation	N
Count 1c (Cfu/m²)	8913.8290	6102.15330	20
Temp 1c (°C)	28.755	.7612	20
Humidity 1c (%)	21.075	2.0576	20
Gas 1c (ppm)	85.050	40.7837	20

Correlations

		Count 1c (Cfu/m²)	Temp 1c (°C)	Humidity 1c (%)
Pearson Correlation	Count 1c (Cfu/m²)	1.000	-.194	.186
	Temp 1c (°C)	-.194	1.000	-.700
	Humidity 1c (%)	.186	-.700	1.000
	Gas 1c (ppm)	-.235	-.281	.195
Sig. (1-tailed)	Count 1c (Cfu/m²)	.	.207	.216
	Temp 1c (°C)	.207	.	.000
	Humidity 1c (%)	.216	.000	.
	Gas 1c (ppm)	.160	.115	.205
N	Count 1c (Cfu/m²)	20	20	20
	Temp 1c (°C)	20	20	20
	Humidity 1c (%)	20	20	20
	Gas 1c (ppm)	20	20	20

Fig 15

ANOVA[a]

Model		Sum of Squares	df	Mean Square	F	Sig.
1	Regression	94236746.401	3	31412248.800	.820	.502[b]
	Residual	613252477.210	16	38328279.826		
	Total	707489223.610	19			

a. Dependent Variable: Count 1c (Cfu/m²)

b. Predictors: (Constant), Gas 1c (ppm), Humidity 1c (%), Temp 1c (°C)

fig 16

Coefficients[a]

Model		Unstandardized Coefficients		Standardized Coefficients	t	Sig.
		B	Std. Error	Beta		
1	(Constant)	55744.455	92602.450		.602	.556
	Temp 1c (°C)	-1704.262	2671.697	-.213	-.638	.533
	Humidity 1c (%)	292.652	967.112	.099	.303	.766
	Gas 1c (ppm)	-46.939	36.288	-.314	-1.294	.214

One-Sample Statistics

	N	Mean	Std. Deviation	Std. Error Mean
Temp 1c (°C)	20	28.755	.7612	.1702
Humidity 1c (%)	20	21.075	2.0576	.4601
Gas 1c (ppm)	20	85.050	40.7837	9.1195
Count 1c (Cfu/m²)	20	8913.8290	6102.15330	1364.48296

One-Sample Test

Test Value = 0

	t	df	Sig. (2-tailed)	Mean Difference	95% Confidence Interval of the Difference Lower
Temp 1c (°C)	168.936	19	.000	28.7550	28.399
Humidity 1c (%)	45.807	19	.000	21.0750	20.112
Gas 1c (ppm)	9.326	19	.000	85.0500	65.963
Count 1c (Cfu/m²)	6.533	19	.000	8913.82900	6057.9333

Fig 17

Non parametric test

Correlations

		Temp 1c (°C)	Humidity 1c (%)	Gas 1c (ppm)
Temp 1c (°C)	Pearson Correlation	1	-.700**	-.281
	Sig. (2-tailed)		.001	.230
	N	20	20	20
Humidity 1c (%)	Pearson Correlation	-.700**	1	.195
	Sig. (2-tailed)	.001		.411
	N	20	20	20
Gas 1c (ppm)	Pearson Correlation	-.281	.195	1
	Sig. (2-tailed)	.230	.411	
	N	20	20	20
Count 1c (Cfu/m²)	Pearson Correlation	-.194	.186	-.235
	Sig. (2-tailed)	.414	.431	.319
	N	20	20	20

Correlations

			Temp 1c (°C)	Humidity 1c (%)
Spearman's rho	Temp 1c (°C)	Correlation Coefficient	1.000	-.491*
		Sig. (2-tailed)	.	.028
		N	20	20
	Humidity 1c (%)	Correlation Coefficient	-.491*	1.000
		Sig. (2-tailed)	.028	.
		N	20	20
	Gas 1c (ppm)	Correlation Coefficient	-.542*	.312
		Sig. (2-tailed)	.014	.181
		N	20	20
	Count 1c (Cfu/m²)	Correlation Coefficient	-.316	.348
		Sig. (2-tailed)	.175	.133
		N	20	20

Fig 18
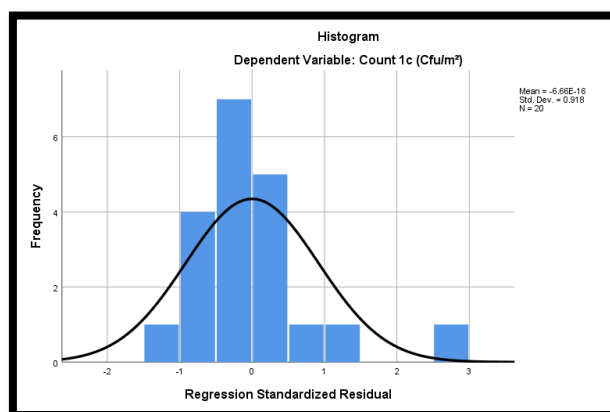
Fig 19
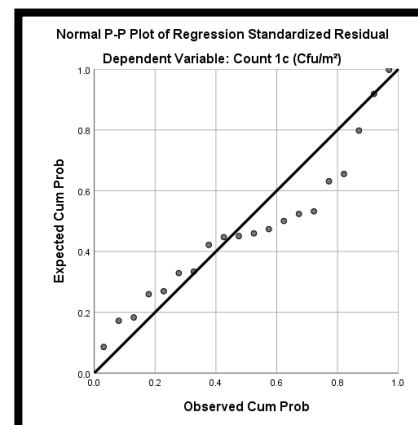
Fig 20
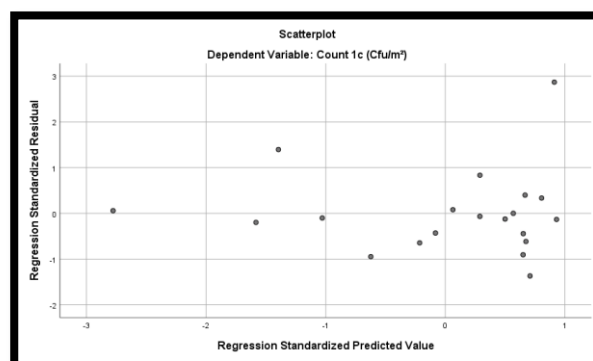
Fig 21

Day 2 Evening

Location	Temp 1d (°C)	Humidity 1d (%)	Gas 1d (ppm)	Count 1d (cfu)	Count 1d (Cfu/m²)
MBG	29.9	7.5	75	213	19722.22
CMB	29.8	6.4	58	170	15740.74
BT-3	29.6	10.7	60	211	19537.03
BT-1	29.6	9.2	58	167	15462.96
BT-Office	29.4	8.8	56	145	13425.92
Staffroom	29.5	8	81	97	8981.48
Datacentre	29.4	8.1	69	205	19907.4
Coffee Kuteera	30.4	5.1	47	172	15925.92
R & D	29.4	11.9	221	150	13888.88
Canteen	31.4	5.4	53	165	15277.77
Power electronics	29.5	12.9	80	122	11296.29
Environmental Lab	29.5	9.5	89	165	15277.77
Indoor	31	6.1	52	245	22685.18
Store room	29.7	9.1	88	163	15092.59
BEE	29.5	11.2	60	242	22407.4
EEE	29.6	10.5	54	178	16481.48
Relay lab	29.4	7.2	55	111	10277.77
Concrete Lab	29.8	7.9	53	54	5000
Chemical Room	29.4	9	228	56	5180.18
Parking	31.3	9	72	200	18518.51

Table 4

Descriptive Statistics

	Mean	Std. Deviation	N
Count 1d (Cfu/m²)	15004.3745	4971.69030	20
Temp 1d (°C)	29.855	.6428	20
Humidity 1d (%)	8.675	2.0986	20
Gas 1d (ppm)	80.450	50.8418	20

Correlations

		Count 1d (Cfu/m²)	Temp 1d (°C)	Humidity 1d (%)
Pearson Correlation	Count 1d (Cfu/m²)	1.000	.333	-.029
	Temp 1d (°C)	.333	1.000	-.536
	Humidity 1d (%)	-.029	-.536	1.000
	Gas 1d (ppm)	-.385	-.299	.373
Sig. (1-tailed)	Count 1d (Cfu/m²)	.	.076	.452
	Temp 1d (°C)	.076	.	.007
	Humidity 1d (%)	.452	.007	.
	Gas 1d (ppm)	.047	.100	.053
N	Count 1d (Cfu/m²)	20	20	20
	Temp 1d (°C)	20	20	20
	Humidity 1d (%)	20	20	20
	Gas 1d (ppm)	20	20	20

Fig 22

ANOVA^a

Model		Sum of Squares	Df	Mean Square	F	Sig.
1	Regression	127369016.135	3	42456338.712	1.985	.157^b
	Residual	342267368.922	16	21391710.558		
	Total	469636385.057	19			

a. Dependent Variable: Count 1d (Cfu/m²)

b. Predictors: (Constant), Gas 1d (ppm), Temp 1d (°C), Humidity 1d (%)

Fig 23

Coefficients^a

Model		Unstandardized Coefficients B	Std. Error	Standardized Coefficients Beta	t	Sig.
1	(Constant)	-79049.228	61837.420		-1.278	.219
	Temp 1d (°C)	3028.144	1971.471	.391	1.536	.144
	Humidity 1d (%)	774.386	621.067	.327	1.247	.230
	Gas 1d (ppm)	-38.153	22.673	-.390	-1.683	.112

One-Sample Statistics

	N	Mean	Std. Deviation	Std. Error Mean
Temp 1d (°C)	20	29.855	.6428	.1437
Humidity 1d (%)	20	8.675	2.0986	.4693
Gas 1d (ppm)	20	80.450	50.8418	11.3686
Count 1d (Cfu/m²)	20	15004.3745	4971.69030	1111.70375

One-Sample Test

					95% Confidence Interval of the Difference
			Test Value = 0		
	T	df	Sig. (2-tailed)	Mean Difference	Lower
Temp 1d (°C)	207.725	19	.000	29.8550	29.554
Humidity 1d (%)	18.487	19	.000	8.6750	7.693
Gas 1d (ppm)	7.077	19	.000	80.4500	56.655
Count 1d (Cfu/m²)	13.497	19	.000	15004.37450	12677.5518

fig24

Non parametric test

Correlations

		Temp 1d (°C)	Humidity 1d (%)	Gas 1d (ppm)
Temp 1d (°C)	Pearson Correlation	1	-.536*	-.299
	Sig. (2-tailed)		.015	.201
	N	20	20	20
Humidity 1d (%)	Pearson Correlation	-.536*	1	.373
	Sig. (2-tailed)	.015		.105
	N	20	20	20
Gas 1d (ppm)	Pearson Correlation	-.299	.373	1
	Sig. (2-tailed)	.201	.105	
	N	20	20	20
Count 1d (Cfu/m²)	Pearson Correlation	.333	-.029	-.385
	Sig. (2-tailed)	.152	.905	.094
	N	20	20	20

Correlations

			Temp 1d (°C)	Humidity 1d (%)
Spearman's rho	Temp 1d (°C)	Correlation Coefficient	1.000	-.477*
		Sig. (2-tailed)	.	.033
		N	20	20
	Humidity 1d (%)	Correlation Coefficient	-.477*	1.000
		Sig. (2-tailed)	.033	.
		N	20	20
	Gas 1d (ppm)	Correlation Coefficient	-.479*	.581**
		Sig. (2-tailed)	.033	.007
		N	20	20
	Count 1d (Cfu/m²)	Correlation Coefficient	.383	-.035
		Sig. (2-tailed)	.096	.885
		N	20	20

Fig 25
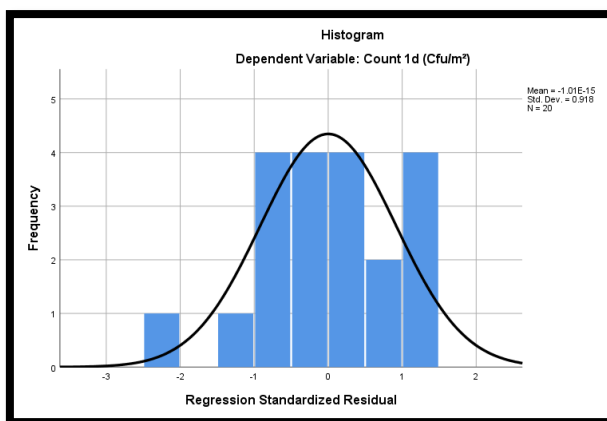
Fig 26
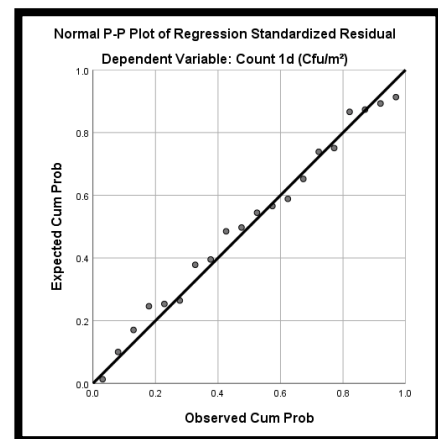
Fig 27
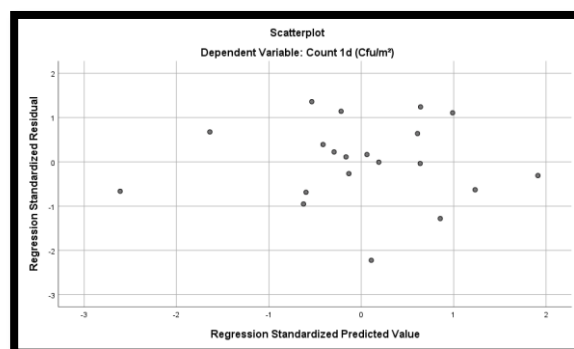
Fig 28

Table description :

Table description :

A Pearson correlation is a number between -1 and 1 that indicates the extent to which two variables are linearly related.(fig 15,22)

The one-way analysis of variance (ANOVA) is used to determine whether there are any statistically significant differences between the means of three or more independent(unrelated) groups (fig 16,23)

When you perform a **t-test**, you're usually trying to find evidence of a significant difference between population means (2-sample **t**) or between the population mean and a hypothesized value (1-sample The **t**-value measures the size of the difference relative to the variation in your sample data.(fig17, 24)

Spearman's Rho is a non-parametric test used to measure the strength of association between two variables (fig18, 25)

Day 3 Morning

Location	Temp 1e (°C)	Humidity 1e (%)	Gas 1e (ppm)	Count 1e (cfu)	Count 1e (Cfu/m²)
MBG	25.5	9.4	155	73	7418.69
CMB	25.9	9.2	120	55	6547.61
BT-3	24.9	11	140	23	2738.9
BT-1	24.5	8	80	46	5476.19
BT-Office	24	7.4	100	27	3214.28
Staffroom	25.4	7	88	23	2738.09
Datacentre	23.8	8.9	90	44	5238.09
Coffee Kuteera	25.1	12	106	201	17631.57
R & D	25.9	7	140	197	17280.7
Canteen	28.5	5	108	278	24385.96
Power electronics	25.3	9	80	111	9736.84
Environmental Lab	24.7	13	75	106	9298.24
Indoor	25.7	7	90	87	8841.46
Store room	25.1	9	145	17	8333.33
BEE	25.1	12	133	102	8947.36
EEE	25.9	6	90	45	5357.14
Relay lab	24.9	9	120	58	6904.76
Concrete Lab	24.7	14	70	115	10087.71
Chemical Room	26.2	9	100	16	1904.73
Parking	25.6	10	149	230	20175.43

Table 5

Descriptive Statistics

	Mean	Std. Deviation	N
Count 1e (Cfu/m²)	9112.8540	6163.13038	20
Temp 1e (°C)	25.335	.9773	20
Humidity 1e (%)	9.145	2.3435	20
Gas 1e (ppm)	108.950	26.9570	20

Correlations

		Count 1e (Cfu/m²)	Temp 1e (°C)	Humidity 1e (%)
Pearson Correlation	Count 1e (Cfu/m²)	1.000	.553	-.042
	Temp 1e (°C)	.553	1.000	-.477
	Humidity 1e (%)	-.042	-.477	1.000
	Gas 1e (ppm)	.234	.186	-.017
Sig. (1-tailed)	Count 1e (Cfu/m²)	.	.006	.430
	Temp 1e (°C)	.006	.	.017
	Humidity 1e (%)	.430	.017	.
	Gas 1e (ppm)	.160	.216	.471
N	Count 1e (Cfu/m²)	20	20	20
	Temp 1e (°C)	20	20	20
	Humidity 1e (%)	20	20	20
	Gas 1e (ppm)	20	20	20

fig 29

ANOVA[a]

Model		Sum of Squares	Df	Mean Square	F	Sig.
1	Regression	276405423.814	3	92135141.271	3.311	.047[b]
	Residual	445293921.538	16	27830870.096		
	Total	721699345.351	19			

a. Dependent Variable: Count 1e (Cfu/m²)

b. Predictors: (Constant), Gas 1e (ppm), Humidity 1e (%), Temp 1e (°C)

fig 30

Coefficients^a

Model		Unstandardized Coefficients B	Std. Error	Standardized Coefficients Beta	t	Sig.
1	(Constant)	-106529.851	38683.662		-2.754	.014
	Temp 1e (°C)	4188.036	1439.081	.664	2.910	.010
	Humidity 1e (%)	727.738	589.734	.277	1.234	.235
	Gas 1e (ppm)	26.468	45.849	.116	.577	.572

One-Sample Statistics

	N	Mean	Std. Deviation	Std. Error Mean
Temp 1e (°C)	20	25.335	.9773	.2185
Humidity 1e (%)	20	9.145	2.3435	.5240
Gas 1e (ppm)	20	108.950	26.9570	6.0278
Count 1e (Cfu/m²)	20	9112.8540	6163.13038	1378.11785

Test Value = 0

	t	Df	Sig. (2-tailed)	Mean Difference	95% Confidence Interval of the Difference Lower
Temp 1e (°C)	115.939	19	.000	25.3350	24.878
Humidity 1e (%)	17.451	19	.000	9.1450	8.048
Gas 1e (ppm)	18.075	19	.000	108.9500	96.334
Count 1e (Cfu/m²)	6.613	19	.000	9112.85400	6228.4202

Fig 31

Non parametric test

Temp 1e (°C)	Pearson Correlation	1	-.477*	.186
	Sig. (2-tailed)		.033	.433
	N	20	20	20

44

Humidity 1e (%)	Pearson Correlation	-.477*	1	-.017
	Sig. (2-tailed)	.033		.942
	N	20	20	20
Gas 1e (ppm)	Pearson Correlation	.186	-.017	1
	Sig. (2-tailed)	.433	.942	
	N	20	20	20
Count 1e (Cfu/m²)	Pearson Correlation	.553*	-.042	.234
	Sig. (2-tailed)	.011	.859	.320
	N	20	20	20

			Temp 1e (°C)	Humidity 1e (%)
Spearman's rho	Temp 1e (°C)	Correlation Coefficient	1.000	-.378
		Sig. (2-tailed)	.	.101
		N	20	20
	Humidity 1e (%)	Correlation Coefficient	-.378	1.000
		Sig. (2-tailed)	.101	.
		N	20	20
	Gas 1e (ppm)	Correlation Coefficient	.326	.087
		Sig. (2-tailed)	.161	.716
		N	20	20
	Count 1e (Cfu/m²)	Correlation Coefficient	.198	.223
		Sig. (2-tailed)	.403	.344
		N	20	20

Fig 32
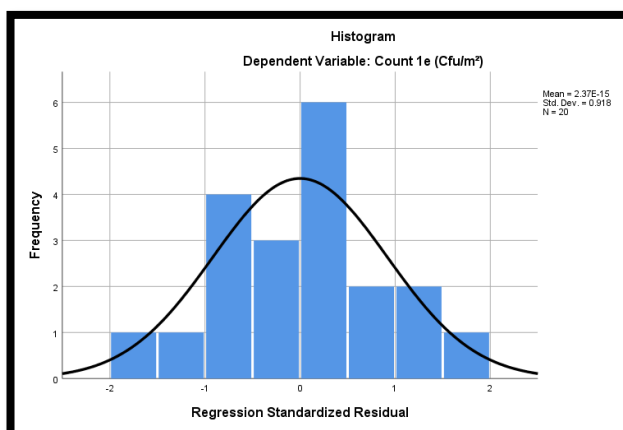
Fig 33
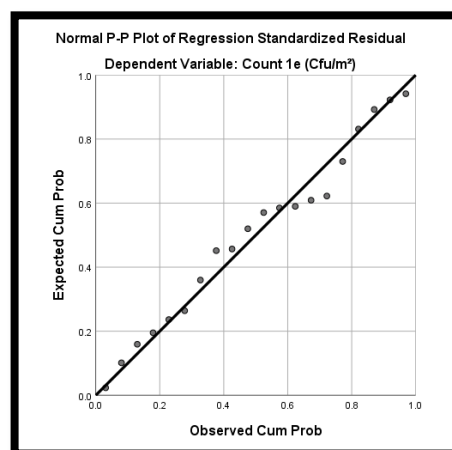
fig 34
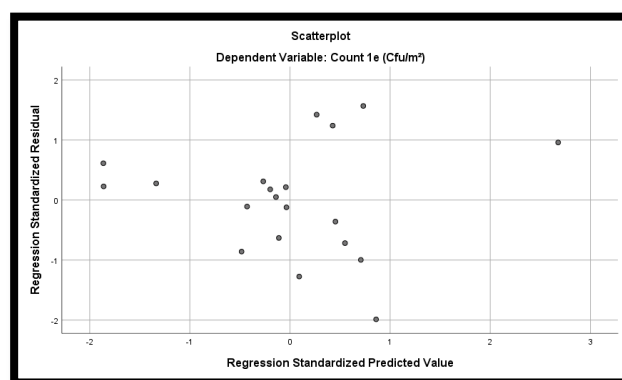
Fig 35

Day 3 Evening

Location	Temp 1f (°C)	Humidity 1f (%)	Gas 1f (ppm)	Count 1f (cfu)	Count 1f (Cfu/m²)
MBG	33	6	48	220	19298.24
CMB	32.5	9.1	56	136	11929.82
BT-3	32.6	9.3	87	85	8638.21
BT-1	32	8	54	92	9349.49
BT-Office	31	5.2	44	60	6097.56
Staffroom	33	9	83	206	18070.1
Datacentre	30	9.7	68	72	7317.07
Coffee Kuteera	34	10	56	421	36921.82
R & D	31	12.2	81	395	34649.12
Canteen	35	6.4	75	333	29210.52
Power electronics	32	17	66	35	4166.66
Environmental Lab	30	14	61	205	17982.45
Indoor	31.4	3.7	67	95	96454.47
Store room	32	6.2	91	173	15175.43
BEE	33	18	83	120	10520.31
EEE	30.7	16.2	78	69	7012.19

Relay lab	31.6	15.1	103	73	7418.69
Concrete Lab	33	14.7	78	240	21052.63
Chemical Room	32	7.8	110	130	11403.3
Parking	31.4	10.7	90	450	39473.68

table 6

Descriptive Statistics

	Mean	Std. Deviation	N
Count 1f (Cfu/m²)	20607.0880	20823.58285	20
Temp 1f (°C)	32.060	1.2588	20
Humidity 1f (%)	10.415	4.1977	20
Gas 1f (ppm)	73.950	17.8251	20

		Count 1f (Cfu/m²)	Temp 1f (°C)	Humidity 1f (%)
Pearson Correlation	Count 1f (Cfu/m²)	1.000	.064	-.397
	Temp 1f (°C)	.064	1.000	-.159
	Humidity 1f (%)	-.397	-.159	1.000
	Gas 1f (ppm)	-.063	.002	.258
Sig. (1-tailed)	Count 1f (Cfu/m²)	.	.394	.042
	Temp 1f (°C)	.394	.	.251
	Humidity 1f (%)	.042	.251	.
	Gas 1f (ppm)	.395	.497	.136
N	Count 1f (Cfu/m²)	20	20	20
	Temp 1f (°C)	20	20	20
	Humidity 1f (%)	20	20	20
	Gas 1f (ppm)	20	20	20

Fig 36

ANOVA[a]

Model		Sum of Squares	Df	Mean Square	F	Sig.
1	Regression	1312419635.935	3	437473211.978	1.011	.414[b]
	Residual	6926390815.951	16	432899425.997		
	Total	8238810451.887	19			

a. Dependent Variable: Count 1f (Cfu/m²)

b. Predictors: (Constant), Gas 1f (ppm), Temp 1f (°C), Humidity 1f (%)

Fig 37

Coefficients^a

Model		B	Std. Error	Beta	t	Sig.
		Unstandardized Coefficients		Standardized Coefficients		
1	(Constant)	38698.127	12624.8.239		.307	.763
	Temp 1f (°C)	-19.541	3844.861	-.001	-.005	.996
	Humidity 1f (%)	-2024.357	1193.502	-.408	-1.696	.109
	Gas 1f (ppm)	48.940	277.464	.042	.176	.862

One-Sample Statistics

	N	Mean	Std. Deviation	Std. Error Mean
Temp 1f (°C)	20	32.060	1.2588	.2815
Humidity 1f (%)	20	10.415	4.1977	.9386
Gas 1f (ppm)	20	73.950	17.8251	3.9858
Count 1f (Cfu/m²)	20	20607.0880	20823.58285	4656.29468

One-Sample Test Test Value = 0

	t	df	Sig. (2-tailed)	Mean Difference	95% Confidence Interval of the Difference Lower
Temp 1f (°C)	113.898	19	.000	32.0600	31.471
Humidity 1f (%)	11.096	19	.000	10.4150	8.450
Gas 1f (ppm)	18.553	19	.000	73.9500	65.608
Count 1f (Cfu/m²)	4.426	19	.000	20607.08800	10861.3512

Fig 38

Non parametric tests

		Temp 1f (°C)	Humidity 1f (%)	Gas 1f (ppm)
Temp 1f (°C)	Pearson Correlation	1	-.159	.002
	Sig. (2-tailed)		.502	.995
	N	20	20	20
Humidity 1f (%)	Pearson Correlation	-.159	1	.258
	Sig. (2-tailed)	.502		.272
	N	20	20	20
Gas 1f (ppm)	Pearson Correlation	.002	.258	1
	Sig. (2-tailed)	.995	.272	
	N	20	20	20
Count 1f (Cfu/m²)	Pearson Correlation	.064	-.397	-.063
	Sig. (2-tailed)	.789	.083	.790
	N	20	20	20

			Temp 1f (°C)	Humidity 1f (%)
Spearman's rho	Temp 1f (°C)	Correlation Coefficient	1.000	-.113
		Sig. (2-tailed)	.	.635
		N	20	20
	Humidity 1f (%)	Correlation Coefficient	-.113	1.000
		Sig. (2-tailed)	.635	.
		N	20	20
	Gas 1f (ppm)	Correlation Coefficient	.004	.261
		Sig. (2-tailed)	.986	.266
		N	20	20
	Count 1f (Cfu/m²)	Correlation Coefficient	.306	-.263
		Sig. (2-tailed)	.189	.262
		N	20	20

Fig 39
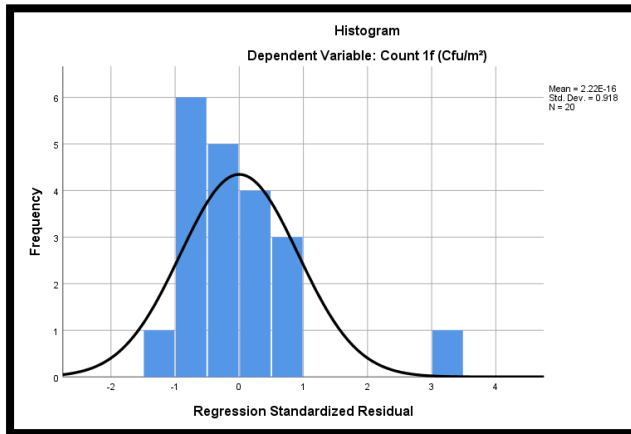
Fig 40
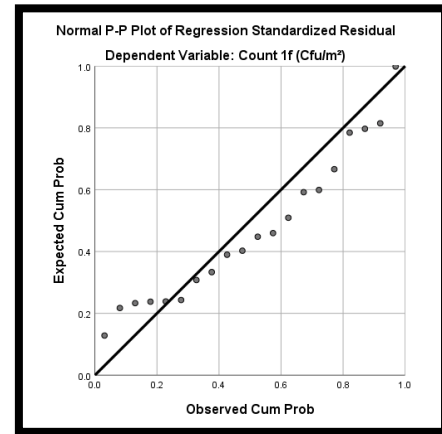
Fig 41
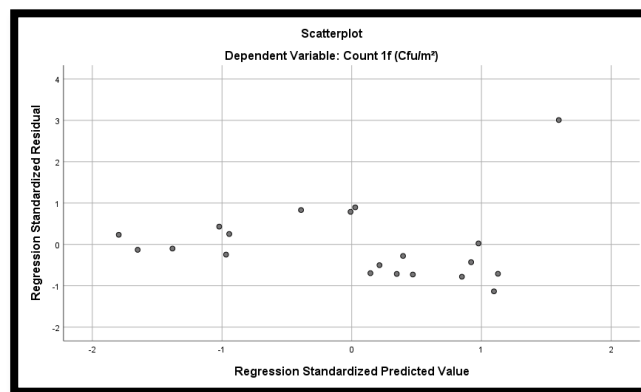
Fig 42

Table description :

A Pearson correlation is a number between -1 and 1 that indicates the extent to which two variables are linearly related.(fig 29,36)

The one-way analysis of variance (ANOVA) is used to determine whether there are any statistically significant differences between the means of three or more independent(unrelated) groups (fig 30,37)

When you perform a t-test, you're usually trying to find evidence of a significant difference between population means (2-sample t) or between the population mean and a hypothesized value (1-sample The t-value measures the size of the difference relative to the variation in your sample data.(fig31, 38)

Spearman's Rho is a non-parametric test used to measure the strength of association between two variables (fig32, 39)

CHAPTER 6
CONCLUSION

Comparing our results with the set standards of IEQ parameters we find a wide range of fluctuations depending on the location based on its occupied or unoccupied state.

Though there are changes compared to one another, these changes when they vary on a large scale we find a greater health risk.

The standards are set for each parameters and their range define its state of health.

From this analysis we found that the p value (sig value in SPSS software) for each of the parameter is greater than 1.

Considering the data we come to a conclusion of Rejecting the Null hypothesis, hence declaring :

"There Is Significant Difference In Microbial Count With Change In Time, External Parameters And Its State Of Occupancy."

Table description :

The one-way analysis of variance (ANOVA) is used to determine whether there are any statistically significant differences between the means of three or more independent(unrelated) groups

When you perform a t-test, you're usually trying to find evidence of a significant difference between population means (2-sample t) or between the population mean and a hypothesized value (1-sample The t-value measures the size of the difference relative to the variation in your sample data.

A Pearson correlation is a number between -1 and 1 that indicates the extent to which two variables are linearly related.

Spearman's Rho is a non-parametric test used to measure the strength of association between two variables

CHAPTER 7
FUTURE SCOPE

7.1. TROUBLE SHOOTS :

1. The electrodes used caused heating effect on the long run, damaging the circuit.
2. The liquid used leaked outside causing shorting of the device.
3. All the device had to be on common voltage ground of 5V, hence either more or lesser voltage demanded components couldn't be connected easily.
4. Since interconnected, one device malfunctioning caused dropping of the other components too.
5. Since intensity is measured, complete blackout had to be maintained. Else it gave false positive results from the external source of light.

7.2 FUTURE SCOPE :

1. The detection can be based on even simpler method, which would not need pumps to add on to the total weight.
2. The detector could be further modified for direct method of microbial detection, instead of using intensity which is an indirect method of estimation.
3. A battery mode of power source can be developed for enhancing its portability.

CHAPTER 8
REFERENCES

1. A Microcantilever-Based Pathogen Detector SCANNING VOL. 25, 297–299 (2003) Demir Akin, Amit Gupta, Rashid Bashir

2. Detection of bacterial cells and antibodies using surface micromachined thin silicon cantilever resonators, J. Vac. Sci. Technol. B 22(6), Nov/Dec 2004

3. This device uses a laser to rapidly detect bacteria, Posted on April 4, 2017 by Microbiology Society

4. Air Samplers for Microbiological Monitoring of Air Quality, Cherwell Laboratories' SAS Microbial Air Sampler Range

5. AIRFLOW INSTRUMENTS & SENSORS Kanomax USA Babichenko S1 , Gala JL2 *, Bentahir M2 , Piette AS2 , Poryvkina L1 , Rebane O1 , Smits B2 , Sobolev I1 and Soboleva N1

6. Non-Contact, Real-Time Laser-Induced Fluorescence Detection and Monitoring of Microbial Contaminants on Solid Surfaces Before, During and After Decontamination Volume 9 • Issue 2 • 1000255 Babichenko et al., J Biosens Bioelectron 2018, J.P. Robinson, B.P. Rajwa, E. Bae, V. Patsekin, A.M. Roumani, A.K. Bhunia, J.E. Dietz, V.J. Davisson, M.M. Dundar, J. Thomas and E.D. Hirleman

7. Using Scattering to Identify Bacterial Pathogens, Carlo Tiebe & Hans Miessner & Bernhard Koch & Thomas Hübert

8. Detection of microbial volatile organic compounds (MVOCs) by ion-mobility spectrometry, Anal Bioanal Chem (2009) 395:2313–2323 DOI 10.1007/s00216-009-3147-4

9. Dr. Ch. Lalitha *Study of indoor air microflora in visakhapatnam city*World journal of pharmacy and pharmaceutical science Volume 7, Issue 4, 20 Feb. 2018,

10. Health impacts of air pollution. (n.d.). Retrieved from https://www.edf.org/health/health-impacts-air-pollution

11. Tian, X., Syvitski, R. T., Liu, T., Livingstone, N., Jakeman, D. L., & Li, Y. (2009). A Method for Structure–Activity Analysis of Quorum-Sensing Signaling Peptides from Naturally Transformable Streptococci. *Biological Procedures Online,11*(1), 207-226. doi:10.1007/s12575-009-9009-9

12. Verbeke, F., Craemer, S. D., Debunne, N., Janssens, Y., Wynendaele, E., Wiele, C. V., & Spiegeleer, B. D. (2017). Peptides as Quorum Sensing Molecules: Measurement Techniques and Obtained Levels In vitro and In vivo. *Frontiers inNeuroscience,11*. doi:10.3389/fnins.2017.00183

13. Craney, A., Hohenauer, T., Xu, Y., Navani, N. K., Li, Y., & Nodwell, J. (2007). A synthetic luxCDABE gene cluster optimized for expression in high-GCbacteria. *Nucleic Acids Research,35*(6). doi:10.1093/nar/gkm086

14. Gram-Positive Bacteria. (n.d.). *SpringerReference* doi:10.1007/springerreference_222936

15. Ibacache-Quiroga, C., Romo, N., Díaz-Viciedo, R., & Dinamarca, M. A. (2018). Detection and Control of Indoor Airborne Pathogenic Bacteria by Biosensors Based on Quorum Sensing Chemical Language: Bio-Tools, Connectivity Apps andIntelligent Buildings. *Biosensing Technologies for the Detection of Pathogens - A Prospective Way for Rapid Analysis*. doi:10.5772/intechopen.72390

16. Park, J., Park, C. W., Lee, S. H., & Hwang, J. (2015). Fast Monitoring of Indoor Bioaerosol Concentrations with ATP Bioluminescence Assay Using an Electrostatic Rod-Type Sampler. *Plos One, 10*(5). doi:10.1371/journal.pone.0125251

17. Park, J., Kim, H. R., & Hwang, J. (2016). Continuous and real-time bioaerosol monitoring by combined aerosol-to-hydrosol sampling and ATP bioluminescence assay. *Analytica Chimica Acta,941*, 101-107. doi:10.1016/j.aca.2016.08.039

18. https://www.downtoearth.org.in/news/science-technology/this-biosensor-attached-to-your-phone-can-sniff-bacteria-62657

VISVESVARAYA TECHNOLOGICAL UNIVERSITY

"JnanaSangama" Belgaum 590 018, Karnataka, India

A Report on
Major Project (16BT8DCPRW)
Titled
"*In Vitro* and *In Silico* Analysis of *Bacopa monnieri* and its effect on mammalian cell "

Submitted in the partial fulfilment of the academic requirements for the award of

Bachelor of Engineering in Biotechnology

Submitted by:

NOOR-UL-AIN-FATIMA (1BM15BT024)
VEENA PRASAD (1BM15BT038)

Students of VIII Semester, Biotechnology

Under the Able Guidance of:
Dr. SAVITHRI BHAT

Associate Professor,

Department of Biotechnology,
B.M.S. College of Engineering,
Bengaluru-560019

B.M.S. College of Engineering
DEPARTMENT OF BIOTECHNOLOGY
Bull Temple Road, Bengaluru - 560019, Karnataka, India.
(June 2019)
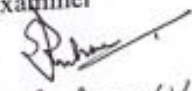
BMS College of Engineering, Bull Temple Road, Bangalore 560019

BONAFIDE CERTIFICATE FOR STUDENT BATCH

This is to certify that the project report titled, "*In Vitro* and *In Silico* Analysis of *Bacopamonnieri* and its effect on mammalian cell." is a bonafide record of the project work done by Noor-Ul-Ain-Fatima with USN 1BM15BT024, Veena Prasad with USN 1BM15BT038 during the academic year 2018- 2019.

Head of the Department	Guide:
Signature:	Signature:
Name: Dr.DivijendraNatha Reddy	Name: Dr. Savithribhat
Seal: HOD-Biotechnology BMS College of Engineering Bangalore-560 019	Designation: Associate Professor
Date: 7/6/19	Date: 6th June 2019

Submitted for the University Examination held on ...7th June, 2019

Internal Examiner	External Examiner
Signature:	Signature:
Name: Dr. Chandraprakash	Name: Dr Reshma SV
Designation:	College/ Designation: PESU
Date: 7/6/19	Date: 7.6.2019

ACKNOWLEDGEMENT

ABSTRACT

Bacopa monnieri (Brahmi) known for enhancing memory and cognition has been used extensively in Indian traditional medicine, Ayurveda for the same. *In vitro* regeneration and optimisation of culture media using Benzylaminopurine and Indole Acetic Acid has been done. Extraction of the various *in vitro* samples (and callus) and field plant was carried out and analysed. The phytocompounds which give the plant its inherent properties were confirmed and antioxidant assays were conducted. Total phenolic content was calculated to be 39.6 mg GAE/g and scavenging activity to be 30-45%. Chromatographic analysis was carried out for the samples. Bacoside A was confirmed using the standard for the compound and HPLC results showed 0.4 – 0.72 mg/ml concentations of Bacoside A in the different extracts. Cytotoxicty properties were tested on SH-SY5Y cells by carrying out MTT Assay with the extracts present. It showed that In the present study, the potential of *Bacopa Monnieri* compounds, to be used as a possible treatment for Alzheimer's has been explored by docking the saponins (31) found in *Bacopa monnieri* with four targets perceived to play an important role in the disease which are beta-secretase (BACE), glycogen synthase kinase-3-beta (GSK3B), acetylcholinesterase (AChE) and amyloid beta, and 2VMK, 1J1B, 4EY7, and 1IYT were the respective PDB IDs. Docking studies using Discovery Studio – CDOCKERand LeadIT and molecular simulation studies using Desmond were performed. The results showed that Bacopaside B, docked the best, followed by Ebelin Lactone. CDOCKER binding energy for BACE, GSK3B, AChE and amyloid beta with Bacopaside B were -69.523, -43.9368, -39.881, and -2.2469 respectively. The binding energy of Ebelin Lactone with the BACE, GSK3B, and AChE were -9.5071, -43.1441 and -62.1722. Compounds extracted from *Bacopa monnieri* can potentially act as a herbal alternative, with less side effects, to the commercial available drugs today.

TABLE OF CONTENTS

LIST OF TABLES

LIST OF FIGURES

1. Introduction

Neurological disorders are some of the hardest diseases to live with and toughest to treat. Neurological disorders are those that affect either the CNS (central nervous system) or the PNS (Peripheral nervous system). They affect the brain, spinal cord, cranial nerves, peripheral nerves, nerve roots, autonomic nervous system, neuromuscular junction, and muscles. (WHO, 2016) According to a report by WHO (World Health Organization), 1 billion people are affected by neurological disorders including Alzheimer's Disease (AD), brain injuries, multiple sclerosis and Parkinson's (WHO 2006, 2007) and an estimated number of 6.8 million people die due to these disorders. 36 million people are affected by Alzheimer's (NIH, 2018) while another 4 million are affected by Parkinson's (Genetics Home Reference, NIH, 2019).

The onset of Alzheimer's Disease and Parkinson's is usually seen in people over the age of 60 (NIH, 2018, National Institute on Aging, NIH, 2017). AD is the most common type of dementia known today. "Dementia is a clinical syndrome that involves progressive deterioration of intellectual function. Various cognitive abilities can be impaired with dementia, including memory, language, reasoning, decision making, visuospatial function, attention, and orientation." (Igor O. Korolev, 2014). AD is mainly caused by the plaque deposits of amyloid beta (Aβ) between nerve cells and neurofibrillary tangles (NFT) of aggregated tau proteins inside the neuronal cells. (NIH, 2018)

For diagnosis patients should undergo cognitive screening every 6–12 months and doctors should look out for signs of functional decline that indicate the onset of Alzheimer's disease and other dementias. There is no cure for the disease known to us and there are no FDA-approved therapies for alzheimer's. There are however FDA approved drugs inhibiting acetylcholinesterase (AChE). Treatment of with an AChE inhibitor has some impact but is has the risks of side effects such as gastrointestinal (GI) symptoms, dizziness, and headache. The drugs only slow down the symptoms of the disease and do not stop or cure it. The drugs used are *donepezil, rivastigmine, galantamine* and *memantine* (Neugroschl, J. et al, 2011, Igor O. Korolev, 2014).

The commercially available drugs have many side effects, and do not cure the disease as well. Medicines extracts from herbs and plants may help to find a cure for the disease or at least to arrest the symptoms and stop the disease for becoming worse. India is rich in tradition knowledge and Aruyveda is a practice that uses the herbs that are rich in medicinal

properties in the treatments administered. There are certain plants that have been named as "Rasayana" and the medicines derived from these plants are rich in antioxidants and are immunomodulatory agents. Some plants that have been classified as "Rasayana" are ashwagandha (*Withania somnifera*), brahmi (*Bacopa Monnieri*) , mandukaparni (*Centella asiatica*), shankapushpi (*Convolvulus pluricaulis*), jatamansi (*Nardostachys jatamansi*) and jyotishmati (*Celastrus paniculatus*). These are also called as "Medhya Rasayanas," implying that these are specific to brain tissues and classed as brain tonics or rejuvenators. (Kaur N et al, 2017, Susmitha Sahoo, 2017)

Bacopa Monnieri is one of these plants that is said to have many medicinal properties and said to be a neural tonic. There are studies that have proved that it helps fight against neurodegenerative diseases including Alzheimer's disease. (Susmitha Sahoo, 2017).

In the present study, the focus is *Bacopa monnieri*. Extraction of effective compound will be done from field grown plants and tissue cultured, to analyse and test the obtained extracts on mammalian cells.

2. Review of Literature

2.1 Neurological Disorder

Alzheimer's disease causing genes have not yet been found today, but the presense of apolipoprotein E (APOE) gene on chromosome 19—increases a person's risk getting the disease (NIH, 2017). The main pathways by which Alzheimer's is caused is by deposition of plaque, which is amyloid β (Aβ) peptides and by formation of neurofibrillary tangles, which mainly involves misfolding and tangling of tau protein, as well as an increase in acetylcholinesterase, causing the breakdown

on acetylcholine. The formation of NFT has directed been correlated with cognitive decline, while the formation of plaque correlation reaches a plateau, which implies that NFT formation may be one of the main reasons for the continual decline seen in patients. (Lee et al, 2011).

A lot of research has been done in the recent past of how various plant extracts can help cure the disease. This has become one of important paths for finding a cure for AD, since the drugs we have today do not help cure the disease completely and leave the patient with a number of side effects. Plant extracts from *Murraya koenigii* (Curry leaf), *Daucus carota* extract (carrot), *Moringa oleifera* (Drumstick tree), *Ginkgo Biloba* (Ginkgo/Maidenhair tree), *Cassia obtisufolia* (Sicklepod), *Desmodium gangeticum* (Sal Leaved Desmodium), *Melissa officinalis*(Lemon Balm), and *Salvia officinalis* (Garden sage, common sage) which all work with various mechanisms to help cure the disease. (M Obulesu et al, 2011, Prasan R Bhandari, 2013.)

2.2 About *Bacopa Monnieri*

The plant has been used as a nootropic and to improve learning, memory. It is from the family S*crophulariaceae* and is a small plant with a number of branches, small oblong leaves. Small purples or white flowers can been seen. It is found throughout the Indian subcontinent, mostly in wetlands and in Australia, Nepal, China, Sri Lanka, parts of USA and Africa. It is also known as water hyssop, brahmi, *Bacopa monniera*, and *Herpestis monniera*. (Aguiar, S. et al, 2013, Kashmira J. Gohil et al, 2010

Bacopa Monnieri is a succulent herb, having various medicinal properties, belonging to the following classification:

Kingdom Plantae – Plants

Subkingdom Tracheobionta – Vascular plants Super division Spermatophyta – Seed plants Division Magnoliophyta – Flowering plants Class Magnoliopsida – Dicotyledons Subclass Asteridae

Order Scrophulariales

Family Scrophulariaceae – Figwort family Genus *Bacopa*

Species *monnieri* (L.)

2.3 *In Vitro* Regeneration in *Bacopa Monnieri* (Plant Tissue Culture)

As it has various neurological properties, it can be utilized to derive drugs using the compounds found in the plant. For abundance of plant material and high concentration of the required compounds in the plants and conservation of germplasm, *in vitro* regeneration can be done. This will help in extraction of large quantities of the compounds from the plant which can be grown in abundance as the plant itself is very small in nature. The plant slowly being lost from their natural habitats due to indiscriminate collection for pharmaceutical demands and *in vitro* regeneration will help tackle this problem. (Richa Jain et al, 2013)

S.No.	Explant	PGR Combination	Result	Reference
1.	Node	BAP+NAA	Shooting	Richa Jain et al, 2013
2.	Leaf and node	IAA +BAP	Shooting	Rahul Keshav, et al, 2018
3.	Node	IAA+BAP	Shooting	Chandra Gurnani et al, 2012
4.	Apical buds and nodes	IAA+BAP	Shooting	Shub Sonia Kapil, et al, 2014

Table 2.1 *In vitro* regeneration – PGR combinations

2.3.1 **Extraction and Phytochemical Analysis**

Extraction of the required compounds done is methanol has been proved to be more the most effective and has yielded the best results so far. (Watoo Phrompittayarat *et al,* 2007, Shahare M. D *et al,* 2010).

Sonication of the extract has been done to ensure the breakage of cells, and to obtain the required compounds. Research done by H. V. Annegowd et al, 2010 states that extraction done by sonication for 30 min in methanol produced the prominent results for the extraction, phenolic, flavonoid, and antioxidants measurements. Rency Elizabeth Thomas, et al, 2015, have also used sonication for extraction and have reported good results.

Bacopa monnieri is said to have a number of phytocompounds present, which give the plant some of its important medicinal properties and properties that are important for compounds to be employed in drugs. Some of those are antimicrobial, antihelmentic and antidiarrhoeal to name a few. (Tiwari *et al*, 2011, Moghadasian MH *et al*, 2000, Pushpendra Kumar Jain *et al*, 2016) Confirmations of these compounds were done using the following tests.

Phytochemical	Confirmatory Test	Outcome
Saponin	20 ml of water added to extract, shaken for 10 min. Foam formation confirms the presence.	Confirmed the presence
Flavonoids	Extracts were treated with drops of lead acetate solution, formation of yellow color precipitate indicates the presence	Confirmed the presence
Alkaloids	Extract was treated with dilute HCl and then with Mayer's reagent. Formation of yellow coloured precipitate confirms presence	Confirmed the presence
Tannins	Extract was treated with 1% gelatin solution with NaCl, formation of white precipitate indicates tannins	Confirmed the presence
Steroids	1ml of extract was treated with 10ml of chloroform and then with 10ml concentrated sulphuric acid. Formation of red colour indicates the presence	Confirmed the presence
Phytosterols	Extract treated with chloroform and with concentrated sulphuric acid, shaken and allowed to stand. Golden yellow colour confirms presence	Confirmed the presence

Anthraquinone	Extract was boiled with sulphuric acid and then chloroform was added. Yellow/brown precipitate confirms the presence.	Confirmed the absence

Table 2.2 – Phytochemical Tests

Paras Jain *et al*, 2017, Rahul Gupta *et al*., 2016, Ghafar *et al*, 2009 reported the above results for the presence of phytochemical compounds.

2.3.2 Antioxidant properties - Total Phenolic Content and DPPH Assay

The plant is said to have antioxidant properties which help the cells fight against oxidative damage and act against free radicals. Most of this antioxidant property has been proved to arise from phenolic compounds present in the plant. (T Anand *et al*, 2011, Sharan Suresh Volluri *et al* 2011) The total phenolic content can be checking using Folin-Ciocalteu method and comparing the optical density measure with gallic acid standard curve, as described by Singleton and Rossi, 1965 originally. (Suman Chandra *et al*, 2014)

Anti-oxidation property quantification is also done using DPPH method where the scavenging activity of the extract is determined. The antioxidant extracts donate their hydrogen atoms to free radicals to make them to form non-radical species There have been various studies to show that *Bacopa monnieri* has properties that help reduce oxidative stress in brains. (Tamara Simpson *et al,* 2015)

2.3.3 Chromatographic analysis

The chromatographic analysis that have been done for the plant are TLC (thin layer chromatography), HPTCL (High performance thin layer chromatography) and HPLC (High performance liquid chromatography) for various compounds present in the plant. HPLC for twelve saponins has been performed (Murthy PB et al 2006) while some have done it only for Bacoside A (Watoo Phrompittayarat et al 2017; Manoharan Mohana et al 2016). Various TLC solvent systems have been used to separate the compounds of *Bacopa monnieri* which show promising results (Kumar, R., et al 2015; Mehta Sonam et al, 2017).

There have been numerous papers which have done the analysis for field plant like in while others have done it for in vitro regenerated plants like Bożena Muszyńska et al, 2016. Field

acclimatized plant and *in vitro* regenerated plants have also been compared (Pragya Bhardwaj1 et al, 2017). Methanolic extraction was done in most of the papers referred to, and is proved to like the best result among all the papers referred to until now and elution, while done in various mobile phases, was usually detected at 205 nm for HPLC.

2.3.4 MTT assay

MTT assay has previously been carried out for different extract solvents such as ethanol, methanol acetone, hexane. These extracts have been exposed to different cell lines such as HT-29 colon cancer, (Vinut.S. Nandagaon et al, 2013), MCF-7 and MDA-MB 231 cell line (Md. Nasar Mallick et al, 2013), and Human Cancer Cell lines, namely, Colon (HT29, Colo320, and Caco2), Lung (A549), Cervix (HeLa, SiHa), and Breast (MCF-7, MDAMB-231) (Md. Nasar Mallick et al 2017) to name a few.

2.4. In-Silico
2.4.1 Targets:

1. BACE1

A**β** Plaque formation is one of the primary causes of Alzheimer's Disease. Amyloid Plaques are generated by the cleavage of Amyloid Precursor Protein (APP). One of the key enzymes involved in this cleavage is the **β** Secretase enzyme. Inhibiting this enzyme would prevent the breakdown of APP, hence preventing the Amyloid plaque formation. (Vassar, R, 2004).

The present study focuses on the potential of the *Bacopa monnieri* compounds to interact and inhibit the targets responsible for Alzheimer's, BACE1 being one of them, using *In Silico* research. (Kumar A. *et al*, 2015)

2. GSK3-**β**

One of the two main reasons for the pathogenesis of Alzheimer's is the formation of Neurofibrillary tangles (NFT), which is the result of hyperphosphorylation of the TAU protein. Glycogen Synthase **β** is one of the key enzymes involved in the hyperphosphorylation of TAU which makes it a potential target for the treatment of Alzheimer's disease.

The current research has explored the potential of the compounds present in *Bacopa monnieri to* inhibit the activity of GSK3-**β** using *In Silico* Approach. (D. Sivaraman et al, 2015)

3. AcheE

An increased activity of Acetylcholinesterase is seen in Alzheimer's patients. This results in the breakdown of acetylcholine resulting in the various symptoms and pathogenicity of the disease. One of the targets, thus chosen, is acetylcholinesterase to reduce the amount of acetylcholine broken down in the patients. (García-Ayllón et al, 2015) The mechanism of prevention of AChE from acting is for the proposed drugs to bind to the protein and prevent the protein from acting on acetylcholine.

Previous *In Silico* work has been done involving docking of AChE with *Bacopa monnieri* compounds to check the effect of a few of the compounds. The PDB ID chosen, 4EY7, was obtained from that paper (Ramasamy, S. et al, 2015). The preparation of protein protocol was obtained from the same paper.

4. 1IYT

The beta amyloid plaque that is formed outside the neural cells, are insoluble in nature. These plaques found in Alzheimer's patients aggregate and cause pathogenicity of the disease. The method of action of the proposed ligands would be to bind the the amyloid fibrils and prevent the aggregation of the plaque. This may help reduce the symptoms of the patient.

The paper referred to have performed docking with different phytocompounds from different plants to check the effect on the fibril. The PDB ID chosen (1IYT) and method of preparation of the compound were obtained from the same paper. (Shruthila, N. *et al*, 2013)

2.4.2 Ligands Chosen:

Ligands chosen for docking were taken from various papers, which had reports saponins in *Bacopa monnieri* along with their structures.

Saponins - targets	Reference

Bacopaside IX,X,XI	Zhou, Y. et al, 2009
1. Bacopaside XI and XII	Bhandari P. et al, 2009
1. Bacopaside III, Bacopasaponin G, and Bacopasides A, B, and C	Hou, C.-C., et al, 2002
1. Bacoside A3, Bacopaside II, Bacopasaponin C, Bacopaside N2, Bacopaside N1, Bacopaside III bacopaside IV, Bacopasaponin G, Bacopasaponin A, Bacopasaponin B, Bacopasaponin D	Majumdar S. et al, 2013
1. Bacosides A(3), Bacopaside II, Bacopaside I, Bacopaside X , Bacopasaponin C , Bacopaside N2 Bacopasaponin F , Bacopaside N1, Bacopaside III , Bacopaside IV and Bacopaside V	Murthy PBS et al, 2006
1. Ebelin Lactone, Bacogenin A1	Ramasamy, S. et al, 2015

Table 2.3 – Ligands

2.4.3 Selection of Standard Drugs

Drug	Phase	Function
JNJ-54861911	I/II	BACE inhibitor
E2609	I/II	BACE inhibitor, Anti-amyloid
Donepezil	FDA approved	AChE inhibitor
Rivastigmine	FDA approved	AChE inhibitor
Nilotinib	I/II	Tyrosine kinase inhibitor (anti-tau), anti-amyloid
Anavex 2-73	I/II	GSK3B inhibitor (anti-tau)

Table 2.4 – Standard drugs chosen

(Cummings, J. et al, 2018, McGleenon BM et al, 1999)

3.Materials and Methodology

Materials

- *Bacopa monnieri* plant
- MS media, Plant Growth Regulators (Indole acetic acid, benzyl amino purine), calcium carbonate
- Chemicals for phytochemical tests – hydrochloric acid, sulfuric acid, lead acetate, Mayer's reagent, gelatin, sodium chloride
- Chemicals for antioxidant tests - total phenolic content – gallic acid, sodium carbonate, FC reagent, DPPH, Ascorbic Acid, methanol

Glassware - test tubes, tissue culture bottles, petri plates

Animal Cell Culture:

Trypsinized cell suspension, Trypan blue, Haemocytometer with coverslip, Inverted microscope, Pipette, Tips

MTT Assay

SH-SY5Y cells, MTT, PBS (Phosphor Buffer Saline), DMSO, Microtitre plate (96 wells), CO_2 incubator

Methodology

3.1 *In vitro* regeneration

3.1.1: Collection of Plant material

Bacopa monnieri to be procured from University of Agricultural Sciences, Bangalore and identified by authorized personnel.

3.1.2: Media for micropropagation & organogenesis

MS Media Preparation and Sterilization

Weigh the required amount of Media powder (42.08g/L) and dissolve it by heating and add CaCl2 to the media. Next, add the plant growth hormones as decided (IAA (Indole Acetic Acid) and 6-BAP (6 Benzylamino purine) in various concentrations. Pour media into test

tubes and autoclave at 121 °C for 15 minutes at 15 psi. After autoclaving pour media into the petri plates inside the LAF.

3.1.3: Sterilization & inoculation of leaf and nodal explants

Surface sterilization

A twig of *Bacopa monnieri* collected and washed with tween -20. Follow with several washes of tap water until the tween -20 clears off from the twig.

Explant preparation

Incubate the twigs in 0.1% HgCl2 for 3-4 min followed by several washes with sterile water and remove the leaves separately for the inoculation and separate the internode from the nodes

Apical bud and nodes with meristematic regions ready for inoculation.

Explant inoculation

Cut the edges of the leaves and inoculate in the petri plate comprising MS media with PGR and

inoculate the nodes and apical bud in the slats having MS media with PGR.

3.1.4: Optimization of PGR & culture conditions

Varied concentration of the plant growth hormones were added to optimize the conditions
IAA - Indole Acetic Acid, BAP- 6 Benzylaminopurine

	Concentration of IAA (mg/L)	Concentration of BAP (mg/L)
A	0	0
B	0.01	0
C	0.01	2
D	0.01	5

E	0.01	10

Table 3.1 – Plant growth hormone concentrations

(Richa Jain et al, 2013)

3.2: Extract preparation and analysis

3.2.1 Extraction

Leaves and stem should be for 48 hours and powdered and 10 ml of methanol to be added to 0.2 g of powder obtained and sonicate for 30 min, maintain at 35 ℃ with an ice pack. The extract is to be decanted and then centrifuged at 5000 rmp for 10 minutes, twice. (Watoo Phrompittayarat et al, 2007)

Phytochemical Analysis

The phytohemical tests to be performed with the extract.

1. Saponin - 20 ml of water added to extract, shaken for 10 min. Foam formation confirms the presence.
2. Flavonoids - Extracts to be treated with drops of lead acetate solution, formation of yellow color precipitate indicates the presence
3. Alkaloids - Extract to be treated with dilute HCl and then with Mayer's reagent. Formation of yellow coloured precipitate confirms presence
4. Tannins - Extract to be treated with 1% gelatin solution with NaCl, formation of white precipitate indicates tannins
5. Steroids - 1 ml of extract to be treated with 10 ml of chloroform and then with 10 ml concentrated sulphuric acid. Formation of red colour indicates the presence
6. Phytosterols- Extract treated to be chloroform and with concentrated sulphuric acid, shake and allowed to stand. Golden yellow colour confirms presence
7. Anthraquinone-Extract to be boiled with sulphuric acid and then chloroform to be added. Yellow/brown precipitate confirms the presence.

(Rahul Gupta et al., 2016, Kh. Lemino Singh et al 2013)

3.2.2: Antioxidant analysis

Total Phenolic Content

To measure the total phenolic content of the extract, the optical density must be measured using Gallic acid as the standard phenolic compound.

Gallic Acid Standard Curve was prepared (to be done with triplicates):
Gallic Acid solution of 50,100,150,200, 250 μg/ml - was prepared from stock (1 mg/ml) and add 5 ml of Folin Ciocalteau (FC reagent) (1:10 v/v) to all test tubes. After 2 minutes, add 4 ml of Sodium Carbonate to all test tubes. Leave in the dark for 30 minutes. Check Optical Density at 765 nm. To check the phenolic content in extracts only Folin Ciocalteau reagent and Sodium Carbonate is to be added, and Optical Density to be measured. Increased absorbance of the reaction mixture indicates increased reducing power. . (Suman Chandra et al, 2014)

DPPH Assay

DPPH is to be prepared by adding 0.0118g of DPPH in 10mL of methanol. Take varying concentrations of Ascorbic Acid (0.2 -1 mg/ml), 50 ul of each concentration or add the same volume of sample. The volume is to be made upto 150 μl by using 100 μl methanol. This is followed by the addition of 150μl DPPH and 1 ml methanol. The mixture is to be incubated at room temperature for 15 minutes. The OD is taken in UV Spectrophotometer at 517 nm.

The % Scavenging Activity can be calculated by using the formula:

% Scavenging Activity = Absorbance of Control – Absorbance of Test Sample   * 100
                                                    Absorbance of Control

3.2.3 Chromatographic Analysis

High Performance Liquid Chromatography

Reverse phase HPLC (Shimadzu, Japan) was performed with C18 column. The mobile phase used was acetonitrile:water (67:33). PDA detector was used at a wavelength of 190 to 300 nm and results were extracted at 205 nm. The flow rate was 1.6 ml/min with a run time of 20 minutes, performed at room temperature.

Standard was dissolved in methanol and the plant extracts in methanol were taken and calibration of the standard was done from 0.2 mg/ml to 1 mg/ml. 30 μl of the samples were injected into HPLC (Manoharan Mohana et al 2016)

Thin Layer Chromatography:

Spot 5 µl of extract/ standard on the plates, and allow it to dry. Prepare solvent system and let it acclimatize. Place plate in solvent system and allow it to elute. Observe under UV light. Detect compounds using Iodine vapours in an airtight chamber and by exposing the plates to caffeic acid.

Optimization of the TLC plates were previous done and the best solvent system now chosen for further analysis.

TLC (thin layer chromatography) solvent system was optimized by checking 5 different solvent systems namely

- toluene: ethyl acetate: methanol: formic acid (3:3.5:2.5:1) (Kumar et a*l*, 2015)
- chloroform: methanol (9:1) paper 2 (Mehta Sonam et al, 2017)
- n butanol: acetic acid: water (12: 1: 1) (Jiang Z et al, 2016)
- dichloromethane : methanol: water (4.5:1:1) (Jiang Z et al, 2016)
- toluene: ethyl acetate: methanol: glacial acetic acid (3:4:3:1) (Shinde et al, 2011)
- ethyl acetate : methanol : water (7:3:1)

3.2.4 MTT assay protocol
Animal Cell Culture:

Filter sterilization: medium required for cells to grow should be filter sterilized, the components are filter sterilized by passing the solution through a membrane filter of pore size 0.22µ. The membrane filter is held in a suitable assembly, the assembly together with filter is sterilized by autoclaving before use. Laminar flow cabinets are used to create aseptic conditions by blowing filter sterilized air through HEPA (high efficiency particulate air) filters.

Wiping with 70% ethanol: The surfaces that cannot be sterilized by other techniques for instance platform of laminar hood, hands are sterilized by wiping them thoroughly with 70% alcohol. All the materials used for culturing should be surface sterilized.

1. Preparation of cell growth medium
   Checking which culture media and culture supplements the cell line requires before starting cultures is common. Culture media and supplements should always be sterile. FBS (Fetal Bovine Serum) was added at 10% and antibiotics as required. Media was prepared as per the protocol. Sterile supplements was added as required and then dispensed into sterile containers

2. Checking cells

The morphology or cell shape was checked as regular intervals Attached cells were mainly attached to the bottom of the flask, round and plump or elongated in shape.Media was pink-orangish or pale pink in colour depending on the media used. Distinct changes to the medium such as turbidity, presence of particles visible in suspension and a rapid decline in pH (yellow colour, indicating acidity) are all indicators of bacterial contamination.

3. Sub-culturing and Splitting

Cells were regularly sub cultured and split as need for propagating or performing experiments. The cells were observed under the microscope. Flask was placed in incubator – 37°C, 5% CO2. Place the flask upright and remove the spent media from flask, add trypsin give three washes so that the cells dissociate from the substratum, if necessary, incubate the flask at 37°C for 1 or 2 minutes. When the dissociation is complete add 5ml of complete media to inhibit tryptic activity which may damage the cells. Disperse the cells as per the requirement.

4. Changing media

If cells have been growing well for a few days but were not yet confluent then they will require media changing to replenish nutrients and keep correct pH. The media colour and cell state were observed and the media was changed accordingly.

Estimation of viability and enumeration of cells

The cell suspension was mixed thoroughly with pipette, 50μl of the suspension was transferred in eppendorf tube and 250μl of trypan blue (1:5 dilution) was added, mixed properly. Haemocytometer was cleaned gently on the surface with 70% ethanol, coverslip was placed. Using a pipette 10μl was added. The slide was placed on the microscope , using 10X objective ,total number of cells were counted. Stained cells are considered as dead cells and unstained cells are considered as viable cells.

Estimation of viable cells can be done by using following formula:

Percentage of viable cells= No: of viable cells/ total no: of cells X 100

Calculation of concentration of cells per ml is as follows:

Each quadrant had - 40,35,45,39 viable cells

Dilution factor is $2*10^4$

Total no: of viable cells/ml = (total viable cell count/4) (dilution factor)

Total no: of viable cells = 159

Total no: of viable cells/ml = $(159/4)*(2*10^4/ml)$

$= 80*10^4$/ml

Total no: of viable cells/ml $= 8*10^5$/ml

Estimation of proliferation of cells

Preparation of test solutions

For cytotoxicity studies, each methanolic extract of different concentrations were taken and mixed to obtain the desired concentration and dissolved in distilled DMSO and volume was made up with DMEM supplemented with 2 % inactivated FBS to obtain a stock solution of 1 mg/ml concentration and sterilized by filtration. Serial two fold dilutions (0-320μg/ml) were prepared from this for carrying out cytotoxic studies.

Reagent Preparation

- MTT stock solution: Put 5mg/10 ml MTT in PBS.
- MTT working solution: 1:10 dilution of stock in PBS.

SHSY5Y cell line was procured from Skanda Life Sciences, stock cells was cultured in DMEM medium supplemented with 10% inactivated Foetal Bovine Serum (FBS), penicillin (100 IU/ml), streptomycin (100 μg/ml) in an humidified atmosphere of 5% CO_2 at 37°C until confluent. The cell was dissociated with TPVG solution (0.2 % trypsin, 0.02 % EDTA, 0.05 % glucose in PBS).

The viability of the cells are checked and centrifuged. Further, cells were seeded in a 96 well plate and incubated for 24 hrs at 37°C, 5 % CO_2 incubator. The monolayer cell culture was trypsinized and the cell count was adjusted to 1.0 x 10^5 cells/ml using DMEM containing 10% FBS. To each well of the 96 well microtiter plate, 100 μl of the diluted cell suspension (50,000 cells/well) was added.

(did not do this) After 24 h, when a partial monolayer was formed, washed the monolayer once with medium and 100 μl of different test concentrations of test drugs were added on to the partial monolayer in microtiter plates. The plates were then incubated at 37°C for 1 days in 5% CO_2 atmosphere, further microscopic examination was carried out, observations were noted for every 24 h. After 1 day, the test solutions in the wells were discarded and 50 μl of MTT (5 mg/10 ml of MTT in PBS) was added to each well. The plates were gently shaken and incubated for 4 h at 37°C in 5% CO_2 atmosphere. The supernatant was removed and 100 μl of DMSO was added and the plates were gently shaken to solubilise the formed formazan. The absorbance was measured using a micro plate reader at a wavelength of 540 nm. The percentage growth inhibition was calculated using the following formula and

3.3 *In Silico* methodology

Part 3.3.1: Selection of Targets

BACE

GSK3B

AChE

Beta amyloid

Part 3.3.2: Selection of PDB Structures Of Targets And Chains

Papers selected for choosing the PDB structures - work done with Alzheimer's docking studies and checked if full length chains are present by checking for missing residues.

BACE (2VKM), GSK3B (1J1B), AChE (4EY7), Beta amyloid (1IYT)

3.3.3: Choosing chains for docking

Check the papers for the structures of the PDB formats present and the PDB page for information of chain, check for ions complexes, etc. Analyse and choose the chains for docking (Example: 4EY7 – AChE)
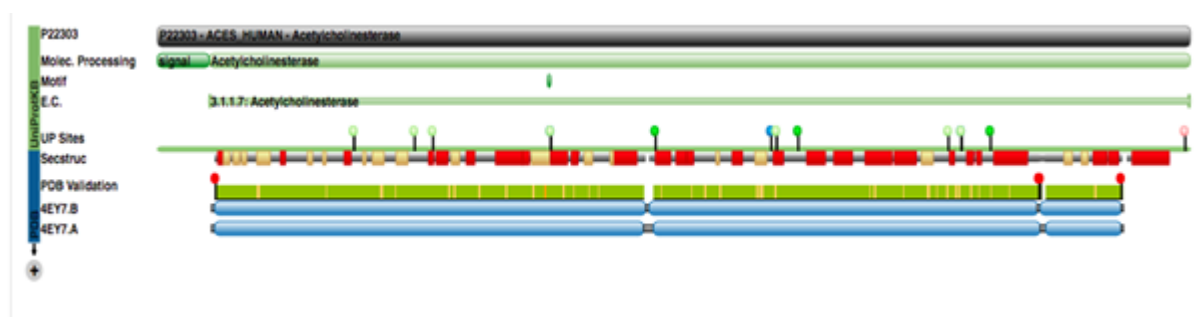
Figure 3.1 – AChE chains chosen for docking

1J1B - missing residues found

Homology modelling done using SWISS-MODEL for homology modelling

Obtain FASTA sequence of the protein and submit it for modeling and choose the best one with maximum homology and download as PDB format

3.3.4: Preparation of ligand library

Refer to papers with ligands structures and confirmation of the compounds in *Bacopa monnieri* and obtain the structures from PubChem and verifying the structure from papers referred and draw the structures in ChEMBL if the structure was not found in PubChem

3.3.5: Selection of Standard Drugs - (Cummings, J. et al, 2018, McGleenon BM et al, 1999)

Drug	Phase	Function
JNJ-54861911	I/II	BACE inhibitor
E2609	I/II	BACE inhibitor, Anti-amyloid
Donepezil	FDA approved	AChE inhibitor
Rivastigmine	FDA approved	AChE inhibitor
Nilotinib	I/II	Tyrosine kinase inhibitor (anti-tau), anti-amyloid
Anavex 2-73	I/II	GSK3B inhibitor (anti-tau)

Table 3.2 – Standard drugs

3.3.6: Preparation Of Ligands and Ligand Library

Download the structures of all the ligands from Pubchem and open one ligand in Discovery Studio and drag all the other ligands to the same window and click on 'Small Molecules' tab. Under the 'Prepare and Filter Ligands' tab, click 'Prepare Ligands'.Set Input Ligands to 'All' in the window that opens. Click 'Run' and save the prepared library as a Mol2 file.

Figure 3.2 – Ligand Library

3.3.7: Visualization of the Ligands
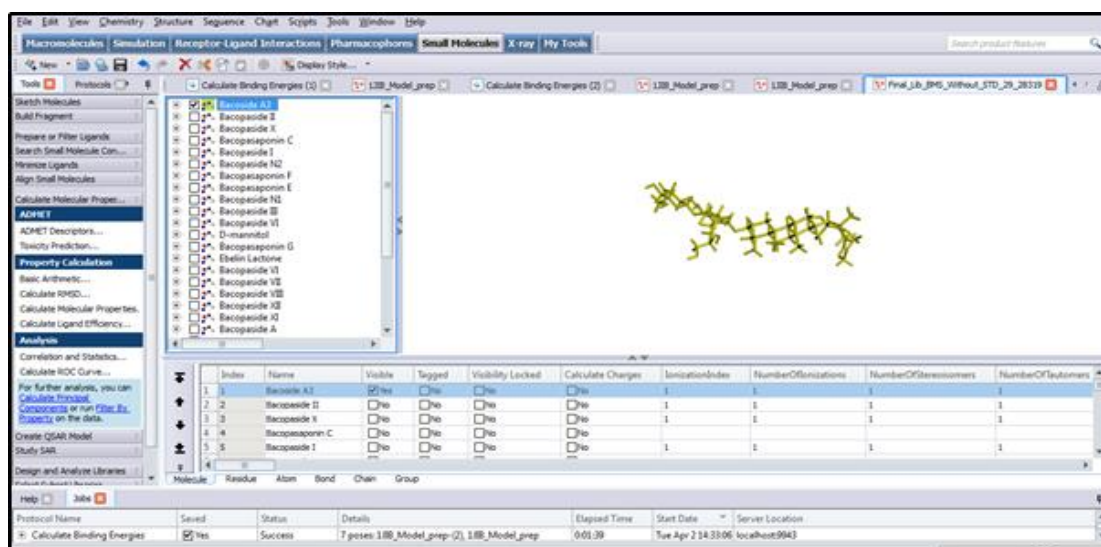
Figure 3.3 – Visualization of ligands

3.3.8: Prediction of ADMET Descriptors

Click on the 'Small Molecules' tab. Under 'Calculate   Molecular Properties', click on 'ADMET   Descriptors'.View the results.

3.3.9: Protocol for Toxicity Prediction

Click on Small Molecules tab followed by 'Calculate Molecular Properties' and ADMET. Now, click on Toxicity prediction, and specify what tests need to be done

3.3.10: Preparation of Protein for Docking

Open the protein in Discovery Studio and click 'Ctrl H' after opening the protein. Click and delete the identical chains and the ligands in the chains that were deleted. Also, delete water molecules if required. Click 'Macromolecule' and then 'Prepare Protein'. A window will open. Keep all the parameters same. Click 'Run' Double click the 'Results'. Check for the phrase No missing segments" in the results. -implies the preparation is proper.

3.3.11: Visualization of the Protein after preparation
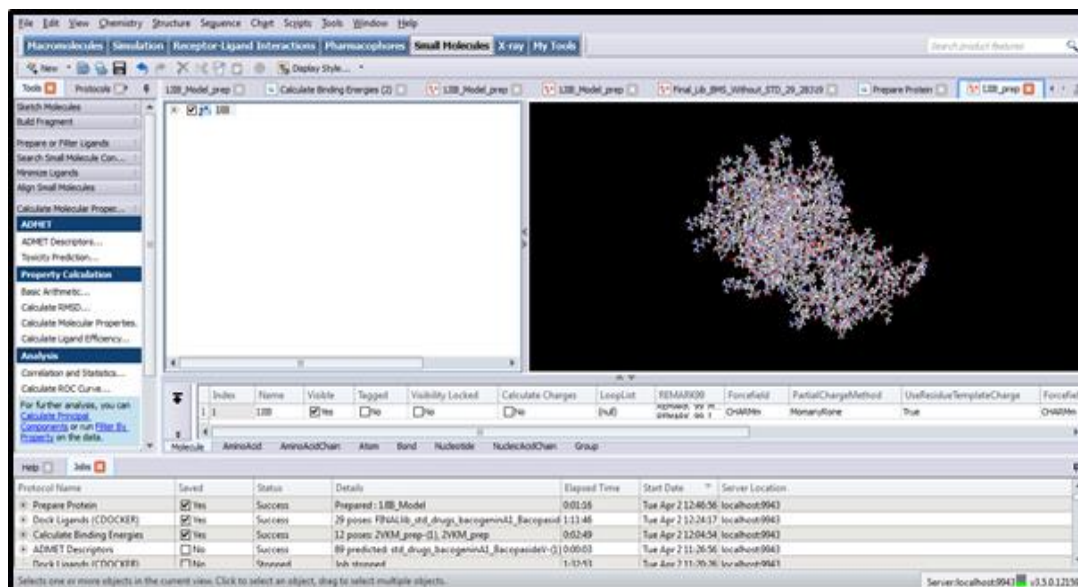
Figure 3.4 – Visualization of protein

3.3.12: Protocol for Docking using CDOCKER

Obtain protein structures from RCSB – PDB and the targets from Pubchem. Prepare the protein for docking using CDOCKER Open the prepared protein in Discovery Studio. Select drug molecules. Click 'Receptor Ligand interaction' followed by 'Define and Edit Binding Site', and 'Current Selection'. Delete the drug - reference based docking. Open the ligands file library in Discovery Studio. Under the tab 'Docking Optimization' Click on Dock Ligand (CDOCKER)

In the window that opens, Select all for Input Ligand. (The library that contains all the prepared ligands/drugs which is open in the software). Select the required number of Top Hits and Click 'Run

Figure 3.5 – Docking in CDOCKER

1IYT - no ligand- entire protein taken as target
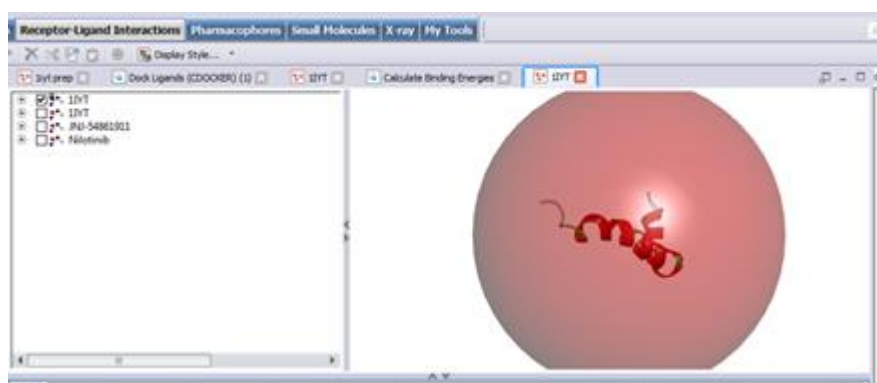
Figure 3.6 – 1IYT docking sphere

3.3.13: Calculation Of Binding Energy

After completion of Docking, open and view the results. For the calculation of Binding Energy, click on Receptor Ligand Interaction and Under the tab 'Scoring', click on 'Calculate Binding Energies'

1JIB - (without standard)
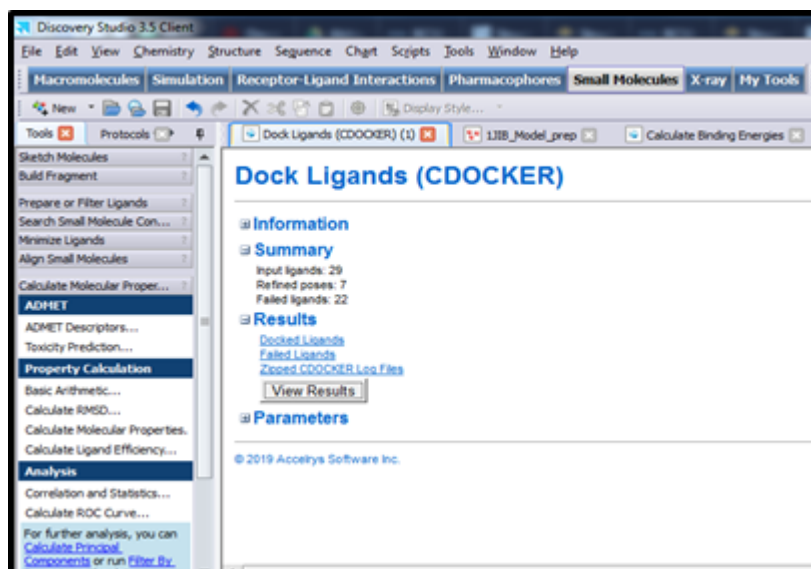
Figure 3.7 – CDOCKER result page

Binding Energy

Figure 3.8 – Binding energy

• Under 'Docking', click 'Define Flex Docking', choose 'Top 1' and click 'Apply and Dock'

3.3.14: Simulation Protocol using Desmond

Simulation was performed using Desmond in Linux Operating System using high end computers having Graphics Card. Open the terminal by pressing Ctrl+Alt+T. Enter the commands for opening Maestro. Import the complex file of the docked protein and prepare it for simulation.

Solvation is to be done by adding the boundary box, minimize the volume and add salt ions. Molecular Dynamics is done for 10ns, and by specifying the processing unit as GPU.
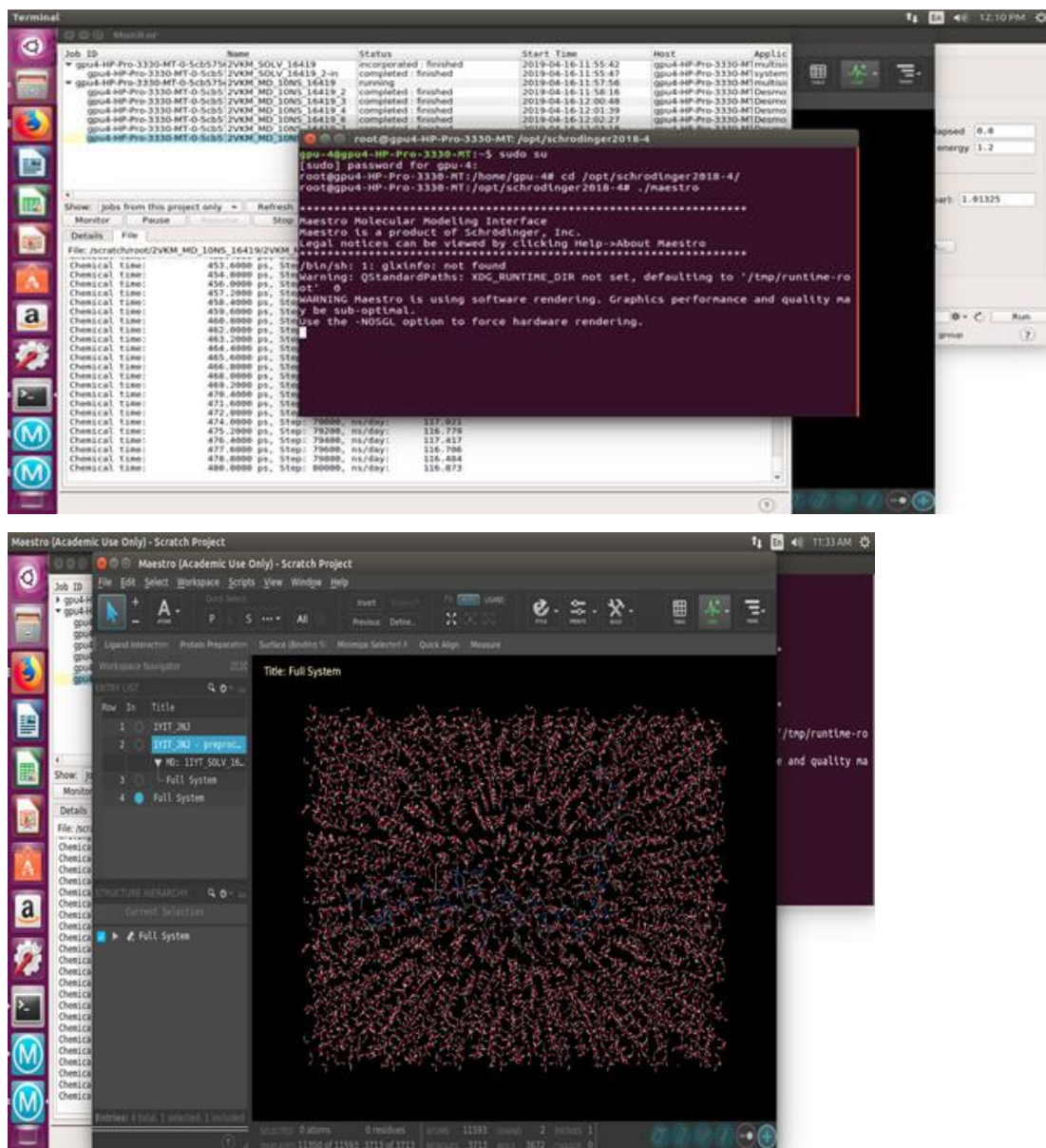
Figure 3.9 Solvation in Desmond

3.3.15: Molecular Simulation
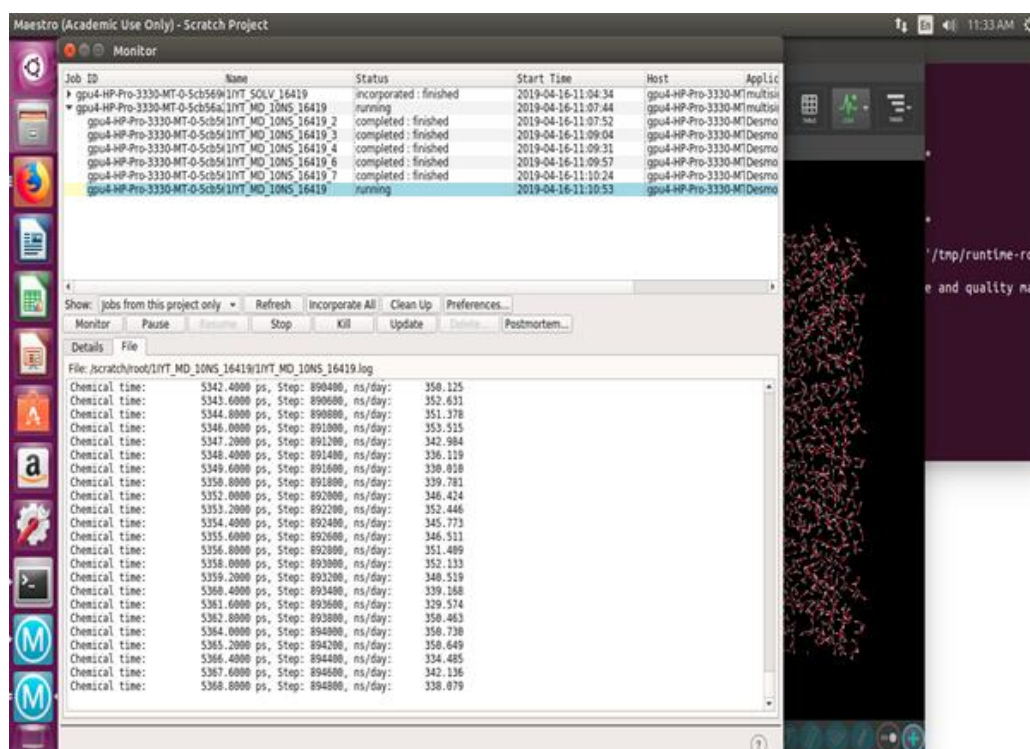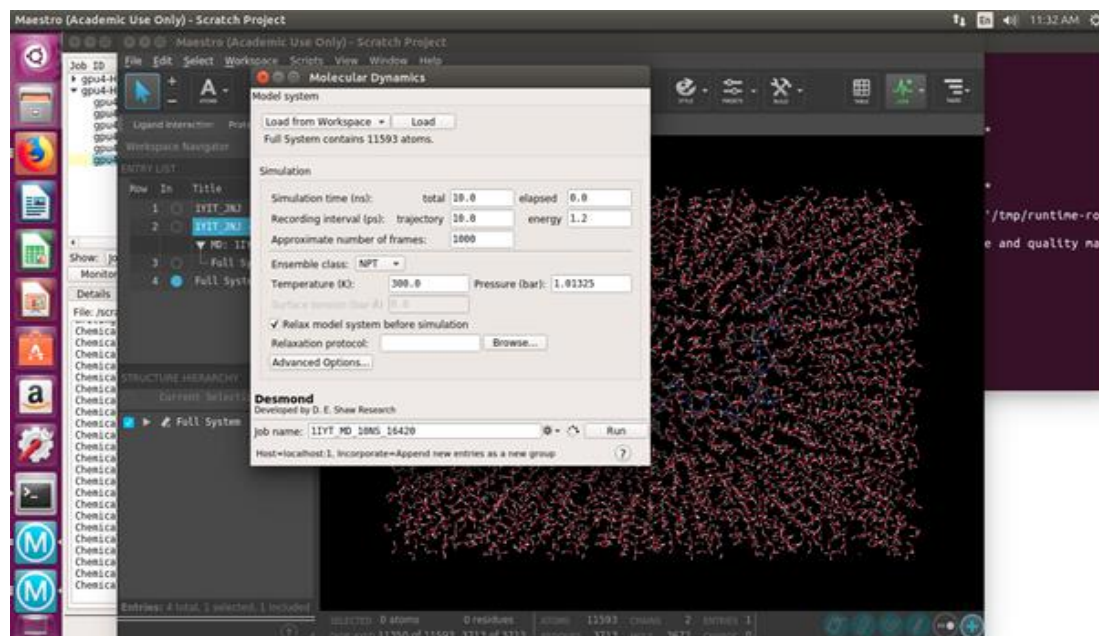
Figure 3.10 – Simulation in Desmond

3.3.16: Simulation Protocol using Discovery Studio

Open the Complex file of the docked protein using Discovery Studio and apply Forcefield.
Go to simulations Tab, under 'Run Simulation' under 'Tools', Click Calculate Energy.
Under 'Dynamics', click 'Standard Dynamics Cascade'. Here specify the nanoseconds. In
Discovery Studio, 1ns= 1,00,000 Production Steps

3.3.17: Protocol for Preparation of Complex Files

Open prepared protein file containing the bound drug. Next, open Binding Energy Results of the docking previously done. Copy and paste the required compound (drug) in the protein window.

Drag the drug inside the protein and remove the site sphere. Apply Force Field and save as pdb file.

Part 5.2.18: Protocol For Viewing the Interactions between the Protein and the Drug and to obtain 2D diagram

Open PDB structure of prepared protein, remove any bound drug. Copy and paste the required drug from binding energy results and drag it inside the protein Click "chain" . then under Receptor Ligand interactions tab, click "define ligand". In the toolbar, click in ligand interaction, and then "nonbond" to view the values of various interaction parameters. Click on "show 2D diagram" and save it as an image file

3.3.19: LigPlot Protocol

Open LigPlot in Linux (open terminal in the folder, type "sudo java -jar.LigPlus") and open the PDB file (complex) in LigPlot. Visualise the interaction and save the file as image

3.3.20: Protocol for obtaining 3D diagram

Open the complex file of the protein with the drug (compound) bound. In the toolbar, under nonbond interaction tab, select ligand interaction. Right click, select "display" and under the graphics tab, choose option "ultra high" and make the background colour white. RIght click, select "add label", choose the object as amino acid. Under nonbond interactions tab (below), select only H-bonds. Select the drug molecule, right click, select "display". Under graphics tab, choose ball and stick, change colour. Under Receptor Ligand Interactions tab, under display receptor surface tab, click on H-bond. Rotate to view the drug molecule for best visualization. Save the result obtained as an image file

3.3.21: Protocol for Docking in LeadIT

Click 'Load or prepare Receptor' to load the protein. Click 'Next'. Click on Chain A and don't select the drug. Keep all of the parameters same.Click on molecule. Choose Library to upload the ligand library.

4.Results

4.1 In Vitro **Results**

Concentration	Inoculation	Shoot Number (20 days)	Shoot Number (45 days)	Rooting &/Callus
IAA – 0, BAP - 0	1	1	2	+
	2	2	4	+
	3	1	3	+
	4	x	x	x
	5	1	3	x
	1	1	2	x

IAA – 0.01 mg/L **BAP - 0**	**2**	**2**	**3**	**+**
	3	**x**	**x**	**x**
	4	**x**	**x**	**x**
	5	**x**	**x**	**x**
IAA – 0.01 mg/L **BAP – 2 mg/L**	**1**	**x**	**x**	**x**
	2	**1**	**2**	**x**
	3	**1**	**1 callusing observed**	**x**
	4	**x**	**x**	**x**
	5	**x**	**x**	**x**
IAA – 0.01 mg/L **BAP - 5**	**1**	**x**	**x**	**x**
	2	**x**	**x**	**x**
	3	**x**	**x**	**x**
	4	**2**	**2 callusing observed**	**x**
	5	**x**	**x**	**x**
IAA – 0.01 mg/L **BAP – 10 mg/L**	**1**	**2**	**3**	**+**
	2	**1**	**4**	**x**
	3	**x**	**x**	**x**
	4	**2**	**2 callusing observed**	**+**
	5	**1**	**2**	**x**

Table 4.1 *in vitro* regeneration results

Observed on 25/4/19, inoculated on 20/2/19 into tissue culture bottle (Shoots - 20 day old)

Concentration	Original Shoot	Proliferated Shoots Number (2 months)	Rooting
IAA – 0, BAP - 0	1	10 - (5-8 cms)	
	2	11 - (5-8 cms)	
	3	7 (2-6 cms)	
	4	5 (2-6 cms)	
	5	10 (2-6 cms)	
IAA – 0.01 mg/L BAP - 0	1	15 (2-5cms)	
	2	10 (2-5 cms)	
	3	10 (2-5 cms)	
IAA – 0.01 mg/L BAP – 2 mg/L	1	15 (3-6 cms)	Rooting seen in all
	2	7 (3-6 cms)	
IAA – 0.01 mg/L BAP - 5 mg/L	1	6 (2-5 cms)	
	2	15 (2-5 cms)	
IAA – 0.01 mg/L BAP – 10 mg/L	1	9 (2-6 cms)	
	2	13 (2-6 cms)	
	3	20 (2-6 cms)	
	4	15 (3-9 cms)	

Table 4.1 *in vitro* regeneration results

IAA - 0 mg/ml

BAP- 0 mg/ml   Various concentrations BAP+IAA

As observed after 2 months
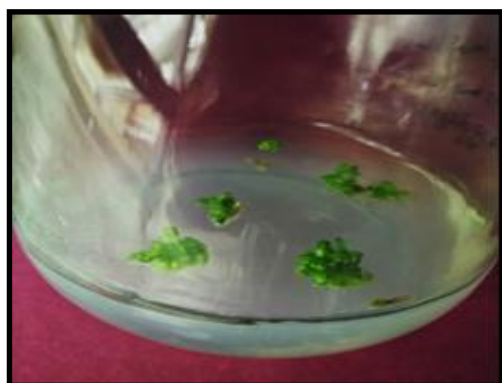
Callusing observed initially   Callusing observed after two months
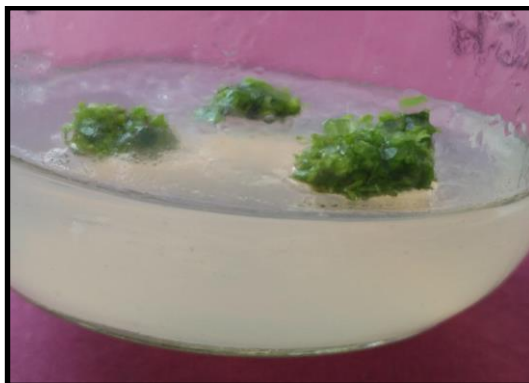
Callus incubated at 26±2 ±°C after 10 days

Callus incubated at $20\pm2 \pm°C$

Rooting as observed after 1 month

IAA - 0 mg/ml

BAP- 0 mg/ml (After two months)

PTC as harvested after two months

Figure 4.1 – In vitro growth

Temperature Dependency of Shoot Growth

Shoots (3 week old) inoculated in tissue culture bottle on 20.2.19

Tissue Culture Bottle Kept at 26±2°C	Tissue Culture Bottle Kept at 20±2°C
Number of Shoot observed from the callus 10 days	Number of Shoot observed from the callus 10 days
11±5.656854249	4±0.7071067812
7±3.535533906	3±2.828427125

Table 4.2 - Temperature dependency of shoot growth in callus

As per the studies done by Rahul Keshav Zote et al, 2018, the concentrations of both BAP and IAA were increased from 1mg/L to 3mg/L in steps of one, and the shoot formation showed an increase from 33.38% to 57.61% in that order. Whereas no such gradual increase proportional to the increase in concentrations was noted. The highest number of shoots were obtained in the media devoid of the PGR (43 shoots), followed by 42 shoots from the media having 0.01 and 10 mg/l concentration of IAA and BAP respectively. This difference in results could be attributed to the fact that the concentration of both the auxin and the cytokinin have been equally varied in the study of Rahul Keshav Zote et al, 2018. Whereas in our study the concentration of the auxin IAA has been kept at a constant 0.01 mg/L in all but one combination where it is 0mg/L and the concentration of BAP has been increased gradually but not in equal steps.

To study the effect of temperature on the growth and proliferation of shoots one sample was kept at a temperature of 26±2°C while the others were at 20±2°C. It was observed that the sample kept at a higher temperature sprouted more shoots as compared to the sample kept at a lower temperature.

In the research carried out by T. Soundararajan et al, 2011, micropropagation of *Bacopa monnieri* was performed with the two temperature ranges 25±2°C and 28-30°C. No significant difference in the shoot regeneration was observed. The reason could be that both the temperature ranges considered are higher than 25°C, and shoot growth has been good for both of them. Had they considered temperatures lesser than 22°C, there might have been a possibility where they would have obtained a difference in the result with less shoots being regenerated in the lower temperature range, as has been observed in the present study.

4.1.2 Phytochemical results

According to Prashanth Tiwari et al, 2011, saponins, flavonoids, alkaloids, tannins, and anthraquinone have antimicrobial properties. Saponins are also said to be anti-cancerous, anthelmintic. Flavonoids, alkaloids, tannins, and steroids are all said to be antidiarrhoeal. Phytosterol controls cholesterol, and steroids also have anti-inflammation properties. Anas Rasheed et al 2017, Moghadasian MH, 2000, Pushpendra Kumar Jain et al 2016, also support the presence of these properties in the phytochemicals. If the extracts of the plant are to be used in formulation of medicines, these properties due to the presence of the phytochemicals present will be very helpful.

Phytochemical	Presence/ Absence (+/-)	Image
SAPONINS (bacosides)	+	
FLAVONOIDS (Flavanones and flavanonols, Apigenin)	+	
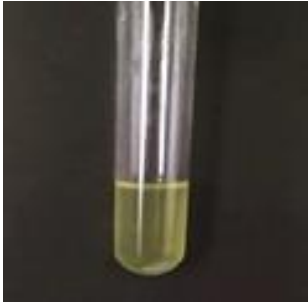
ALKALOIDS Rahmine, Nicotine, And Herpestine	+	
TANNINS	+	
STEROIDS	+	
PHYTOSTEROLS (sitosterol and stigmasterol)	+	
ANTHRAQUINONE	-	

Table 4.3 Phytochemical results

(Ref: - Rahul Gupta et al., 2016, Kh. Lemino Singh et al 2013)

The results obtained were the same for most of the tests as reported by Paras Jain et al, 2016, Monic Shah, et al, 2012, Pawar et al, 2016, Rahul Gupta et al, 2016, except Praveen R, et al, 2016 who tested negative for the presence of steroids.

Part 5.2.3: Antioxidant analysis

Total Phenolic Content

During the various physiological processes happening in vivo, free radicals are generated. Owing to pathological conditions, they are overproduced causing oxidative stress and leading to a number of diseases like cardiovascular-neurological diseases, cancer etc. Taking natural antioxidants can prove to be an effective remedy against oxidative damage. The term antioxidant refers to free radical scavengers, inhibitors of lipid peroxidation and chelating agent. Phenolic compounds possess a wide spectrum of biological effects including antioxidant and free radical scavenging. Anti-oxidant properties of *Bacopa monnieri*, owing to the large amount of saponins present, can offer protection from free radical damage in cardiovascular disease and certain types of cancer (Sharan Suresh Volluri et al, 2011)

OBSERVATIONS
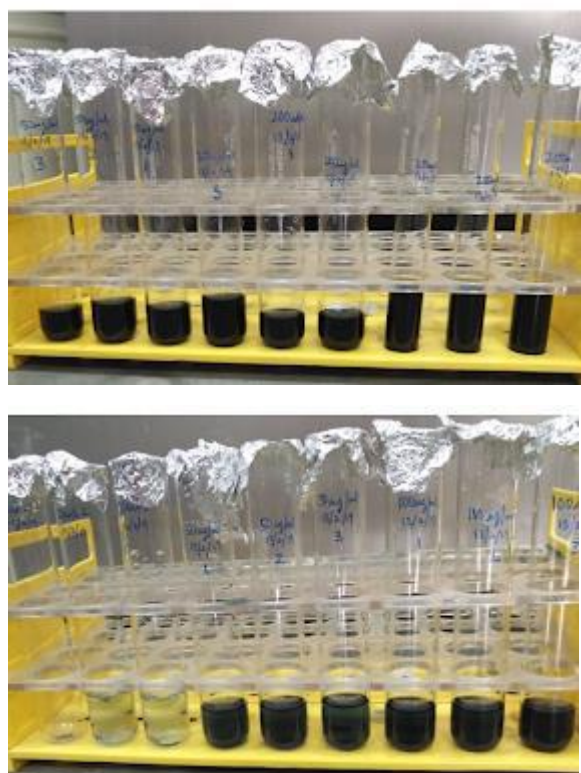
Fig. 4.2 :Triplicates taken for the gallic acid standard curve

OD as read at 765 nm:

Gallic Acid Concentration	OD at 765 nm			Average	Standard Deviation
	1	2	3		
0					
50	0.201	0.19	0.173	0.188	0.014
100	0.222	0.234	0.204	0.220	0.015
150	0.311	0.353	0.301	0.322	0.028
200	0.411	0.379	0.394	0.395	0.016
250	0.516	0.461	0.466	0.481	0.030
Sample	0.367	0.401	0.403	0.390	0.020

Table 4.4 Total Phenolic content
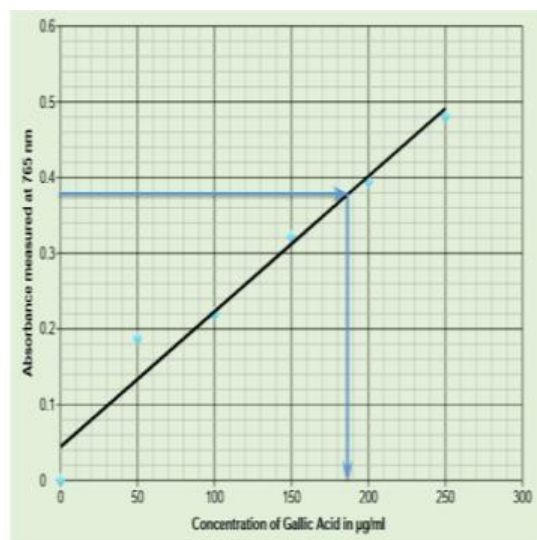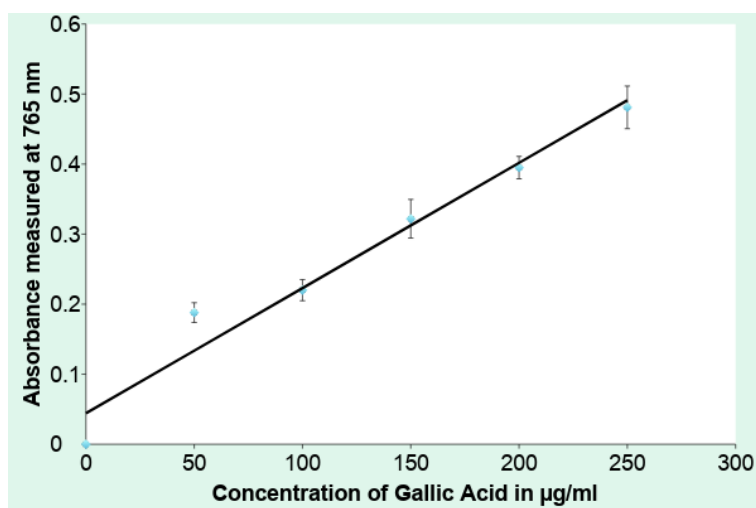
Fig. 4.3 :Standard Curve for Gallic Acid

Extract concentration – in terms of Gallic Acid Concentration was extrapolated to be 192 µg/ml

Total phenolic = Conc of gallic acid(mg/ml) * vol of extract in ml * dilution factor

Content   Weight of plant taken in g

(in mg GAE/g)

Total phenolic content = $\dfrac{0.198 * 0.5 * 4}{0.01}$ = 39.6 mg GAE/g

Total Phenolic content was calculated to be 39.6 mg GAE/g in the field plant sample of *Bacopa monnieri* obtained. Phenolic compounds undergo a complex redox reaction with the phosphotungstic and phosphomolybdic acids present in the Folin-Ciocalteu reagent to give a colour change that can be observed and measured to infer the total phenolic content (Abd Ghafar et al, 2009).

Sharan Suresh Volluri et al, 2011 and Paras Jain et al, 2017 got a lesser total phenolic content than ours which are 27.76 mg/GAE and 24.75 mg GAE/g respectively, and Shah et al 2012 got a result of 58 mg GAE/g for a herbal extract that they had obtained which is more than the value measured by us.

The difference in values may be due to the different extraction protocols followed by the different scientists. Sharan Suresh et al and Shah et al used Soxhlet apparatus and Paras Jain et al used maceration (48 hours) for extraction, but the specifications of Soxhlet apparatus were not given. Sharan Suresh et al obtained plants from the wild, while Paras Jain et al obtained plants from a botanical garden. Shah et al tested the total phenolic content of a herbal extract obtained by them

DPPH assay

S.L. No.	Concentration	Volume in µl	Methanol	DPPH	Methanol	OD	Scavenger Activity (%)
1.	0.1mgm/L	50				0.98	15.6
2.	0.2 mg/mL	50				0.8	32
3.	0.4 mg/mL	50				.66	44.5

4.	0.6 mg/mL	50	100µl	150µl	1mL	.27	77.31
5.	0.8 mg/mL	50				.1	91.5
6.	1.0 mg/mL	50				.06	94.9

Table 4.5 – Ascorbic acid standard curve and scavenging activity
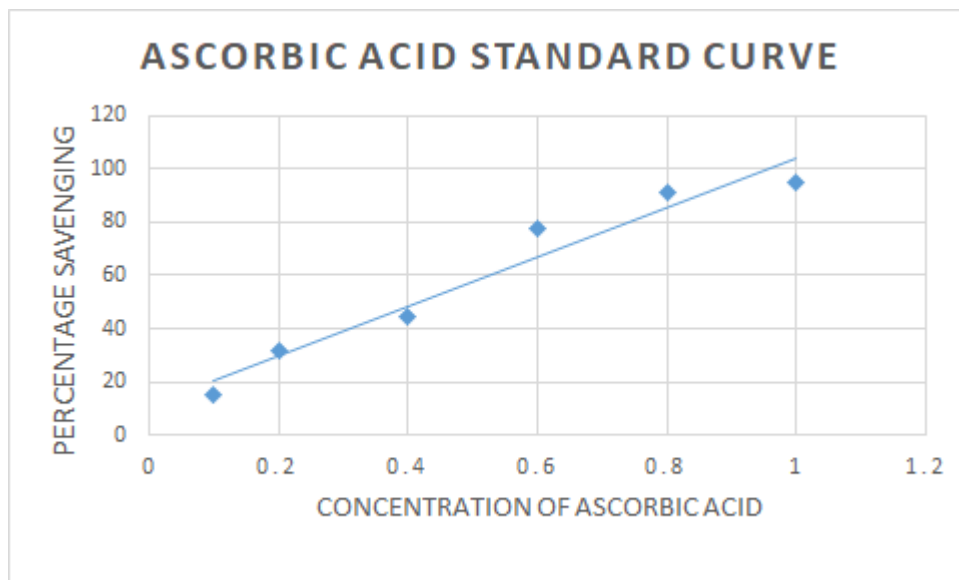
Figure 4.4 – – Ascorbic acid standard curve and scavenging activity

Control : 1.19

Field Plant Extract

S.L. No.	Concentration µg/ml	Sample	Methanol	DPPH	Methanol	OD	Scavenger Activity (%)
1.	31.25	50µl	100µl	150µl	1mL	0.719	31.17
2.	62.5					0.734	33.94
3.	125					0.749	36.42
4.	250					0.756	37.05
5.	500					0.786	38.31
6.	100					0.819	39.57

Table 4.6 – Scavenging Activity of field plant extract

In vitro (treated) Extract

S.L. No.	Concentration µg/ml	Sample	Methanol	DPPH	Methanol	OD	Scavenger Activity (%)
1.	31.25					0.848	25.42
2.	62.5					0.7555	26.97
3.	125	50µl	100µl	150µl	1mL	0.8875	28.73
4.	250					0.779	31.00
5.	500					0.869	36.51
6.	100					0.821	34.53

Table 4.7 – Scavenging Activity of *in vitro* (treated with PGR) extract

Callus Extract

S.L. No.	Concentration µg/ml	Sample	Methanol	DPPH	Methanol	OD	Scavenger Activity (%)
1.	31.25					0.891	25.12
2.	62.5					0.8495	28.61
3.	125	50µl	100µl	150µl	1mL	0.808	32.10
4.	250					0.7955	33.15
5.	500					0.7945	33.23
6.	100					0.676	43.19

Table 4.8 – Scavenging Activity of callus extract
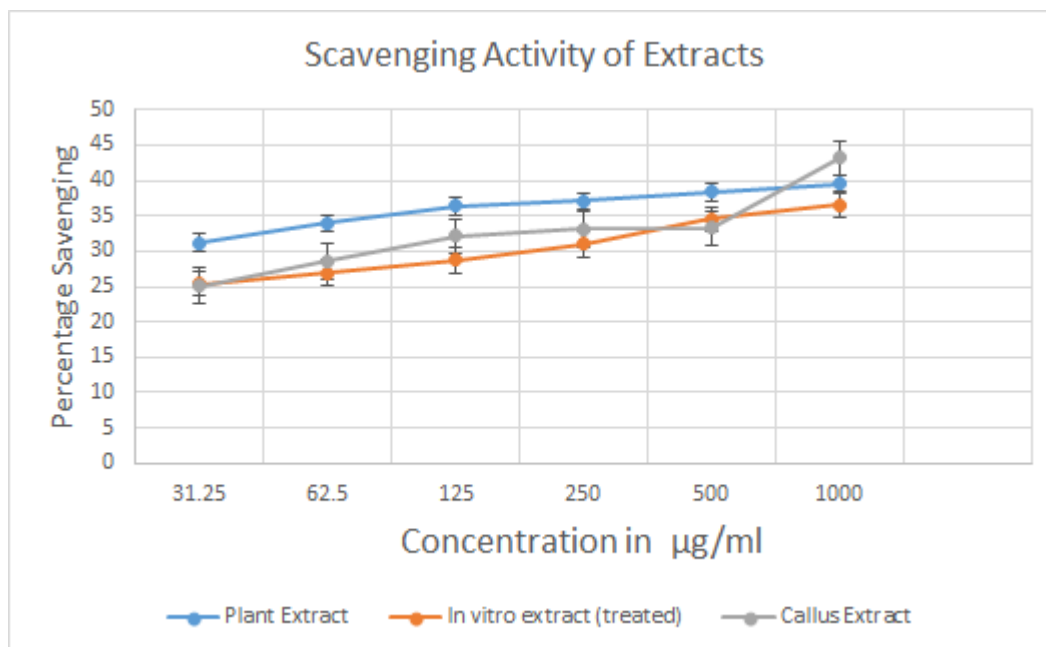
Figure 4.5 – Scavenging activity of extracts

The scavenging activity was calculated to be 25-45%. An increase in the concentration of extract showed an increase in the scavenging activity. The antioxidant extracts donate their hydrogen atoms to free radicals to make them to form non-radical species There have been various studies to show that *Bacopa monnieri* has properties that help reduce oxidative stress in brains. (Tamara Simpson et al 2015) Other studies have been performed to determine the antioxidant properties using different methods, including DPPH (Manohar Mohana et al, 2016, Vinut.S. Nandagaon, et al 2013)

Part 4.1.3 Chromatographic Analysis

High Performance Liquid Chromatography

Bacoside A Standard Results

Concentration in mg/ml	Retention Time	Area	Retention Time (min)	Area
0.0	0.2332	18016	1.750	10027
0.2	2.383	3865327	1.776	63474
0.4	2.326	5708099	1.777	79881
0.6	2.355	9101483	1.8	89042
0.8	2.37	12832550	1.788	95266

Table 4.9 – Bacoside A – HPLC results
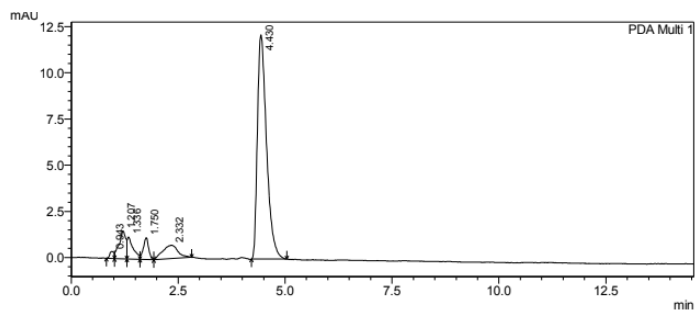
Concentration – 0.0 mg/ml (only methanol)
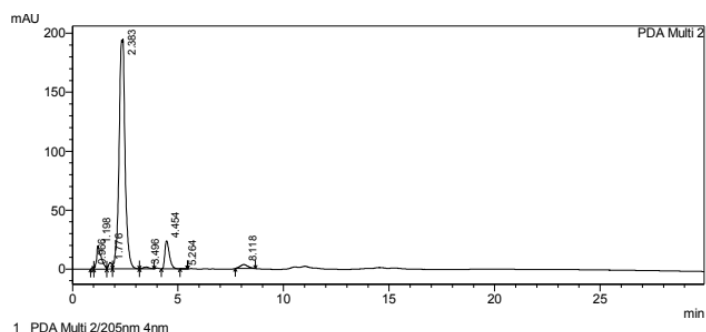
Concentration – 0.2 mg/ml
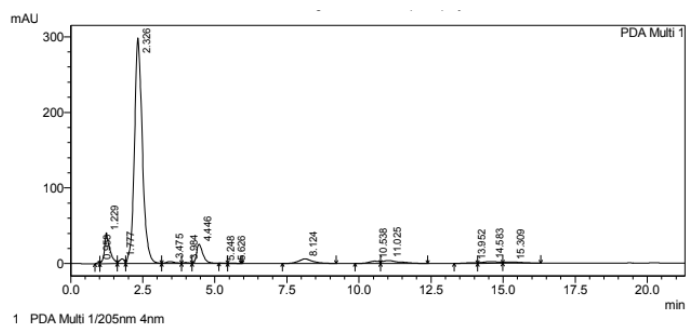
Concentration – 0.4 mg/ml
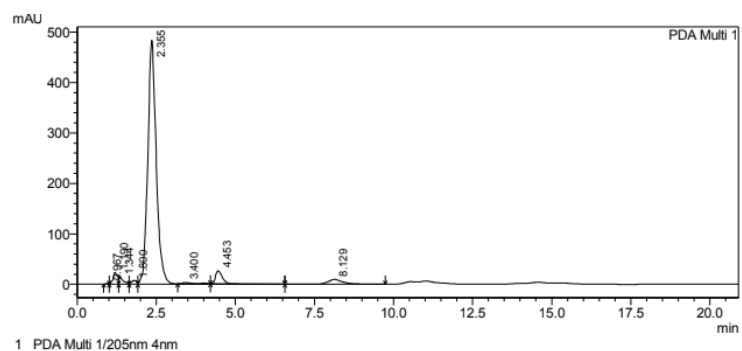
Concentration – 0.6 mg/ml
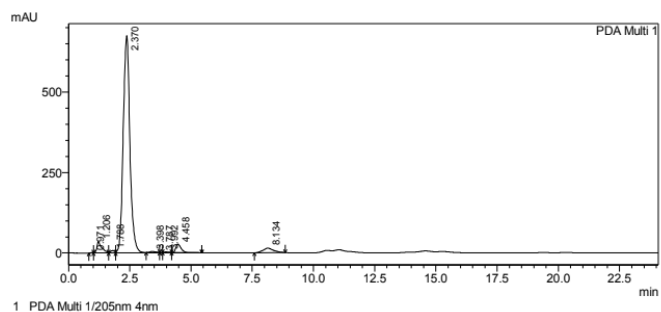
Concentration – 0.6 mg/ml
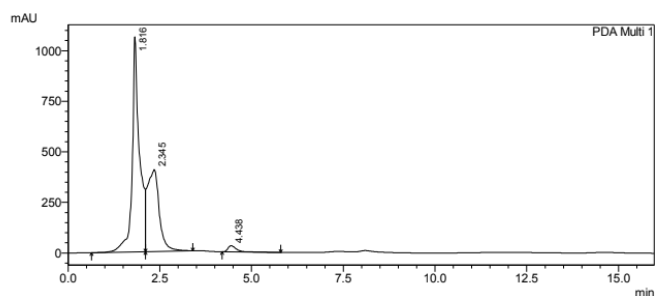
Sample A – Field extract
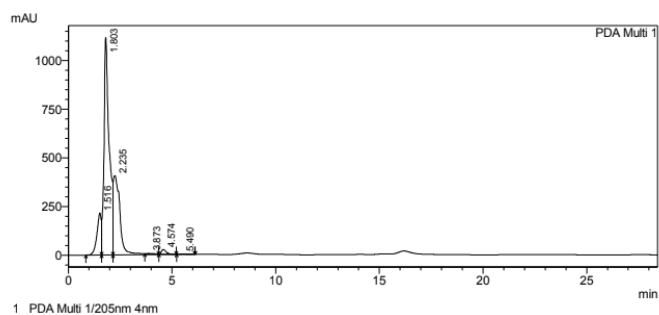
Sample B – *in vitro (*untreated) extract
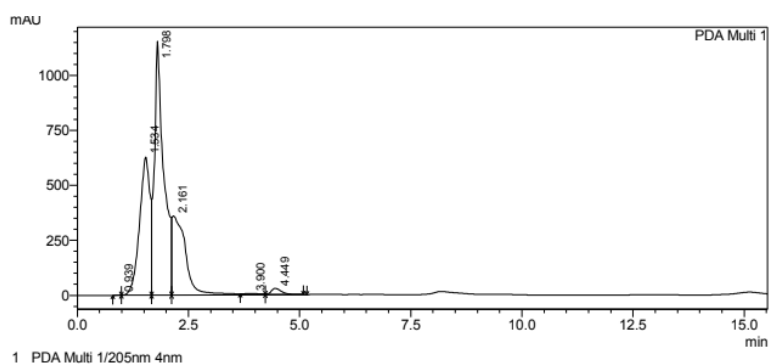
Sample C – *in vitro (*treated) extract
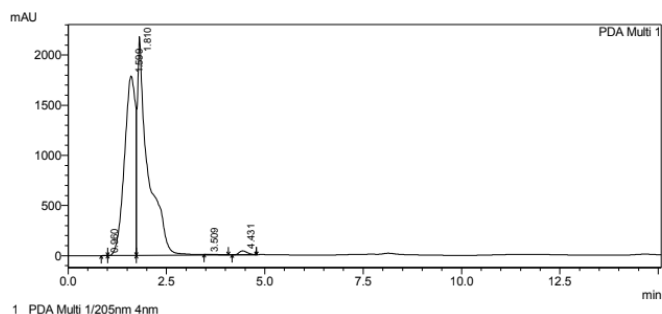
Sample D – callus extract

Figure 4.6 – HPLC graphs
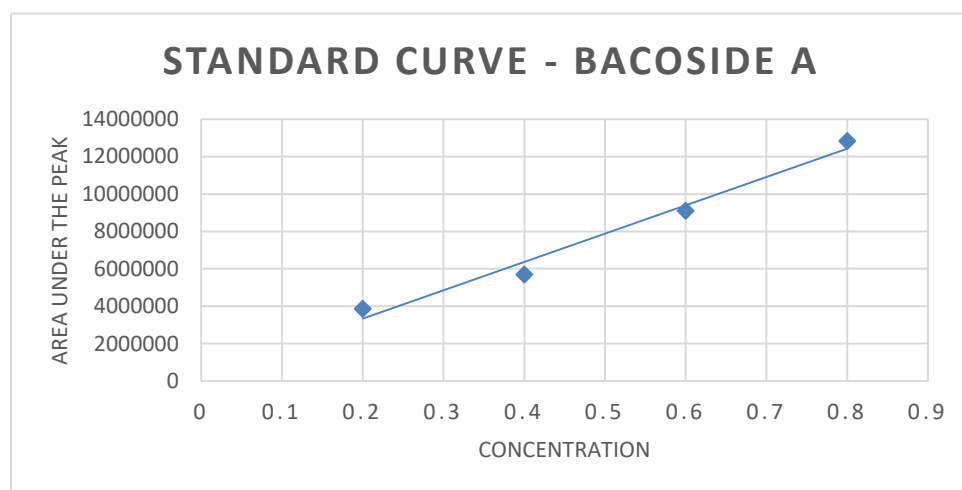
Figure 4.7 – HPLC bacoside A standard curve

The retention time for Bacoside A was analysed to be 2.3±0.2 min. According to that retention time and area of peak found in the extracts, the concentrations were extrapolated from the above graph.

Extract	Retention time	Area
A	2.345	9066286
B	2.235	9240897
C	2.161	7761379

Orange line – untreated in vitro
Blue line – field extract
Green line – treated in vitro
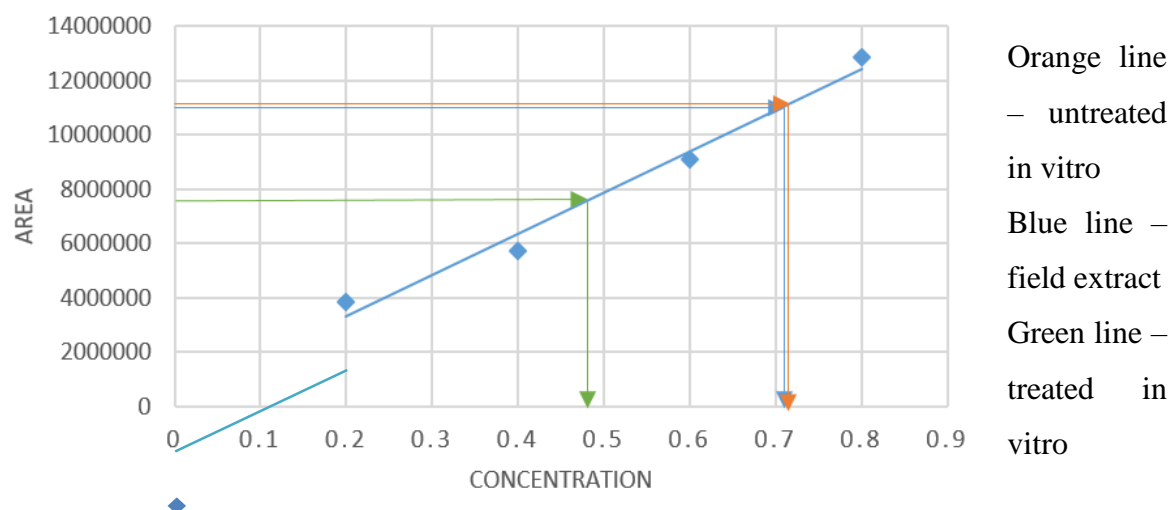
Figure 4.7 – HPLC extract concentration

The concentrations for in vitro treated, field, and untreated extracts were calculated to be 0.48 mg/ml, 0.71 mg/ml and 0.72 mg/ml.

There was another peak which was at 1.8±0.2 which showed very high concentrations in the extracts, but lesser in the standard.

Table Bacoside A Standard peak values at retention time of 1.8±0.2 min

Retention Time (min)	Concentration in mg/ml	Area
1.776	0.2	63474
1.777	0.4	79881
1.8	0.6	89042
1.788	0.8	95266

Retention time	Extract	Area
1.816	Field	14908575
1.803	In vitro untreated	19794219
1.798	In vitro treated	16863534
1.81	Callus	40900153

Table 4.9 – HPLC results

This peak may be of another compound that is highly expressed in the plant. The results also show that the callus has 2.5 times the concentration of the compound than the others.

Thin layer chromatography

Thin layer chromatography solvent system was optimised by trying various systems and finally concluding which system eluted out the components the best and in which identification of the particular compounds could be done. The system used was ethyl acetate:methanol:water (7:3:1).

S - Standard

A - Field plant extract

B - In vitro regenerated (untreated) extract

C - In vitro regenerated (treated) extract

D - Callus extract

E - Callus (temperature effect) extract

As observed under UV light at 365 nm

Figure 4.8 – a. TLC visualised under UV (365 nm)

The bands that have eluted out in D (callus) and E (callus - temperature effect) can promintely be observed, more so than the bands seen in the other samples.

As observed after exposing the extracts to Caffeic Acid

Figure 4.8 – b. TLC stained with caffeic acid

After exposing to Caffeic Acid, we can see the standard Bacoside A being detected the strongest. Bands in A, and B are seen clearly while in C and D, the bands were very light.

Figure 4.8 – c. TLC stained with iodine vapours

The bands in S, C, and D were clearly identified while A, B and E were stained lightly.

R$_f$ value = <u>**Distance moved my solute**</u>

                      Distance moved my solute front

R$_f$ values for

Distance moved my solute front =7.5 cm

Distance moved my Bacoside A = 5.5 cm

Distance moved by solutes	Rf value
5.5 (Bacoside A)	0.7337
5.3	0.706.
4 (prominent in field extract)	0.533
3 (prominent in callus extracts)	0.4

Table 4.10 – TLC retention factors

Other studies for TLC have obtained different R_f values in different solvent systems. An Rf value of 0.78 was obtained by Om Prakash et al, 2008 in dichloromethane: methanol: water (4.5: 1.0: 0.1 v/v/v) and in chloroform:glacial acetic acid:methanol:water in the ratio 16:8:3:2 Rf was 0.95 for the same compound (Manoharan Mohana et al, 2016). This value may be due to the fact that they ran HPTLC and not TLC. It was observed that the R_f obtained by others were all also above 0.70, which is similar to the results obtained in this study.

4.1.4 MTT assay results
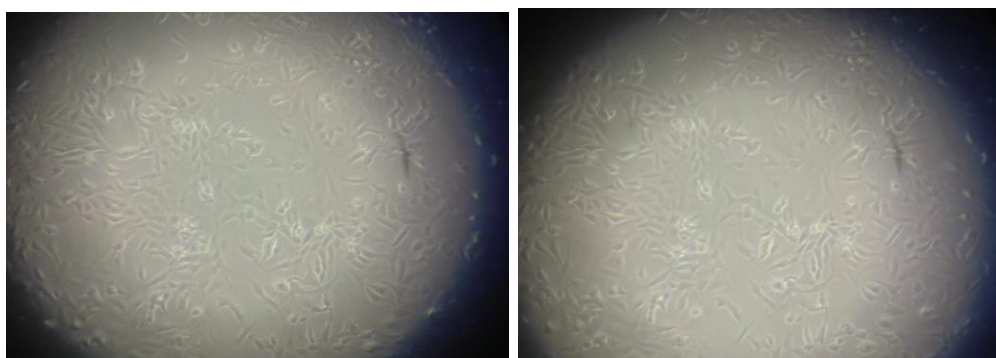
SHSY5Y Cells
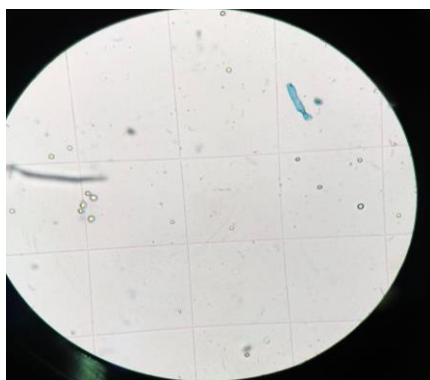
Stained with tryphan blue
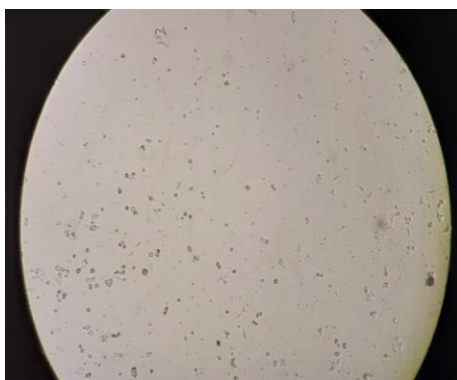
After seeding (6 hours later)

After exposing to extracts (24 hours)
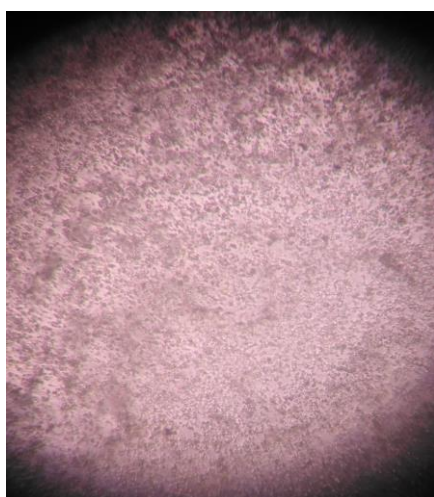
Standard
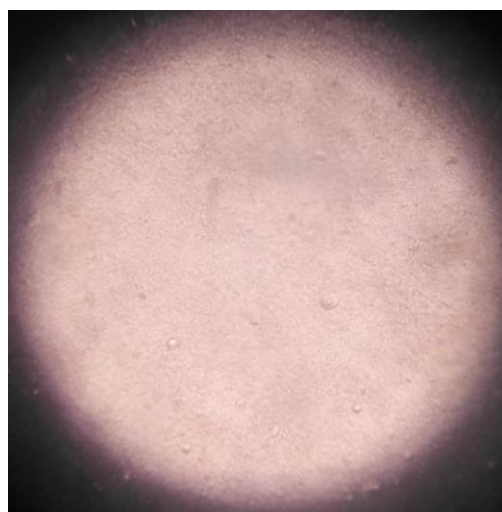
Field extract
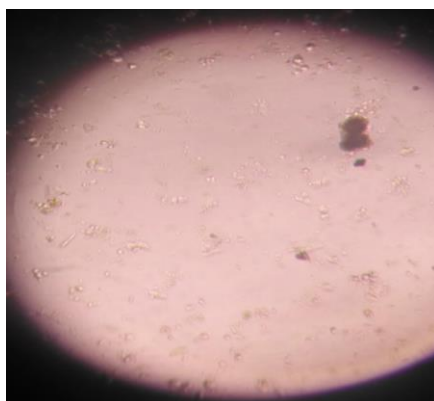
In vitro extract

Callus extract

Methanol

H2O2
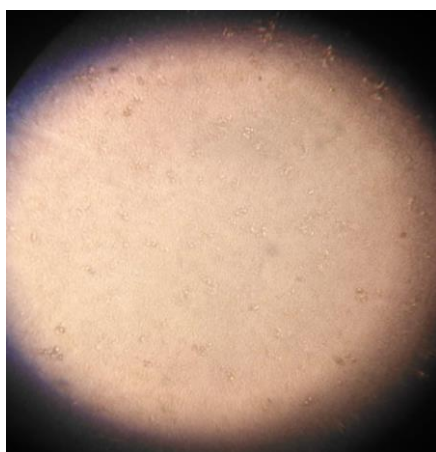
Control

Figure 4.9 – Animal cell culture and MTT Assay

Table Percentage Inhibiton

Methanol (µM)	Average	% inhibiton
1000	0.547333	34.1
500	0.183	77.97
250	0.129667	84.38
125	0.099667	88
62.5	0.088	89.4
H2O2 (µM)	Average	% inhibiton
1000	0.076	90.85
500	0.098	88.2
250	0.096333	88.4
125	0.066	92.05
62.5	0.076333	90.81
Field (µg/ml)	Average	% inhibiton
500	0.100667	87.96
250	0.050333	93.98
125	0.096667	88.35

62.5	0.069333	91.65
31.25	0.081	90.25
Callus (μg/ml)	**Average**	**% inhibiton**
500	0.097333	88.28
250	0.064333	92.25
125	0.100667	87.96
62.5	0.103	87.6
31.25	0.059333	92.85
Treated in vitro (μg/ml)	**Average**	**% inhibiton**
500	0.094667	88.61
250	0.083667	89.93
125	0.093333	88.76
62.5	0.090333	89.12
31.25	0.058	93.01
Standard (μg/ml)	**Average**	**% inhibiton**
500	0.169	79.65
250	0.102	87.71
125	0.083667	90
62.5	0.097667	88.25
31.25	0.095	88.56

Table 4.11 – Percentage inhibition

MTT discussion?

4.2 *In Silico* Result

PDB ID	Description	NMR	Resolution (Å) - X ray	Initial potential energy (kcal/mol)	Final potential energy (kcal/mol)	
2VK M	Crystal structure of GRL-8234 bound to BACE (Beta-secretase)		2.05	-15,015.59	-24276.94967	
1J1B	Homology modelling			-13710.24271	-22351.99925	
4EY7	Crystal Structure of Recombinant Human Acetylcholinesterase in Complex with Donepezil		2.3509	-16619.8344	-32919.70678	
1IYT	Solution structure of the Alzheimer's disease amyloid beta-peptide (1-42)	X		-859.87735	-1620.72538	

Table 4.12: Protein description and PDB ID

These are the properties of the PDB files chosen for the four targets.

ADMET Properties

SL no	Compound	AlogP	PSA_2D	Plasma protein binding	Hepato-toxicity	CYP2D6 binding	Aqueous solubility	BBB penetration	Intestinal absorption	
1	Bacoside A3	-0.338	279.595	FALSE	FALSE	FALSE	2	4	3	
2	Bacopaside II	-0.47	279.595	FALSE	FALSE	FALSE	2	4	3	

3	Bacopaside X	0.172	258.78	FALSE	FALSE	FALSE	2	4	3	
4	Bacopasaponin C	0.041	258.78	FALSE	FALSE	FALSE	2	4	3	
5	Bacopaside I	-0.872	298.797	FALSE	FALSE	FALSE	3	4	3	
6	Bacopaside N2	0.767	220.104	FALSE	FALSE	FALSE	3	4	3	
7	Bacopasaponin F	-1.574	339.087	FALSE	FALSE	FALSE	1	4	3	
8	Bacopasaponin E	-1.064	318.271	FALSE	FALSE	FALSE	2	4	3	
9	Bacopaside N1	0.898	220.104	FALSE	FALSE	FALSE	2	4	3	
10	Bacopaside III	0.364	239.306	FALSE	FALSE	FALSE	3	4	3	
11	Bacopaside VI	1.409	199.289	FALSE	FALSE	FALSE	3	4	3	
12	D-mannitol	-2.941	124.892	FALSE	FALSE	FALSE	5	4	3	
13	Bacopasaponin G	1.919	178.473	FALSE	FALSE	FALSE	2	4	3	
14	Ebelin Lactone	6.271	47.046	TRUE	FALSE	FALSE	1	0	1	
15	Bacopaside VI	0.364	239.306	FALSE	FALSE	FALSE	3	4	3	
16	Bacopaside VII	0.172	258.78	FALSE	FALSE	FALSE	2	4	3	
17	Bacopaside VIII	-1.574	339.087	FALSE	FALSE	FALSE	1	4	3	
18	Bacopaside XII	-1.706	339.087	FALSE	FALSE	FALSE	1	4	3	
19	Bacopaside XI	0.364	239.306	FALSE	FALSE	FALSE	3	4	3	
20	Bacopaside A	-0.132	141.139	FALSE	FALSE	FALSE	4	4	1	
21	Bacopaside B	1.568	177.914	FALSE	FALSE	FALSE	3	4	3	
22	Bacoside A1	1.919	178.473	FALSE	FALSE	FALSE	2	4	3	
23	Bacopasaponin A	1.919	178.473	FALSE	FALSE	FALSE	2	4	3	
24	Bacoside A2	0.041	258.78	FALSE	FALSE	FALSE	3	4	3	
25	Bacopasaponin B	1.788	178.473	FALSE	FALSE	FALSE	2	4	3	
26	Bacopasaponin D	1.277	199.289	FALSE	FALSE	FALSE	2	4	3	
27	Bacoside C	0.192	186.844	FALSE	FALSE	FALSE	3	4	3	
28	pseudojujubogenin	**4.26**	59.491	TRUE	FALSE	FALSE	2	1	0	
29	Jujubogenin	4.392	59.491	TRUE	FALSE	FALSE	1	1	0	
30	Bacopaside V	1.277	199.289	FALSE	FALSE	FALSE	3	4	3	
31	Bacogenin A1	4.204	67.861	FALSE	FALSE	FALSE	2	1	0	

Table 4.13: ADMET properties

SL no	Compound	AlogP	PSA_2D	Plasma protein binding	Hepato-toxicity	CYP2D6 binding	Aqueous solubility	BBB penetration	Intestinal absorption
1	E2609	0.763	106.627	FALSE	FALSE	FALSE	2	3	0
2	ANAVEX 2-73	1.78	12.134	FALSE	FALSE	TRUE	3	1	0
3	Donepezil	3.009	38.365	TRUE	FALSE	FALSE	2	1	0
4	JNJ-54861911	1.311	107.884	FALSE	TRUE	FALSE	3	3	0
5	Nilotinib	4.98	97.107	FALSE	TRUE	FALSE	1	4	1
6	Rivastigmine	1.038	32.787	FALSE	TRUE	FALSE	4	2	0

Table 4.14: Standards drugs ADMET properties:

Plasma protein binding   FALSE - poorly bounded

                                         TRUE - highy bounded

Hepatotoxicity   TRUE - toxic

                                         FALSE - non-toxic

CYP2D6 binding   TRUE - inhibitor

                                         FALSE - non-inhibitor

Aqueous solubility   1 - poor

                                         2 - low

                                       3 - good

                                       4 - very good

BBB penetration   0 - very good

                                       1 - good

                                     2 - moderate

                                     3 - low

4 - undefined

Intestinal absorption   0 - good

1 - moderate

2 - poor

3 - very poor

4 - undefined
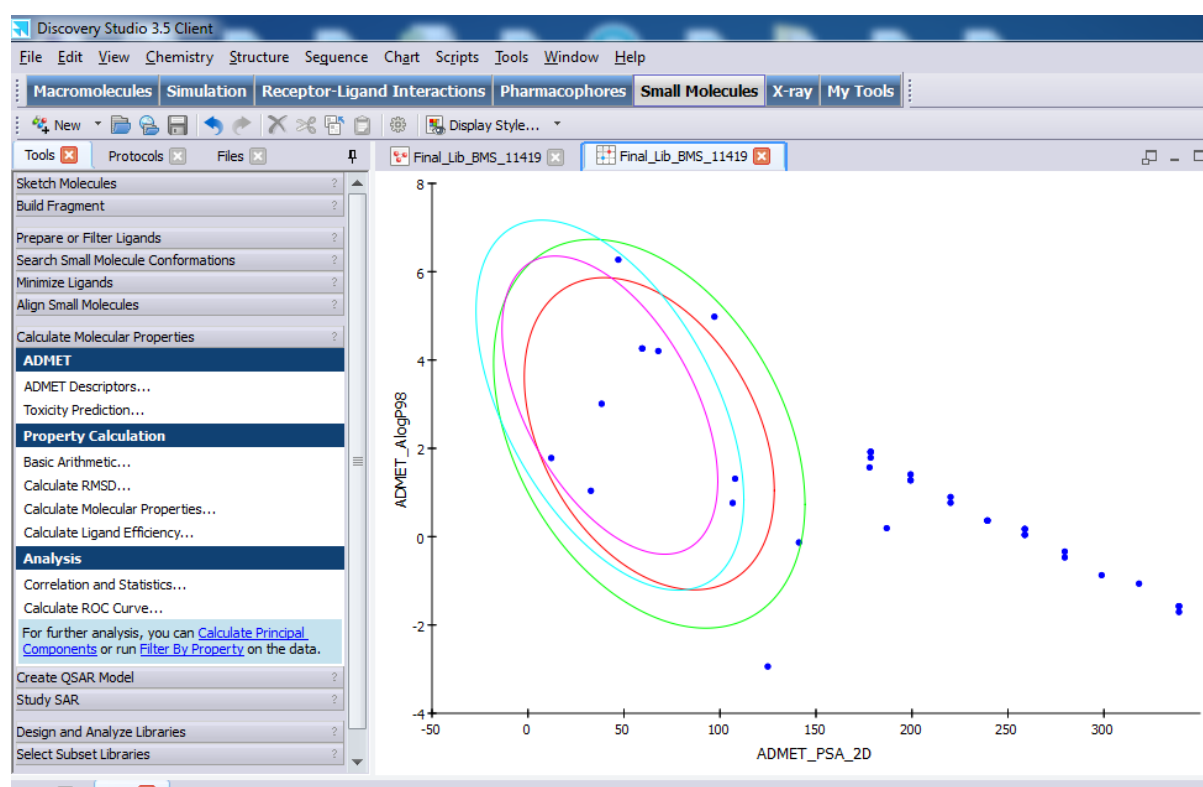
Figure 4.10 – ADMET properties

From the above results, the main property to be checked is Blood Brain Barrier. The compounds which have good blood brain barrier are Ebelin Lactone (best) and Bacogenin A1, jujubogenin and pseudo jujubogenein are the ones that follow second. Other properties that are also checked in ADMET properties are Plasma protein binding, hepatotoxicity, CYP2D6 binding, aqueous solubility and intestinal absorption.

We can also see the ADMET properties of standard drugs and drugs undergoing clinical trials. We can observe that compound which do not have good ADMET properties are being considered to be FDA approved drugs or already are.

Toxicity Prediction

Compounds	NTP Carcinogenicity Call (Male Rat)	NTP Carcinogenicity Call (Female Rat)	Developmental Toxicity Potential (DTP)	Skin Irritation	Ames Mutagenicity
Bacoside A3	Green	Red	Green	Green	Green
Bacopaside II	Green	Red	Green	Green	Green
Bacopaside X	Green	Red	Green	Green	Green
Bacopasaponin C	Green	Red	Green	Green	Green
Bacopaside I	Green	Red	Green	Green	Green
Bacopaside N2	Green	Red	Black	Red	Green
Bacopasaponin F	Green	Red	Green	Green	Green
Bacopasaponin E	Green	Red	Green	Green	Green
Bacopaside N1	Green	Red	Green	Red	Green
Bacopaside III	Green	Red	Red	Red	Green
Bacopaside VI	Red	Red	Green	Red	Green
Bacopasaponin G	Red	Red	Green	Red	Green
Ebelin Lactone	Red	Red	Red	Red	Green
Bacopaside VI	Green	Red	Red	Red	Green
Bacopaside VII	Green	Red	Green	Green	Green
Bacopaside VIII	Green	Red	Green	Green	Green
Bacopaside XII	Green	Red	Green	Green	Green
Bacopaside XI	Green	Red	Red	Red	Green
Bacopaside A	Green	Green	Green	Red	Red

Bacopaside B	Black	Red	Red	Red	Green
Bacopasaponin A	Red	Red	Green	Red	Green
Bacoside A2	Green	Red	Green	Green	Green
Bacopasaponin B	Red	Red	Green	Red	Green
Bacopasaponin D	Green	Red	Black	Red	Green
Bacoside C	Green	Red	Red	Red	Green
Pseudojujubogenin	Red	Red	Red	Red	Green
Jujubogenin	Red	Red	Red	Red	Green
Bacopaside V	Red	Red	Green	Red	Green
Bacogenin A1	Green	Red	Green	Green	Green

Table 4.15 – Toxicity prediction

Compounds	NTP Carcinogenicity Call (Male Rat)	NTP Carcinogenicity Call (Female Rat)	Developmental Toxicity Potential (DTP)	Skin Irritation	Ames Mutagenicity
E2609	Green	Green	Red	Green	Green
ANAVEX 2-73	Green	Red	Green	Green	Green
Donepezil	Red	Green	Red	Red	Green
JNJ-54861911	Green	Green	Green	Green	Red
Nilotinib	Green	Green	Red	Green	Red
Rivastigmine	Green	Red	Green	Red	Green

Table 4.16 Standard drugs toxicity prediction

These are toxicity predictions that can be done using Discovery Studio, for various tests. Green is means non toxic, black is tolerable, and red is toxic. These tests results are influenced by and rely on the ADMET properties results for the calculations.

Docking results from: CDOCKER (Discovery Studio)

Sl No	Target Name	Target PDB ID	Compound Name	Cdocker Energy Value	Cdocker Interaction	Binding Energy
1	BACE	2VKM	Bacopaside N2	-952.033	-5.22441	645.182
2	BACE	2VKM	Bacopaside N1	-795.822	-18.9142	501.245
3	BACE	2VKM	Bacopaside III	-236.931	30.8207	-30.2931
4	BACE	2VKM	D-mannitol	13.5385	34.0195	-65.0962
5	BACE	2VKM	Bacopasaponin G	-517.736	-24.1228	228.221
6	BACE	2VKM	Ebelin Lactone	-148.107	18.1573	-9.5071
7	BACE	2VKM	Bacopaside A	5.7335	46.49	-53.8796
8	BACE	2VKM	Bacopaside B	26.2924	68.6274	-69.5237
9	BACE	2VKM	Bacopasaponin B	-360.314	23.1435	67.2556
10	BACE	2VKM	Bacopaside C	22.703	71.296	-87.8889
11	BACE	2VKM	Jujubogenin	-203.211	-4.53375	23.8174
12	BACE	2VKM	Pseudojujubogenin	-203.211	-4.53375	23.8174
13	BACE	2VKM	Bacopaside V	-347.277	36.8127	-2.15397
14	BACE	2VKM	Bacogenin A1	-180.028	11.1766	-1.44359

Table 4.17: 2VKM CDOCKER results

Sl No	Target Name	Target PDB ID	Compound Name	Cdocker Energy Value	Cdocker Interaction	Binding Energy
1	BACE	2VKM	E2609	1.57426	46.855	-4.85009

2	BACE	2VKM	ANAVEX 2-73	-6.17047	32.8294	0.00027
3	BACE	2VKM	Donepezil	5.43336	51.6339	0.00027
4	BACE	2VKM	JNJ-54861911	17.2783	47.421	-13.0168
5	BACE	2VKM	Nilotinib	24.2183	56.756	-7.56361
6	BACE	2VKM	Rivastigmine	30.793	42.4188	0.00027

Table 4.18 Standard drugs - docking results for CDOCKER with 2VKM (beta secretase)

Sl No	Target Name	Target PDB ID	Compound Name	Cdocker Energy Value	Cdocker Interaction	Binding Energy
1	GSK-3B	1JIB	D-mannitol	1.14433	22.848	-18.1427
2	GSK-3B	1JIB	Ebelin Lactone	-58.4989	35.655	-43.1441
3	GSK-3B	1JIB	Bacopaside A	3.12946	38.7198	-51.6203
4	GSK-3B	1JIB	Bacopaside B	36.666	56.6393	-43.9368
5	GSK-3B	1JIB	Bacopaside C	17.486	63.1021	-67.938
6	GSK-3B	1JIB	Jujubogenin	-104.377	41.0953	-19.1169
7	GSK-3B	1JIB	pseudojujubogenin	-104.377	41.0953	-19.1169
8	GSK-3B	1JIB	Bacogenin A1	-78.9335	39.4103	-12.8981

Table 4.19 Docking results from: CDOCKER (Discovery Studio) results - 1J1B (GSK3B)

1	GSK-3B	1JIB	E2609	0.551733	45.5381	-49.5755
2	GSK-3B	1JIB	ANAVEX 2-73	5.58395	33.8547	-54.5905
3	GSK-3B	1JIB	Donepezil	1.52649	44.3299	25.5027
4	GSK-3B	1JIB	JNJ-54861911	13.4258	40.7322	-67.4729
5	GSK-3B	1JIB	Nilotinib	29.5693	53.9954	-115.138
6	GSK-3B	1JIB	Rivastigmine	27.4167	32.3446	-25.5152

Table 4.20 Standard drugs - docking results for CDOCKER with 1J1B (GSK3B)

Sl No	Target Name	Target PDB ID	Compound Name	Cdocker Energy Value	Cdocker Interaction	Binding Energy
1	AChE	4EY7	Bacopaside N2	-553.761	-23.1752	264.795
2	AChE	4EY7	Bacopaside N1	-319.554	-8.5062	13.7949
3	AChE	4EY7	Bacopaside III	-311.729	-8.27938	24.5964
4	AChE	4EY7	Bacopaside IV	-300.523	-4.87067	-3.36088
5	AChE	4EY7	D-mannitol	3.54826	28.6785	-17.4243
6	AChE	4EY7	Bacopasaponin G	-327.912	-5.63619	40.6074
7	AChE	4EY7	Ebelin Lactone	-69.2045	36.3771	-62.1722
8	AChE	4EY7	Bacopaside VI	-294.193	5.58311	45.6012
9	AChE	4EY7	Bacopaside XI	-317.159	-1.47792	34.7291
10	AChE	4EY7	Bacopaside A	1.82197	48.0188	-39.881
11	AChE	4EY7	Bacopaside B	38.4876	62.8168	-84.5665
12	AChE	4EY7	Bacoside A1	-237.748	26.6016	-54.1989
13	AChE	4EY7	Bacopasaponin B	-270.931	9.53526	8.81541
14	AChE	4EY7	Bacopasaponin D	-324.252	10.8738	-1.54889
15	AChE	4EY7	Bacopaside C	1.68343	63.0374	-9.27375
16	AChE	4EY7	Jujubogenin	-174.695	9.83944	11.4903
17	AChE	4EY7	Pseudojujubogenin	-174.695	9.83944	11.4903
18	AChE	4EY7	Bacopaside V	-263.677	16.4092	-9.36664
19	AChE	4EY7	Bacogenin A1	-165.811	-0.0130026	6.96318

Table 4.21 Docking results from: CDOCKER (Discovery Studio) results - 4EY7 (AChE)

Sl No	Target Name	Target PDB ID	Compound Name	Cdocker Energy Value	Cdocker Interaction	Binding Energy	
1	AChE	4EY7	E2609	14.685	65.7016	-370.60	
2	AChE	4EY7	ANAVEX 2-73	19.8749	53.0949	-202.19	
3	AChE	4EY7	Donepezil	17.8285	57.3379	-148.17	
4	AChE	4EY7	JNJ-54861911	21.5274	48.792	-270.594	
5	AChE	4EY7	Nilotinib	32.7777	65.6879	-96.585	
6	AChE	4EY7	Rivastigmine	38.3359	46.869	-214.85	

Table 4.22 Standard drugs - docking results for CDOCKER with 4EY7 (AChE)

Sl No	Target Name	Target PDB ID	Compound Name	Cdocker Energy Value	Cdocker Interaction	Binding Energy	
1	Amyloid beta	1IYT	D-mannitol	-9.26701	13.3311	-37.5269	
2	Amyloid beta	1IYT	Bacopaside B	0.0548213	20.7563	3.23345	

Table 4.23 Docking results from: CDOCKER (Discovery Studio) results-1IYT (beta amyloid)

Sl No	Target Name	Target PDB ID	Compound Name	Cdocker Energy Value	Cdocker Interaction	Binding Enegrgy
1	Amyloid beta	1IYT	JNJ-54861911	-11.7015	16.5833	-24.5429
2	Amyloid beta	1IYT	Nilotinib	-5.00597	24.3505	12.7932

Table 4.24 Standard drugs - docking results for CDOCKER with 1IYT (beta amyloid)

After obtaining the CDOCKER docking scores, we have to calculate binding energy. Here, only the compounds for which negative values for Binding Energy were considered. Binding energy is the energy released when a drug binds to the target. Negative binding

energy implies that energy is released during binding. Positive implies that it requires energy for the bonds to be formed.

Protein	PDB ID	Binding sphere radius (Å)	Co-ordinates (Å)		
			X	Y	Z
BACE	2VKM	11.1749	-2.77542	-3.71585	31.7604
GSK-3B	1J1B	8.26013	37.2939	-7.64626	-33.1729
AChE	4EY7	9.70264	-13.9818	-43.9714	27.8911
Amyloid Beta	1IYT	31.0687	-0.0805833	0.0181101	0.160041

Table 4.25 Docking sphere and coordinates in CDOCKER

The binding sphere radius is the radius of the binding site that was obtained from previously bound drugs to the target. The coordinates are the ones of the docking site hence obtained for referenced docking.

Sl No	Target Name	Target PDB ID	Compound Name	Score
1	BACE	2VKM	Bacopaside N2	1.901
2	BACE	2VKM	Bacopaside III	-1.9502
12	BACE	2VKM	bacopaside IV	-0.0515
3	BACE	2VKM	D-mannitol	-17.7967
4	BACE	2VKM	Bacopasaponin G	-0.1775
5	BACE	2VKM	ebelin lactone	-10.6741
6	BACE	2VKM	Bacopaside VI	-1.7662
7	BACE	2VKM	Bacopaside A	-21.6607
8	BACE	2VKM	Bacopaside B	-32.5013
9	BACE	2VKM	Bacoside A1	-3.7828
10	BACE	2VKM	Bacopasaponin A	5.9082
11	BACE	2VKM	Bacopasaponin B	-9.817
12	BACE	2VKM	Bacopasaponin D	4.7439
13	BACE	2VKM	Bacopaside C	-23.5423
14	BACE	2VKM	Jujubogenin	-5.3681
15	BACE	2VKM	Pseudojujubogenin	-5.3681
16	BACE	2VKM	Bacopaside V	-3.0653

| 17 | BACE | 2VKM | Bacogenin A1 | -5.761 |

Table 4.26 LeadIT docking score for 2VKM (BACE)

Sl No	Target Name	Target PDB ID	Compound Name	Score
1	BACE	2VKM	E2609	-28.1927
2	BACE	2VKM	ANAVEX 2-73	-12.4808
3	BACE	2VKM	Donepezil	-23.1802
4	BACE	2VKM	JNJ-54861911	-29.6877
5	BACE	2VKM	Nilotinib	-43.4175
6	BACE	2VKM	Rivastigmine	-19.633

Table 4.27 Standard drugs-LeadIT docking score for 2VKM(BACE)

Sl No	Target Name	Target PDB ID	Compound Name	Score
1	GSK-3B	1J1B	Bacopaside III	1.2665
2	GSK-3B	1J1B	D-mannitol	-13.5154
3	GSK-3B	1J1B	Bacopasaponin G	-3.8795
4	GSK-3B	1J1B	ebelin lactone	-6.8949
5	GSK-3B	1J1B	Bacopaside XI	-2.1121
6	GSK-3B	1J1B	Bacopaside A	-8.6089
7	GSK-3B	1J1B	Bacopaside B	-21.8116
8	GSK-3B	1J1B	Bacopasaponin D	-4.202
9	GSK-3B	1J1B	Bacopaside C	-20.68
10	GSK-3B	1J1B	Jujubogenin	-5.2205
11	GSK-3B	1J1B	Pseudojujubogenin	-5.2205
12	GSK-3B	1J1B	Bacogenin A1	-6.4454

Table 4.28 LeadIT docking score for 1J1B (GSK3B)

Sl No	Target Name	Target PDB ID	Compound Name	Score
1	GSK-3B	1J1B	E2609	-22.9148
2	GSK-3B	1J1B	ANAVEX 2-73	-11.7207
3	GSK-3B	1J1B	Donepezil	-18.0469
4	GSK-3B	1J1B	JNJ-54861911	-23.2242
5	GSK-3B	1J1B	Nilotinib	-32.7905
6	GSK-3B	1J1B	Rivastigmine	-12.6716

Table 4.29 Standard drugs-LeadIT docking score for 1J1B (GSK3B)

Sl No	Target Name	Target PDB ID	Compound Name	Score
1	AChE	4EY7	D-mannitol	-19.8104
2	AChE	4EY7	Bacopaside A	-20.8494
3	AChE	4EY7	Bacopaside B	-27.124
4	AChE	4EY7	Bacopaside C	-19.8776

Table 4.30 LeadIT docking score for 4EY7 (AChE)

Sl No	Target Name	Target PDB ID	Compound Name	Score
1	AChE	4EY7	E2609	-33.6574
2	AChE	4EY7	ANAVEX 2-73	-18.8117
3	AChE	4EY7	Donepezil	-24.0995
4	AChE	4EY7	JNJ-54861911	-34.106
5	AChE	4EY7	Nilotinib	-35.6079
6	AChE	4EY7	Rivastigmine	-16.7592

Table 4.31 Standard drugs-LeadIT docking score for 4EY7(AChE)

Sl No	Target Name	Target PDB ID	Compound Name	Score
1	Amyloid beta	1IYT	Bacoside A3	10.5699
2	Amyloid beta	1IYT	Bacopaside II	10.1551
3	Amyloid beta	1IYT	Bacopaside X	7.6946
4	Amyloid beta	1IYT	Bacopasaponin C	8.718
5	Amyloid beta	1IYT	Bacopaside I	11.5452
6	Amyloid beta	1IYT	Bacopaside N2	7.4268
7	Amyloid beta	1IYT	bacopaside N1	5.0928
8	Amyloid beta	1IYT	Bacopaside III	8.6532
9	Amyloid beta	1IYT	bacopaside IV	2.381
10	Amyloid beta	1IYT	D-mannitol	-3.5023
11	Amyloid beta	1IYT	Bacopasaponin G	1.8384
12	Amyloid beta	1IYT	ebelin lactone	-3.7969

13	Amyloid beta	1IYT	Bacopaside VI	11.9062
14	Amyloid beta	1IYT	Bacopaside VII	12.7409
15	Amyloid beta	1IYT	Bacopaside VIII	23.79
16	Amyloid beta	1IYT	Bacopaside XI	7.728
17	Amyloid beta	1IYT	Bacopaside A	1.5575
18	Amyloid beta	1IYT	Bacopaside B	-2.2469
19	Amyloid beta	1IYT	Bacoside A1	6.7401
20	Amyloid beta	1IYT	Bacopasaponin A	10.3211
21	Amyloid beta	1IYT	Bacopasaponin B	0.7886
22	Amyloid beta	1IYT	Bacopasaponin D	3.7236
23	Amyloid beta	1IYT	Bacopaside C	-0.4269
24	Amyloid beta	1IYT	Jujubogenin	-2.9311
25	Amyloid beta	1IYT	Pseudojujubogenin	-2.9311
26	Amyloid beta	1IYT	Bacopaside V	5.6325
27	Amyloid beta	1IYT	Bacogenin A1	-3.2432

Table 4.32 LeadIT docking score for 1IYT (beta amyloid)

Sl No	Target Name	Target PDB ID	Compound Name	Score
1	Amyloid beta	1IYT	E2609	-14.6897
2	Amyloid beta	1IYT	ANAVEX 2-73	-8.0266
3	Amyloid beta	1IYT	Donepezil	-9.8896
4	Amyloid beta	1IYT	JNJ-54861911	-14.8815
5	Amyloid beta	1IYT	Nilotinib	-23.8756
6	Amyloid beta	1IYT	Rivastigmine	-7.7445

Table 4.33 Standard drugs-LeadIT docking score for 1IYT (beta-amyloid)

	2VKM		1J1B		4EY7		1IYT	
Compound Name	CDOCKER	LeadIT	CDOCKER	LeadIT	CDOCKER	LeadIT	CDOCKER	LeadIT
ebelin lactone	-9.5071	-10.6741	-43.1441	-6.8949	-62.1722			-3.7969
D-mannitol	-65.0962	-17.7967	-18.1427	-13.5154	-17.4243	-19.8104	-37.5269	-3.5023

Bacopaside A	-53.8796	-21.6607	-51.6203	-8.6089	-39.881	-20.8494		1.5575
Bacopaside B	-69.5237	-32.5013	-43.9368	-21.8116	-84.5665	-27.124	3.23345	-2.2469
Bacopaside C	-87.8889	-23.5423		-20.68	-9.27375	-19.8776		-0.4269
Jujubogenin	23.8174	-5.3681	-19.1169	-5.2205	11.4903			-2.9311
Pseudojujubogenin	23.8174	-5.3681	-19.1169	-5.2205	11.4903			-2.9311
Bacogenin A1	-1.44359	-5.761	-12.8981	-6.4454	6.96318			-3.2432

Table 4.34 Docking scores of CDOCKER (Discovery studio) with LeadIT scores comparison for the compounds

After obtaining all the docking scores, a final comparison was made and only the compounds which docked with all/most of the targets in both the softwares were considered for the final evaluation.

	2VKM		1J1B		4EY7		1IYT	
Compound Name	CDOCKER	LeadIT	CDOCKER	LeadIT	CDOCKER	LeadIT	CDOCKER	LeadIT
E2609	-4.85009	-28.1927						-1 .689
ANAVEX 2-73			-54.5905	-11.7207				
Donepezil					-148.179	-24.0995		
JNJ-54861911	-13.0168	-29.6877					-24.5429	-1 .881
Nilotinib			-115.138	-32.7905			12.7932	-2 .875
Rivastigmine					-214.856	-16.7592		

Table 4.35 Docking scores of CDOCKER with LeadIT scores comparison for Standard Drugs
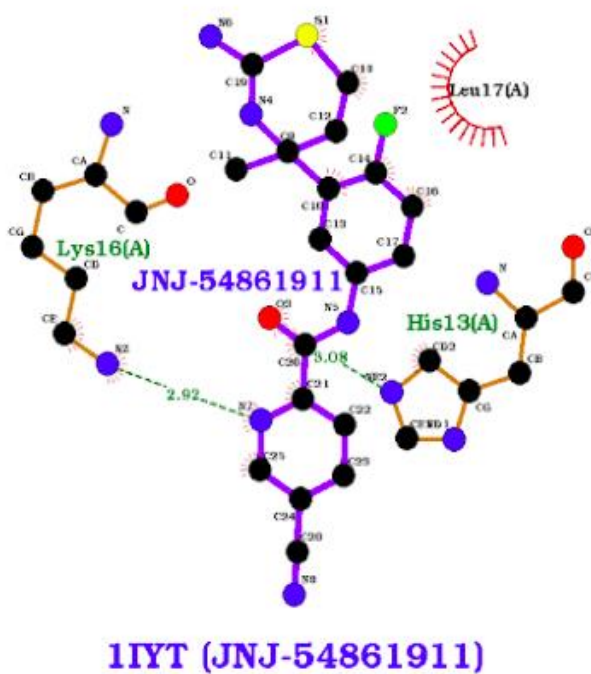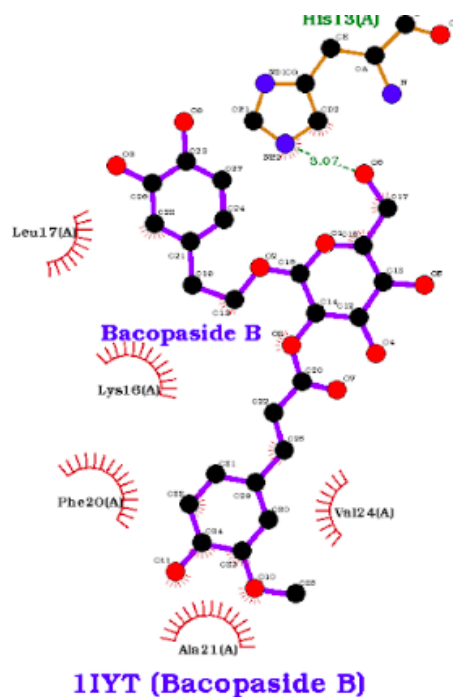
LigPlot interactions

1IYT (Bacopaside B)

1IYT (JNJ-54861911)

Figure 4.11 – Ligplot interaction for 1IYT

Target	Sl no	Compound	Protein -- Ligand	H-bond Length
2VKM	1	JNJ-54861911	GLN$_{73}$A (O) -- N6	2.71
			LYS$_{10}$7A (O) -- N6	3.08

Target	Sl no	Compound	Protein -- Ligand	H-bond Length
	2	E2609	$GLN_{73}A$ (O) -- N8	2.56
			$GLN_{73}A$ (O) -- N7	2.94
	3	Ebelin lactone	-	
	4	Bacogenin A1	GLN_{73} (NE2) -- O27	2.65
			$GLN_{73}A$(O) -- O25	2.65
1J1B		Anavex 2-73	$ASN_{64}B$(O) -- N2	2.72
		Nilotinib	$TYR_{134}B$ (OH) -- N11	3.01
			$LYS_{85}B$(NZ) -- O4	3.1
			$LYS_{85}B$(NZ) -- F3	2.98
		Ebelin lactone	-	
		Bacogenin A1	$CYS_{199}B$ (SG) -- O23	2.78

Target	Sl no	Compound	Protein -- Ligand	H-bond Length
4EY7	1	Rivastigmine	-	
	2	Donepezil	-	
	3	Ebelin lactone	$HIS_{278}A$ (NE2) -- O2	3.17
	4	Bacogenin A1	$TYR_{341}A$(O) -- O25	2.72
			$SER_{293}A$(O) -- O25	2.7
1IYT	1	Bacopaside B	$HIS_{13}A$(NE2) -- O6	3.07
	2	D-mannitol		

	3	JNJ-54861911	LYS$_{16}$A(NZ) -- N7	2.92
			HIS$_{13}$A(NE2) -- O3	3.08
	4	Nilotinib	LYS$_{16}$A(NZ) -- N10	2.74

Table 4.36 LigPlot interactions using complex files

Visualization of the interactions between the drug and the target can be done using LigPlot. The complex files of the drug bound to the target, which were prepared using Discovery Studio, were loaded onto LigPlot, and the diagram were obtained. LigPlot shows interactions at the amino acid level, the interactions between the drug and the target, which was then recorded into a tabular form. These interactions can further be visualised after simulation.
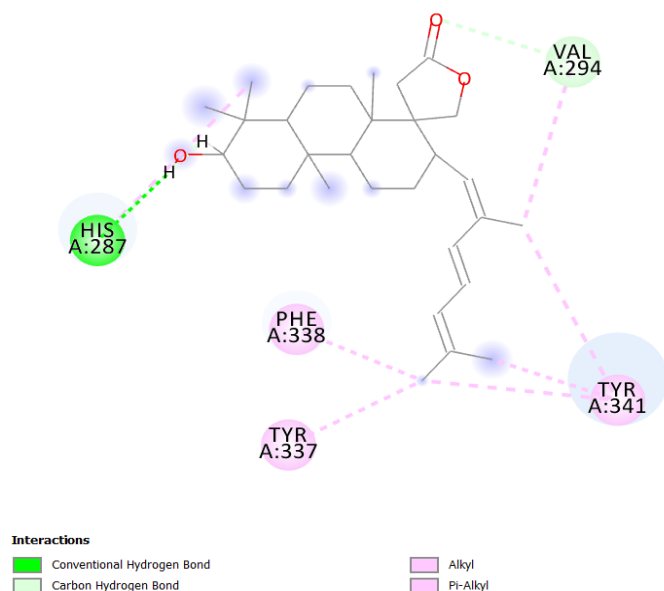

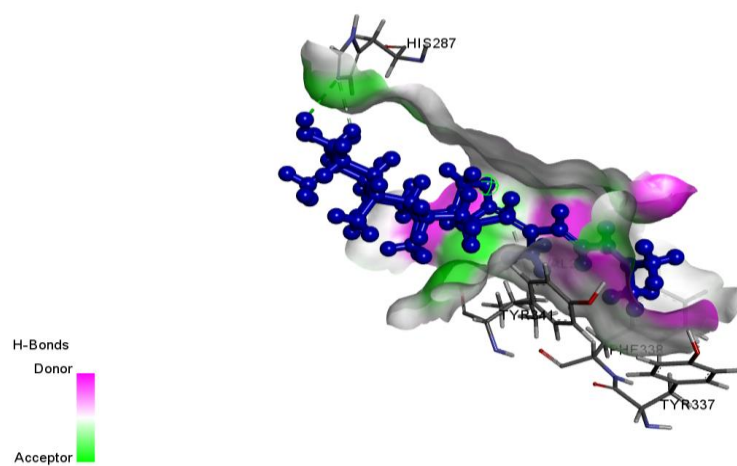Figure 4.12 2D diagram of 4EY7 with Ebelin Lactone

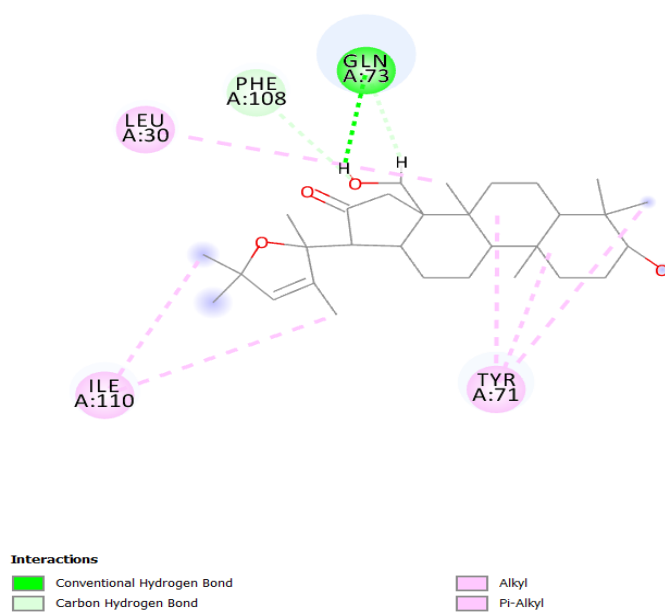Figure 4.13 3D of 4EY7 with Ebelin Lactone

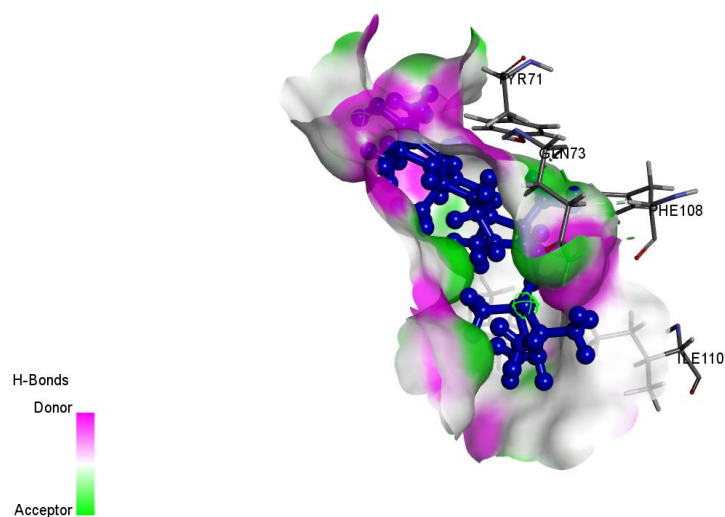Figure 4.14 2D Diagram of 2VKM with Bacogenin A1

Figure 4.15 3D Diagram of 2VKM with Bacogenin A1

These 2D and 3D diagrams, prepared using Discovery Studio, aid in the visualization of the interactions between the drug and target. The Hydrogen bond(s) along with the interactions at the amino acid level can be conveniently visualized and studied.
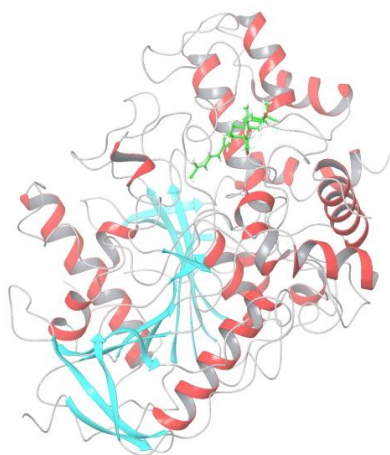
Molecular Simulation Results
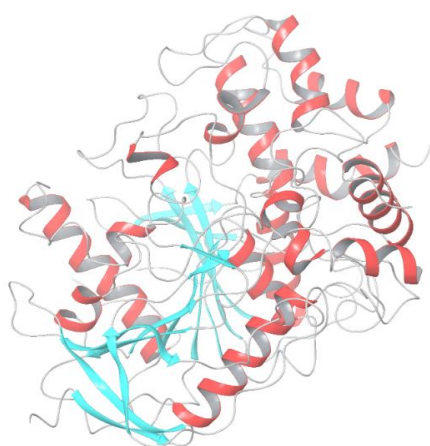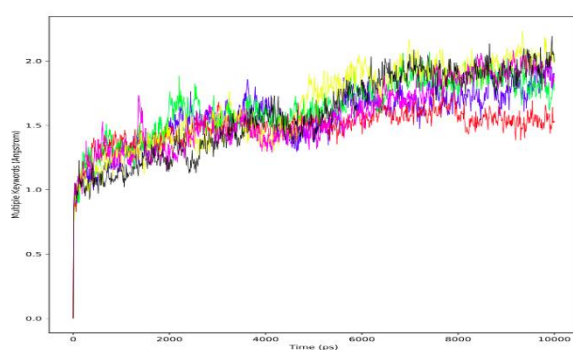

4EY7 (0 ns)
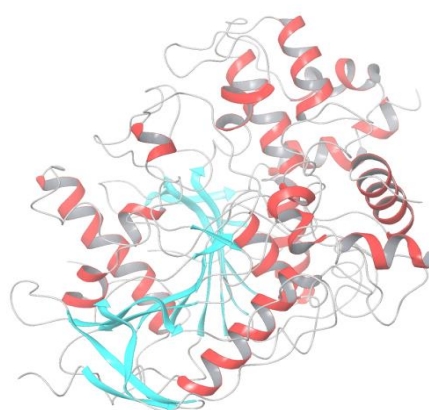
4EY7 (10 ns)

4EY7 with Ebelin Lactone (0 ns)   4EY7 with Ebelin Lactone(10ns)

Figure 4.16 – Simulation results for 4EY7

1.   Blue - Only protein (4EY7)
2.   Red - 4EY7_BAB
3.   Green - 4EY7_BGA
4.   Yellow - 4EY7_EBL
5.   Pink - 4EY7_RSM
6.   Black - 4EY7_DNP

 Figure 4.17 RMSD Graph for 4EY7

Docking Results

From the Docking Scores obtained using the two Commercial Softwares, Discovery Studio and LeadIT, it is observed that Bacopaside B docks with the various targets taken for the study and gives a good docking score. However, the ADMET prediction obtained with Bacopaside B didn't give a favourable result. But it can still be considered because some of the Standard drugs available in the market also didn't give good ADMET result.

The compound that gave the second best result was Ebelin Lactone which docked with only three of the four targets taken but with a considerably good docking Score. Moreover, it also showed good ADMET result. Hence Ebelin Lactone can also be considered as a good compound which can acts a drug.

There have been previous *In Silico* studies of *Bacopa monnieri* done of compounds found

in the plant with various receptors. Bacoside A with LRRK2 (Parkinson's disease) receptor studies have been done (Jain et al, 2013). Docking studies of Bacoside A compounds, intermediates and derivatives have been done with AChE receptor for Alzheimer's and it was found that Ebelin Lactone was most favorable. (Ramasamy et al, 2015). In another study for Zika virus receptors Bacopaside III, and Bacopaside A were identified as leads against multiple targets of Zika virus (Kothandan S. et al, 2018). Docking studies for bacterial inhibitions have also been done with six compounds found in the plant. (Udhaya Lavinya B. et al, 2016).

Conclusion and future prospective

The optimization of culture media and temperature dependent shooting from callus results can help propagate Bacopa monneri *in vitro* to not only grow the plant but also conserve the germ plasm, as it's under threat due to excessive harvesting for its medicinal properties. The phytochemical analysis confirmed the presence of various compounds that give the plant its characteristics. Measuring the total phenolic content and antioxidant properties prove another important aspect of the plate, the mechanism by which it prevents oxidative stress in CNS. Chromatographic techniques were used to compare the nfield, in vitro plant, and callus extracts for the concentration of compounds with a focus of Bacoside A. In TLC, Bacoside A was detected in all, but it was seen that the callus had extra bands which the rest of the extracts did not. There may be compounds which are expressed in callus but not in other forms. HPLC \
MTT

In Silico studies showed that among all the saponins considere, Bacopaside B and Ebelin Lactone were the most promising due to high docking scores and ability to dock with most of the targets well.

Future work:
The successful docking results of Bacopaside B and Ebelin Lactone suggest that *Bacopa monnieri* has the potential cure for Alzhiemer's. The *In Silico* findings can be validated by performing in vitro study on various animal models like *Drosophila melanogaster*.

Also the properties of *Bacopa monnieri* can be further explored by performing the metabolomic and the lipidomic studies of both the field as well as the *In vitro* plant and the comparison between the two.

REFERENCES

1. What are neurological disorders? (2016, May 03). Retrieved from
   https://www.who.int/features/qa/55/en/

2. World Health Organization – Neurological Disorder Report (2006) https://www.who.int/mental_health/neurology/neurological_disorders_report_web.pdf

3. Neurological disorders affect millions globally: WHO report. (2010, December 08).Retrieved from https://www.who.int/mediacentre/news/releases/2007/pr04/en/

4. Parkinson disease - Genetics Home Reference - NIH. (n.d.). Retrieved from https://ghr.nlm.nih.gov/condition/parkinson-disease#statistics

5. Alzheimer's Disease. (2018, April 24). Retrieved from https://www.nih.gov/research-training/accelerating-medicines-partnership-amp/alzheimers-disease

6. Parkinson's Disease. (n.d.). Retrieved from https://www.nia.nih.gov/health/parkinsons-disease

7. Alzheimer's Disease. (2018, April 24). Retrieved from https://www.nih.gov/research-training/accelerating-medicines-partnership-amp/alzheimers-disease

8. **Korolev**, I. (2004). Alzheimer's Disease: A Clinical and Basic Science Review. *Medical Student Research Journal*, **4** (Fall).

9. **Neugroschl, J., &Wang, S**.,"Alzheimer's Disease: Diagnosis and Treatment Across the Spectrum of Disease Severity" *Mount Sinai Journal of Medicine: A Journal of Translational and Personalized Medicine*, **78(4),** 596–612.

10. **Kaur, N., Sarkar, B., Gill, I., Kaur, S., Mittal, S., Dhiman, M., … Mantha, A. K.** (2017). Indian Herbs and their Therapeutic Potential against Alzheimer's Disease and Other Neurological Disorders. In Neuroprotective Effects of Phytochemicals in Neurological Disorders (79–112). *John Wiley & Sons, Inc*.

11. **Sahoo, S**. (2018). A review of some medicinal plants used for nervous disorders. *Journal of Medicinal Plants Studies*, **6(1),** 220-224.

12. **Cummings, J., Lee, G., Ritter, A., & Zhong, K.** (2018). Alzheimer's disease drug development pipeline: 2018. *Alzheimer's & Dementia: Translational Research & Clinical Interventions*, **4**, 195–214.

13. **M.oObulesu**, **soma shekhar Somashekhar**, **Roja Venu**, (2011) Genetics of Alzheimer's Disease: An Insight Into Presenilins and Apolipoprotein E Instigated Neurodegeneration, *The International journal of neuroscience* **121(5):**229-36

14. **Prasan R. Bhandari,** (2013), A comment on effect of plant extracts on Alzheimer's disease: An insight into therapeutic venues, *J Neurosci Rural Pract*, 4(2):236-7

15. **Aguiar, S., & Borowski, T**. (2013). Neuropharmacological Review of the Nootropic Herb *Bacopa monnieri*. Rejuvenation Research, **16(4),** 313–326.

16. **Gohil, K., & Patel, J**. (2010). A review on *Bacopa monniera*: Current research and future prospects. *International Journal of Green Pharmacy*, **4(1),** 1.

17. **Richa Jain1, Bheem Prasad2 and Manju Jain1**. *In- vitro* regeneration of Bacopa monnieri (L.): A highly valuable medicinal plant. *Int.J.Curr.Microbiol.App.Sci* (2013) **2(12):** 198-205

18. **Zote, R. K., Patil, Y. K., Londhe, S., Thakur, V., & Choudhari, N.** (2018). *In vitro* regeneration of Bacopa monnieri (L.) from leaf and stem explants. *International Journal of Chemical Studies*, **6(2),** 1577-1580.

19. **Chandra, S., Khan, S., Avula, B., Lata, H., Yang, M. H., ElSohly, M. A., & Khan, I. A.** (2014). Assessment of Total Phenolic and Flavonoid Content, Antioxidant Properties, and Yield of Aeroponically and Conventionally Grown Leafy Vegetables and Fruit Crops: A Comparative Study. *Evidence-Based Complementary and Alternative Medicine*, **1-9**, 2014

20. **Kapil, S. S., & Sharma, V.** (2014). In-Vitro Propagation of Bacopa Monneri: An Important Medicinal Plant. *International Journal of Current Biotechnology*, **2(1),** 7-10.

21. **Phrompittayarat, W., Putalun, W., Tanaka, H., Jetiyanon, K., Wittaya-areekul, S., & Ingkaninan, K.** (2007). Comparison of Various Extraction Methods of *Bacopa monnieri. Naresuan University Journal*, **15(1),** 29-34.

22. **Shahare M. D., D' Mello P. M.** (2010). Standardization of *Bacopa monnieri* and its Formulations with reference to Bacoside A, by High Performance Thin Layer Chromatography. *International Journal of Pharmacognosy and Phytochemical Research*, **2(4),** 8-12.

23. **Annegowda, H. V., Bhat, R., Min-Tze, L., Karim, A. A., & Mansor, S. M.** (2011). Influence of sonication treatments and extraction solvents on the phenolics and antioxidants in star fruits. *Journal of food science and technology*, **49(4),** 510-4.

24. **Rency Elizabeth Thomas, S. D. Kamat and D. V. Kamat**, (2015) Comparative Study of Antiplatelet Aggregation Activity of *Bacopa monnieri* extracted using Microwave and Ultrasonication, *International Journal of Advances in Pharmacy, Biology and Chemistry*, **4(2),** 2277 - 4688

25. **Prashant Tiwari, Bimlesh Kumar, Mandeep Kaur, Gurpreet Kaur, Harleen Kaur,** (2011), Phytochemical screening and Extraction: A Review, *Internationale Pharmaceutica Sciencia*

26. **Pushpendra Kumar Jain, (**2016), Pharmacognostic Comparison *Bacopa monnieri*, *Cyprus rotundus*, an *Emblica officinalis*, *Innovare Journal Of Ayurvedic Sciences*,**4(4)**

27. **Jain, C., Gupta, A., Tewari, A., Sharma, V., Kumar, V., Mathur, A., & Sharma, S.** (2013). Molecular docking studies of bacoside from *Bacopa monnieri* with LRRK2 receptor. Biologia, **68(6).**

28. **Mohammed Fadlinizal Abd Ghafar, K. Nagendra Prasad, Kong Kin Weng and Amin Ismail,** (2009), Flavonoid, hesperidine, total phenolic contents and antioxidant activities from Citrus species, *African Journal of Biotechnology,* **9(3),** 326-330

29. **Sharan Suresh Volluri et al**, (2011) *In Vitro* Antioxidant activity and estimation of total phenolic content in the methanolic extract of *Bacopa monnieri*,**4 .2** ,

30. **Chandra, S., Khan, S., Avula, B., Lata, H., Yang, M. H., ElSohly, M. A., & Khan, I. A.** (2014). Assessment of Total Phenolic and Flavonoid Content, Antioxidant Properties, and Yield of Aeroponically and Conventionally Grown Leafy Vegetables and Fruit Crops: A Comparative Study. *Evidence-Based Complementary and Alternative Medicine*, **1–9.**

31. <u>**Sowndhararajan K**</u>**,** <u>**Kang SC**</u>**.** (2013) Free radical scavenging activity from different extracts of leaves of Bauhinia vahlii Wight & Arn, <u>*Saudi J Biol Sci.*</u> **20(4):**319-25

32. **Tamara Simpson, Matthew Pase, and Con Stough**, (2015) "*Bacopa Monnieri* as an Antioxidant Therapy to Reduce Oxidative Stress in the Aging Brain," Evidence-Based Complementary and Alternative Medicine, vol. 2015, 9

33. **Phrompittayarat, W., Putalun, W., Tanaka, H., Jetiyanon, K., Wittaya-areekul, S., & Ingkaninan, K.** (2007). Comparison of Various Extraction Methods of *Bacopa monnieri*. *Naresuan University Journal*, **15(1),** 29-34.

34. **Manoharan Mohana, Palghat Raghunathan Padma, (2016),** Free Radical scavenging Activity of the Bacoside fraction from *Bacopa monnieri*, *International Journal of Current Pharmaceutical Research* **8(2)**

35. **Kumar, R., Singh, T., Kumar, D., Singh, M., Kaur, S., & Garg, R.** (2015). Estimation Of Bacoside-A In *Bacopa Monnieri* Aerial Parts Using Tlc Densitometry. *International Journal of Pharmacy and Pharmaceutical Sciences,7***(12).**

36. **Mehta Sonam, Rana Pawan Singh, Saklani Pooja** . (2017);   Phytochemical Screening and TLC Profiling of Various Extracts of *Reinwardtia. Indica. International Journal of Pharmacognosy and Phytochemical Research*9(4); 523-527

37. **Jiang Z, Kempinski C, Chappell J**(2016). Extraction and Analysis of Terpenes / Terpenoids. *Curr Protoc Plant Biol*.;**1**:345-358.

38. **Shinde PB, Aragade PD, Agrawal MR, Deokate UA, Khadabadi SS**.(2011) Simultaneous determination of withanolide a and bacoside a in spansules by high-performance thin-layer chromatography. *Indian J Pharm Sci*.; **73(2):**240-3.

39. **Bożena Muszyńska, Maciej Łojewski, Katarzyna Sułkowska-Ziaja, Agnieszka Szewczyk, Joanna Gdula-Argasińska & Patrycja Hałaszuk** (2016) *In vitro* cultures of *Bacopa Monnieri* and an analysis of selected groups of biologically active metabolites in their biomass, *Pharmaceutical Biotechnology,* 54:11, 2443-2453

40. **Pragya Bhardwaj, Chakresh Kumar Jain, Prashant Mishra, Ashwani Mathur** (2017) Comparative Analysis of Bacoside A Yield in Field Acclimatized and in-vitro Propagated *Bacopa Monnieri*, *Int. J. Pharm. Sci. Rev.* Res., **44(2),** ; Article No. 33, 168-175

41. **Vinut.S. Nandagoan, A.R Kulkarni,** (2013) "*In Vitro* Antioxidant And Cytotoxicity Activity of *Bacopa Monnieri* And Baliospermum Montanum muell Arg." *International Journal of Pharmaceutical Applications* **4(3)**

42. **Mallick MN, Khan W, Parveen R, Ahmad S, Sadaf, Najm MZ, Ahmad I, Husain SA**.(2017) Exploring the Cytotoxic Potential of Triterpenoids-enriched Fraction of *Bacopa monnieri* by Implementing *In vitro*, *In vivo*, and *In silico* Approaches**,** *Pharmacogn Mag.* **13(3):**S595-S606

43. **Mallick MN, Akhtar MS, Najm MZ, Tamboli ET, Ahmad S, Husain SA**. (2015) Evaluation of anticancer potential of *Bacopa monnieri*L. against MCF-7 and MDA-MB 231 cell line, *J Pharm Bioallied Sci.* **7(4):**325-8.

44. **Vinut.S. Nandagaon and A.R Kulkarni** (2013) *In Vitro* Antioxidant and cytotoxicity activity of *Bacopa monnieri* and *Baliospermum montanum* muell Arg. *International Journal of Pharmaceutical Applications*, Vol4, Issue3, 2013, pp 63-67

45. **Vassar, R.** (2004). BACE1: The β-Secretase Enzyme in Alzheimer's Disease. *Journal of Molecular Neuroscience,* 23(1–2), 105–114

46. **Kumar, A., Roy, S., Tripathi, S., & Sharma, A**. (2015). Molecular docking based virtual screening of natural compounds as potential BACE1 inhibitors: 3D QSAR pharmacophore mapping and molecular dynamics analysis. *Journal of Biomolecular Structure and Dynamics*, **34(2),** 239–249.

47. **D.Sivaraman and P.Panneerselvam**, (2015) Screening of Potential Glycogen synthase kinase -3β Inhibitors from Herbal Lead by *In silico* Docking Technique, *International Journal of ChemTech Research*, **8(6),** 834-842

48. **García-Ayllón, M.-S.** (2011). Revisiting the role of acetylcholinesterase in Alzheimer's disease: cross-talk with P-tau and β-amyloid. *Frontiers in Molecular Neuroscience,* **4.**

49. **Ramasamy, S., Chin, S. P., Sukumaran, S. D., Buckle, M. J. C., Kiew, L. V., & Chung, L. Y.** (2015). *In Silico* and *In Vitro* Analysis of Bacoside A Aglycones and Its Derivatives as the Constituents Responsible for the Cognitive Effects of *Bacopa monnieri*. *PLOS ONE*, **10(5),** e0126565

50. **Shruthila, N., P. Narayan, D. J. Kumar, and H. G. Nagendra.** . (2013) "Docking Studies of Plant Polyphenols with Ab fragments suggests determinants that enable design of inhibitors towards preventing aggregation events during Alzheimer's". *International Journal of Pharmaceutical Sciences and Drug Research*, **5(4),** 170-4

51. **Zhou, Y., Peng, L., Zhang, W.-D., & Kong, D.-Y**. (2009). Effect of Triterpenoid Saponins from Bacopa monnieraon Scopolamine-Induced Memory Impairment in Mice. *Planta Medica*, **75(6),** 568–574.

52. **Bhandari P., Kumar N., Singh B., Kaur I** (2009) Dammarane triterpenoid saponins from *Bacopa monnieri*., *Canadian Journal of Chemistry*, **87 (9),** 1230-1234.

53. **Hou, C.-C., Lin, S.-J., Cheng, J.-T., & Hsu, F.-L.** (2002). Bacopaside III, Bacopasaponin G, and Bacopasides A, B, and C from *Bacopa monniera*. *Journal of Natural Products*, **65(12),** 1759–1763.

54. **Majumdar S., Basu A., Paul P., Halder M., Jha S.** (2013) Bacosides and Neuroprotection. In: Ramawat K., Mérillon JM. (eds) Natural Products. *Springer*, Berlin, Heidelberg

55. **Murthy PBS, Raju VR, Ramakrisana T, Chakravarthy MS, Kumar KV, Kannababu S, et al. (**2006) Estimation of twelve bacopa saponins in *Bacopa monnieri* extracts and formulations by high-performance liquid chromatography. *Chem Pharm Bull* (Tokyo); **54(6):**907–911.

56. **McGleenon BM1, Dynan KB, Passmore AP**.(1999) Acetylcholinesterase inhibitors in Alzheimer's disease. *Br J Clin Pharmacol.* Oct;48(4):471-80.

57. **Zote, R. K., Patil, Y. K., Londhe, S., Thakur, V., & Choudhari, N.** (2018). *In vitro* regeneration of *Bacopa monnieri* (L.) from leaf and stem explants. *International Journal of Chemical Studies*, **6(2),** 1577-1580.

58. **T. Soundararajan and C.M. Karrunakaran,** (2011). Micropropagation of *Bacopa monnieri* through Protoplast. *Asian Journal of Biotechnology*, **3:** 135-152.

59. **Mohana M. and Padma P.R.,** (2016), Isolation And Characterization Of The Bacoside Fraction From *Bacopa Monnieri, World Journal Of Pharmacy And Pharmaceutical Sciences*, **5(4),** 1513-1521.